THE NORTH ATLANTIC CURRENT SYSTEM: A SCIENTIFIC REPORT

19-20 April, 1993
Woods Hole Oceanographic Institution
Woods Hole, MA 02543

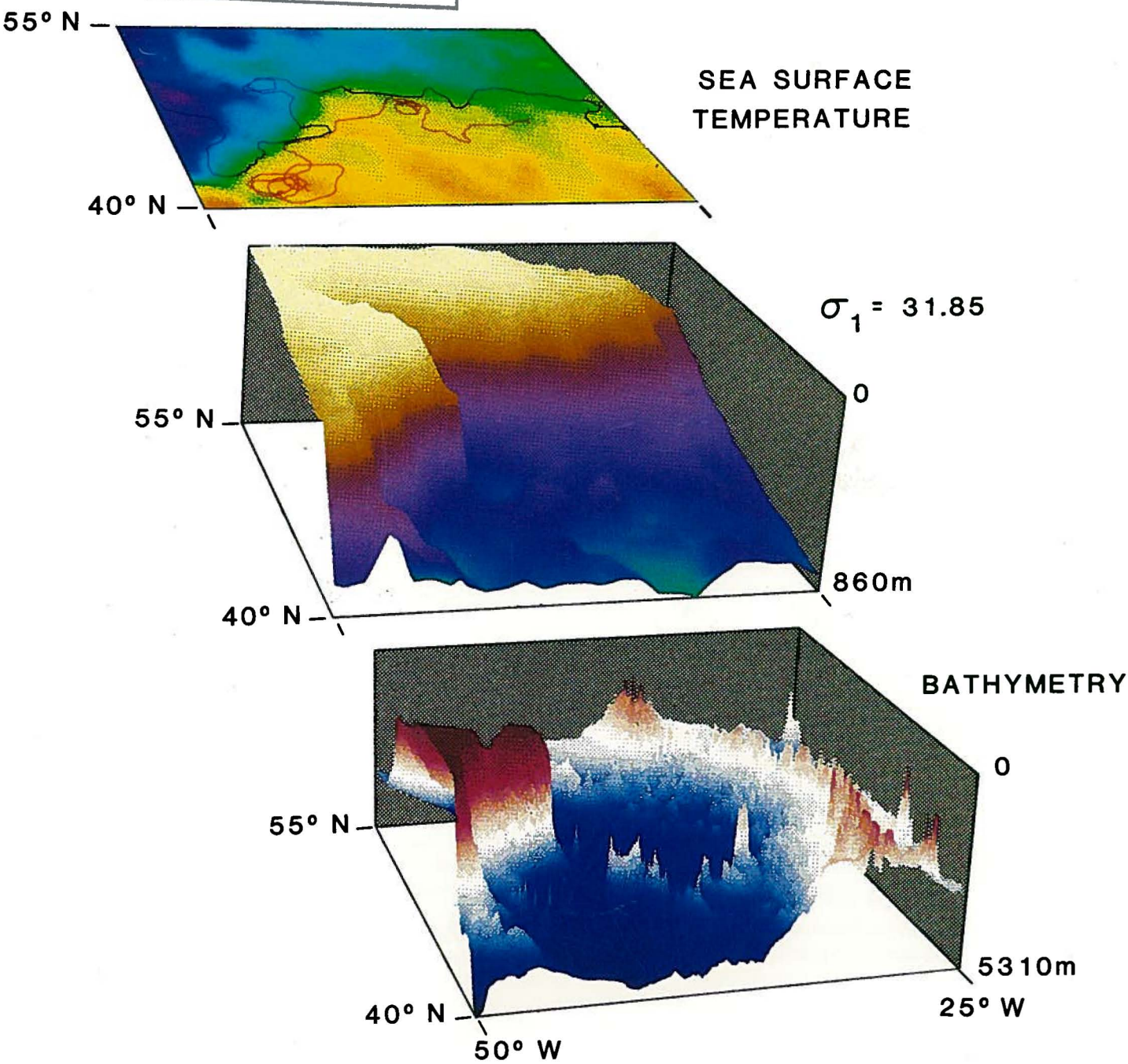

Front Cover

The top panel shows sea surface temperature constructed from a re-analysis of all available hydrographic observations. The extension of warm waters into the northwest (also known as the Loop Current) and the Polar Front near 52°N are evident. The red trajectory (courtesy Prof. W. Krauss, IfM, Kiel) illustrates motion along the North Atlantic Current, while the blue one shows the south- and northward motion of waters in the Labrador Current (courtesy Dr. D. Murphy, International Ice Patrol). The tracks are about 5 months long.

The middle panel shows the mean depth of the $\sigma_1 = 31.85$ surface constructed from a re-analysis of all available hydrographic data. To retain as much structure of the density field as possible, the data were averaged in 1° bins. The mean temperature on this surface is close to 7°C. Note the sharp shoaling of the surface along the path of the North Atlantic Current. The Loop Current is clearly visible as a 'valley' extending to the northwest. (S. Lozier graciously provided her hydrographic analyses for top and middle panels).

The bottom panel shows the bathymetry (constructed from the ETOPO5 data base). The sharp relief of the continental margin and Flemish Cap show up clearly. The Mid-Atlantic Ridge extends north and northwest along the eastern side of the panel.

THE NORTH ATLANTIC CURRENT SYSTEM:

A SCIENTIFIC REPORT

19-20 April 1993

Woods Hole Oceanographic Institution

Woods Hole, MA 02543

Edited by:

Paola Malanotte-Rizzoli
Massachusetts Institute of Technology
Cambridge, MA 02139

Thomas Rossby
University of Rhode Island
Narragansett, RI 02882

PREFACE

On April 19-20, 1993 a two-day workshop was held at the Woods Hole Oceanographic Institution on "The North Atlantic Current (NAC) System". The workshop, which was sponsored by NSF/NOAA/ONR reflected a growing sense of excitement and interest in the oceanographic community in the NAC system and its role in the large scale circulation of the North Atlantic Ocean and Climate of the adjoining landmasses.

The presence of the North Atlantic Current with its warm waters at such high latitudes, and its role in both the wind-driven and thermohaline circulations makes it unique amongst the Western Boundary Currents of the oceans. Being on the one hand part of the wind-driven circulation and on the other hand the upper branch of the "Global Conveyor Belt", the North Atlantic current is indeed an enigma, suggesting fundamental issues about the nature of the coupling between the two 'roles' of the current that will need to be addressed. But it was also clear from the workshop discussions that there remain considerable uncertainty about the basic structure of the NAC. A high level of interest in these questions was evident at the workshop. The lectures, presentations, and the discussion sessions where observational and modelling issues were debated, brought out many ideas for the development and focus of future research of the NAC and surrounding waters.

This report is intended to provide not only a synopsis of the lectures, papers, and ideas that were discussed, but also a scientific statement from the workshop reflecting a growing consensus for initiating a coordinated research effort in the region. For the near-term, the document identifies a number of research activities, which with a modest commitment of resources should be started up soon to investigate the seasonal and interannual variablity of the region. For the longer term, we hope this document will be helpful in developing a national, indeed international research program to chart and understand these poorly understood yet very important waters of the North Atlantic. Again, we wish to thank NSF/NOAA/ONR for sponsoring the workshop!

TABLE OF CONTENTS

VII. Extended Abstracts

THE NORTH ATLANTIC CURRENT SYSTEM: A SCIENTIFIC REPORT

I. INTRODUCTION

The region east of the Grand Banks, where the North Atlantic and Labrador Currents meet, is unique and uniquely important: through this region flow the warm waters that give Central and Northern Europe its temperate climate and even more generally influence climate variability in the entire northern hemisphere. In a geographically limited region, the warm waters of the Gulf Stream meet and join the cold waters of the Labrador Sea. Together, they flow north to higher than 50°N before turning east towards the European continent. As they transit the North Atlantic towards the Norwegian and Irminger Seas, the warm waters surrender enormous quantities of heat to the atmosphere. This process is enhanced by the low temperatures and humidities of the air masses that sweep out over the region from the North American continent, resulting in tremendous evaporative heat losses from the ocean. The upper ocean circulation, however, appears to be mechanically directed by the prevailing atmospheric circulation, although questions remain concerning the impact of the regional thermodynamical coupling of the air and sea on the climate scale. If the thermal coupling of air and sea is considerable then one might suspect that the circulation is driven thermodynamically and steered mechanically! It is also noteworthy that the annual north-south migration of the westerlies subjects the entire region between 35°N and 55°N to both cyclonic and anticyclonic windstresses. What is the effect of these changes in the windstress field on the circulation of the region?

The circulations on the Greenland and Labrador shelves bring significant quantities of fresh water in the form of low salinity water and sea ice southward and this fresh water enters the western Atlantic at various locations along its western margin. Significant changes in sea ice extent in the Greenland and Labrador seas over periods up to a decade, are associated with surface temperature anomalies over the entire region. It is also through this region that the return flow of the global thermohaline circulation must take place. It is generally thought that the strength of the thermohaline circulation is governed by convective processes in the Norwegian, Greenland and Iceland Seas. But the rate of deep water renewal depends not only on the severity of cooling, but also on the salinity of the surface waters, which may not be determined locally but by processes elsewhere including i) the relative strength of evaporation and precipitation (E-P) in the region of the North Atlantic Current, ii) the amount of ice flowing south in the Labrador Current, and iii) exchange of waters between the subtropical and subpolar gyres in the Newfoundland Basin and Southern Labrador Sea. The fact that all of these are large and variable in the region east of the Grand Banks suggests that they may play a big if not central role in governing or modulating the pattern and strength of the circulation over much of the northern North Atlantic Ocean. Taken together, one can see the considerable importance of a regional study of these `crossroads' of the North Atlantic circulation.

The best information we have today about the circulation suggests that there is a broad band of latitudes between about 35°N and 55°N where the surface waters flow from west to east. Some of this transport appears to be part of a general eastward drift; parts of it appear to be concentrated in intense zonal flows, e.g. the Azores Current in the south and the Polar Front in the north with another possible jet at 47°N of unknown temporal and spatial stability. The Azores Current and the jet at 47°N seem to be 'anchored' to major topographic features along the North American continent: the Tail of the Grand Banks and the Flemish Cap, respectively. Similarly, it has been suggested that the Polar Front is locked into place by the Charlie-Gibbs Fracture Zone on the Mid-Atlantic Ridge. But the stability, temporal variability, and partition of water into and transport by each of these zonal flows are essentially unknown. The two extreme cases would occur when most waters turn north at the Tail of the Grand Banks into the North Atlantic Current (as appears to be the case today) and when all waters continue east instead (as appeared to be the case during the last glacial maximum). Between these two extremes can exist a variety of zonal circulations which presumably depend upon a delicate balance between inflow and outflow conditions on the one hand (set by high latitude water mass formation, for example), and water mass modification by the strong surface forcing in the region on the other. This suggests that if we are to improve our understanding of the processes that govern the North Atlantic circulation we must significantly improve our knowledge of the region.

From the above it should be clear that while we have a general idea of the circulation of the region, it is also evident that there are great uncertainties regarding i) transports of mass and heat, ii) spatial and temporal scales variability (including the existence of closed gyre within the Newfoundland Basin), iii) the coupling between the ocean and atmosphere, and iv) the importance of the region to the large scale wind-driven and thermohaline circulation of the North Atlantic. It is inevitable that one should first try to construct a mean field from the variety of observations that have been obtained over the years. But in a region that is known to exhibit substantial change on interannual timescales, it may be particularly difficult if not hazardous to attempt a mean field description based on observations spanning those very time scales of variability! Consequently, improved understanding of the region may not come from attempting a better mean field description (which can only be an average of some set of observations), but by focussing on improving our understanding of the variability of the mass and velocity fields. This must start with efforts to obtain a better description of their temporal and spatial properties and, to the extent possible, the energetics responsible for the observed oceanic variability. We thus put forth the following set of scientific objectives that should be addressed in the near future. The intent is to focus on the region east of the Grand Banks and Newfoundland where the western boundary currents of the subpolar and subtropical gyres meet and interact, and where the exchange of energy and momentum between the atmosphere and ocean is particularly large and variable.

II. SCIENTIFIC OBJECTIVES

I. Interaction between subtropical and subpolar gyres in the North Atlantic
   a. Upper ocean circulation and dynamics including bifurcation processes
   b. Momentum and mass exchange across fronts
   c. Deeper waters and their circulation (mean and eddy fields).

II. Relationship of the North Atlantic Current to variations of
   a. the overall thermohaline cell ('The Conveyor Belt')
   b. Intermediate (mode) water formation

III. Relationship of local seasonal, interannual and secular variability, in the Newfoundland Basin and Southern Labrador Sea, to
   a. surface forcing (heat, water, windstress)
   b. melt waters from the Labrador Sea.

IV. Role of Surface Variations in the Newfoundland Basin in determining the climate of the North Atlantic and adjacent landmasses.

III. OBSERVATIONAL ISSUES

A comprehensive study of the following issues will require a major planning effort. However, it is already known from analyses of historical data sets that there is considerable variability on decadal time scales (e.g. Deser and Blackmon, this report; Levitus, 1982). Our present ability to monitor the region is very limited since the demise of the Ocean Weather Stations. But there are new yet well-established techniques for in-situ monitoring of heat and transport variations. There are certain locations and parameters that are likely to be effective indicators of low frequency transients and change and therefore should be examined closely:

a. Bifurcation at the Tail of the Grand Banks:

This region is enigmatic. Does the Gulf Stream continually split into a NAC and an Azores Current, or is the latter primarily formed from eddies that are shed from the Gulf Stream as it turns north? On the one hand this process must be topographically conditioned, but upstream conditions (advection) must also be very important to events in this region. Similarly, the southward flowing Labrador Current splits into two parts with most waters returning to the north and the remainder flowing west. There is evidence of significant decadal change in L.C. bifurcation which might play a role in the variability over a larger region including the bifurcation of the Gulf Stream itself.

b. Bifurcation of the NAC at Flemish Cap:

What is the partition of NAC transport into the Polar Front and the jet at 47°N, if the latter one actually exists? And, before reaching Flemish Cap, does the NAC transport decrease uniformly from the tail of the Grand Banks indicating a continuous bleeding of NAC water into the Newfoundland Basin?

Regardless of what happens to these flows after they separate from the boundary, it is clear that we have very limited knowledge of the processes responsible for this very important regional variability. Yet, significant change here may be quite important in governing the surface distributions of heat and salt farther north and east over much of the North Atlantic.

c. The circulation in and through the Newfoundland Basin.

Is there a significant recirculation of the surface or deep waters between the Grand Banks and the Mid-Atlantic Ridge, as advocated by Worthington (1976) and Schmitz and McCartney (1993)? Or is there instead a general eastward drift in the region as advocated by Krauss (1986)? Schmitz and McCartney only allow 12 Sv of NAC water to proceed north out of the Newfoundland Basin, in contrast to Krauss' northward transport of 30 Sv. The crucial question is this: what is the total mean northward volume transport in each layer versus the magnitude of the recirculation?

d. Heat storage variability at the site of OWS 'Delta' (and others)

Surface heat flux maps show a maximum in the Newfoundland Basin. The hydrographic time series at the ocean weather stations provide valuable information of temporal change for a window of time in the past. There are simple techniques for resuming and providing continuous coverage of heat storage change. With modest effort, such new time series can be calibrated and linked to the earlier time series not only to determine the variability on the seasonal timescale but also to provide a window on longer (interannual) time scale change.

e. Transport fluctuations (at depth) between Flemish Cap and Milne Seamount.

This region is thought to be an excellent 'choke point' for monitoring the strength of the Deep Western Boundary Current, i.e. part of the lower limb of the 'Conveyor Belt'. Since our present estimates of transport are mostly based on hydrography and not direct measurement, it is probably safe to say that at the present time we have very little insight into or knowledge of the variability of the deep transport.

f. Vertically averaged velocities (transports) on Canadian repeat hydrography.

There is increasing effort to obtain repeated hydrographic sections. It is suggested that all hydrography should have measurements of absolute transport as well, particularly since the measurements are now so easy to obtain.

IV. MODELING ISSUES AND NEEDS

The numerical modeling community has not placed much emphasis, until now, on understanding and realistically simulating the NAC system "per se", with its separation at Flemish Cap, numerous mid-ocean bifurcations, air/sea coupling and mean properties as well as transient instabilities and interactions with the associated mesoscale eddy field. Rather, the NAC has always been considered in the context of the entire Northern Atlantic circulation in efforts such as the CME (Community Modeling Experiment) of WOCE, carried out at NCAR by Holland and Bryan, and at Kiel, Germany by Böning and collaborators (see Böning et al., present report). However, the present results show that GCM's perform poorly in the NAC region. Eddy resolving models have the peculiarity that the main water masses of the NAC flow through Flemish Pass, i.e. west of Flemish Cap instead of around Flemish Cap along the continental slope. Furthermore, eddy intensity is not properly reproduced even in simulations with a 1/6° resolution. The

poor performance of the GCM's, even in the most realistic and fully eddy resolving calculations, coupled with the shortage of simpler, conceptual models of the system make it quite desirable and timely that a concerted modeling effort be initiated as soon as possible. We emphasize that efforts should concentrate not only on "full-physics" simulation calculations but also on "reduced-physics" conceptual models aimed at understanding the NAC system. We outline below some of the important modeling issues that could be addressed with a modest, initial effort.

a) Role of conceptual models

Conceptual modeling is a crucial component in our understanding of the "zero-order" questions raised by the above discussion. Process oriented questions to be addressed in such a modeling effort include: By which mechanisms do the Gulf Stream and the NAC bifurcate at the tail of the Grand Banks and the Flemish Cap respectively? What determines the NAC separation and eastward turn at 51-52°N? What is the role played by topography in setting the pathways of the NAC system? What type of instabilities characterize the NAC jet? By which dynamical mechanisms are the anticyclones produced at the offshore side of the NAC? What is the role of NAC meandering and instabilities in determining the energetic mesoscale eddy field for instance through wave radiation processes? What are the eddy-mean flow interaction processes? Such questions ought to be addressed through simpler, idealized approaches such as one or two layer periodic or inflow/outflow numerical models; box models; contour dynamic models; instability studies of analytical jet shapes; wave-mean flow interaction studies analogous to those carried out in meteorology (Plumb, 1985) or in the Gulf Stream System (Malanotte-Rizzoli et al., 1993).

b) Role of GCM's

A series of basic issues for the NAC System can only be addressed with the use of GCM's which properly place the NAC as an important component of the entire Northern Atlantic circulation, both wind and thermally driven. Important motivations include:

b1) An assessment of the relative importance of mechanical versus thermohaline forcing for the circulation north of 42°N. It is crucial to understand and model the interaction between the wind-driven subpolar and subtropical gyres in the North Atlantic and related intergyre exchange of properties. This is especially critical for the northern/subpolar ocean, where differently from the subtropics, the annual north/south migration of the westerlies reverses the polarity of the wind stress curl.

b2) An understanding of the dynamical influence of the NAC on the overall Atlantic "conveyor belt". If the Atlantic thermohaline cell were shut off, would this shut off the northern branch of the NAC, with consequent cooling of the polar gyre, less heat flux to the atmosphere and a colder Europe?

b3) An understanding of the separation problem of the NAC and why in GCM calculations the NAC flows through the Flemish pass instead of flowing around the Flemish Cap along the continental slope.

b4) An appreciation of the role of coupled air/sea interactions in setting the large scale ocean circulation in the NAC region. Is the NAC System unstable when explicit atmospheric coupling is included? Are coupled, high-frequency air/sea interactions (e.g. winter storms) responsible for a significant portion of the system variance on longer time scales?

To address the above scientific issues one must consider the following urgent needs of GCM's.

i) Availability of a better climatology capable of adequately resolving sharp frontal regions such as the NAC. It is well known that one reason why GCM's perform badly in the NAC region is the use of highly smoothed climatologies such as Levitus.

ii) To understand the influence of lateral boundary conditions (open versus closed) in determining the NADW renewal rates, pathways and consequently the dynamics of the overall thermohaline cell.

iii) To understand the role of surface boundary conditions (flux, robust diagnostics or mixed boundary conditions) in determining the behavior of the thermohaline cell and its properties. This dependence should be assessed not only on the type of surface boundary conditions used but also on the quality of the dataset(s) included in the boundary conditions.

iv) Necessity of improved mixing schemes based upon parameterizations of convection. Process models of deep convection and subduction, leading to deep and intermediate water mass formation respectively, should be used to lead to the formulation of new and better mixing schemes.

References

Krauss, W. (1986) The North Atlantic Current, J. Geophys. Res., 91, 5061-5074.

Levitus, S. (1982) Climatological Atlas of the World Ocean NOAA Professional Paper 13, 173 pp.

Malanotte-Rizzoli, P., N.G. Hogg and R.E. Young (1993) Stochastic wave radiation by the Gulf Stream: numerical experiments, submitted to Deep-Sea Res..

Plumb, R.A. (1986) Three-dimensional propagation of transient quasi-geostrophic eddies and its relationship with the eddy forcing of the time-mean flow, J. Atmos. Sci., 43, 1657-1678.

Schmitz, W.J., J. and M.S. McCartney (1993) On the North Atlantic circulation, Rev. Geophys., 31, 29-49.

Worthington, L.V. (1976) On the North Atlantic circulation: The Johns Hopkins Oceanographic Studies 6, 110 pp.

V. PROPOSED OBSERVATIONAL STUDIES

Ocean Acoustic Tomography in the North Atlantic Current

Peter Worcester, Bruce Cornuelle
Scripps Institution of Oceanography
University of California, San Diego
La Jolla, CA 92093

We propose a small pilot ocean acoustic tomography experiment in the southern Newfoundland Basin with the primary purpose of studying the ocean heat budget, i.e., the seasonal cycle in heat content and its relation to surface fluxes and advection. The proposed experiment would consist of 3-4 tomographic transceivers deployed in an area roughly 500 km square to the east of the main North Atlantic Current, to the north of the Azores Current, and to the south of the Milne Seamounts and the uncertain front at about 45°N (roughly in the region 40-44°N, 39-44°W). The array would not be eddy-resolving, but would exploit the spatial averaging inherent in tomograhic data to measure the spatial mean properties of the region, including the large-scale temperature structure and heat content, barotropic and baroclinic flow, and heat transport, and their evolution in time. Previous tomographic experiments have amply demonstrated the ability to provide accurate measurements of large-scale average temperature structure, heat content, and flow (see, e.g., Dushaw et al., 1993a, Dushaw et al., 1993b, and Worcester et al., 1993a). It is important to keep the array as large as possible, consistent with the expected circulation pattern and bathymetry, to obtain the maximum spatial averaging possible in this eddy-rich region.

This region is near the center of a maximum in net air-sea heat flux during winter (Isemer and Hasse, 1987). The monthly mean net air-sea heat flux shows a seasonal maximum of about 350 W/m^2 from the ocean to the atmosphere in January, centered roughy at 45°N, 41°W, over the Newfoundland Basin. The heat flux drops to about 300 W/m^2 in December and February, but is still a local spatial maximum. This region can therefore be expected to be particularly important in the North Atlantic heat budget. The heat lost to the atmosphere in this region during winter plays an important role in moderating Europe's climate.

Under the overall goal of studying the ocean heat budget are a number of more detailed objectives:

(i) to determine the relative roles of air-sea fluxes and advection in determining near-surface ocean temperatures;

(ii) to study the processes by which the mixed layer deepens in winter and the depth of vertical homogenization;

(iii) to study the formation of mode water that is created in the region with a temperature of about 15°C, and

(iv) to determine if there is a large-scale recirculation of the North Atlantic Current in the southern Newfoundland Basin.

We propose a pilot 1-year experiment. Clearly a 2-year experiment, with recovery and redeployment of the instruments after one year, would be preferable to begin to study seasonal and interannual variability. While such an experiment would be possible, since we have enough tomographic transceivers for two deployments of four

transceivers each, it is probably better to complete a pilot experiment first. The experiment would be a prototype for a longer term regional monitoring effort, perhaps in conjunction with the basin-scale Acoustic Thermometry of Ocean Climate program currently underway. Such a monitoring effort would fit naturally within the context of GOOS, if the results are favorable. This experiment would also serve as a pilot experiment to determine the feasibility of a much larger mesoscale resolving tomographic array to study the NAC and its related eddy field in detail, as described by Worcester (1993).

In the design of such an experiment, there is a trade-off between the use of acoustic transceivers, which both transmit and receive, and of receive only units. Reciprocal measurements made using transceivers provide both temperature and current data. One-way transmissions provide temperature, but not current, with a residual error caused by the neglect of the effect of ocean currents on travel times. The cost and effort to deploy a transceiver is significantly greater than that to deploy a receiver, however, due to the size and battery requirements of the acoustic sources. We recommend 3-4 transceivers be used to provide both heat content and current data. Tomographic receivers placed on moorings of opportunity would increase the spatial coverage and resolution of temperature structure and heat content at relatively low cost, however, and provide an initial test of the feasibility of this approach for long term monitoring.

We envisage a three year proposal. Equipment preparations would take 6-9 months, the actual deployment would last 12 months, and data analysis would require 12-18 months. While the proposed research is potentially relevant to the Long Term Ocean Observations program element, we feel that the pilot experiment is more directly applicable to the Atlantic Climate Change program element.

References

H.-J. Isemer and L. Hasse, The Bunker Climate Atlas of the North Atlantic Ocean, Vol. 2: Air-Sea Interactions, Springer-Verlag, Berlin, 1987.

Dushaw, B.D., P.F. Worcester, B.D. Cornuelle, and B.M. Howe, "Variability of heat content in the North Central Pacific in summer 1987 determined from long-range acoustic transmissions," J. Phys. Oceanogr., in press, 1993a.

Dushaw, B.D., P.F. Worcester, B.D. Cornuelle, and B.M. Howe, "Barotropic currents and vorticity in the North Central Pacific in summer 1987 determined from long-range acoustic transmissions," J. Geophys. Res., submitted, 1993b.

Worcester, P.F., J.F. Lynch, W.M.L. Morawitz, R. Pawlowicz, P.J. Sutton, B.D. Cornuelle, O.M. Johannessen, W.H. Munk, W.B. Owens, R. Shuchman, and R.C. Spindel, "Evolution of the large-scale temperature field in the Greenland Sea during 1988-1989 from tomographic measurements," Geophys. Res. Lett., in press, 1993a.

Worcester, P.F., "Measuring thermal and velocity structure in the Northwestern Atlantic with acoustic tomography," Report of a Workshop on the North Atlantic Current System, Woods Hole, MA, April 19-20, 1993 (this report).

The Variability of the North Atlantic Current

E.T. Katz
Lamont-Doherty Earth Observatory
Route 9W-Dept. of Physical Oceanography
Palisades, NY 10964

Abstract

The temporal and spatial variability of the initial stages of the North Atlantic Current downstream of the Grand Bank will be studied by combining the dense spatial information derived from the TOPEX/POSEIDON altimeter with the continuous time series information from an array of five inverted echo sounders, deployed under the satellite tracks and centered about the 38°W meridian. The observations will begin in the summer of 1994 concurrent with other Canadian and U.S. field programs monitoring the time variable flow into the study area, allowing for study of how upstream conditions in the transitional zone between the Gulf Stream and North Atlantic Current lead to changes in the location and strength of the latter.

I. Description Of The Study Area

One of the more recent schematics of the path of the NAC, published by Krauss (1986)* , is shown in Figure 1. It is based on surface drifter observations and the meridionally shaded region is the area where a northward flow associated with the NAC was observed (with the southern boundary varying between the dashed lines, A and A'). The 38°W meridian is seen to represent a downstream condition after the turning eastward (in the "Northwest Corner") and we therefore focus our observational effort in a region centered about that meridian and reaching from south of the border of eastward flow to north of the strongest eastward flow.

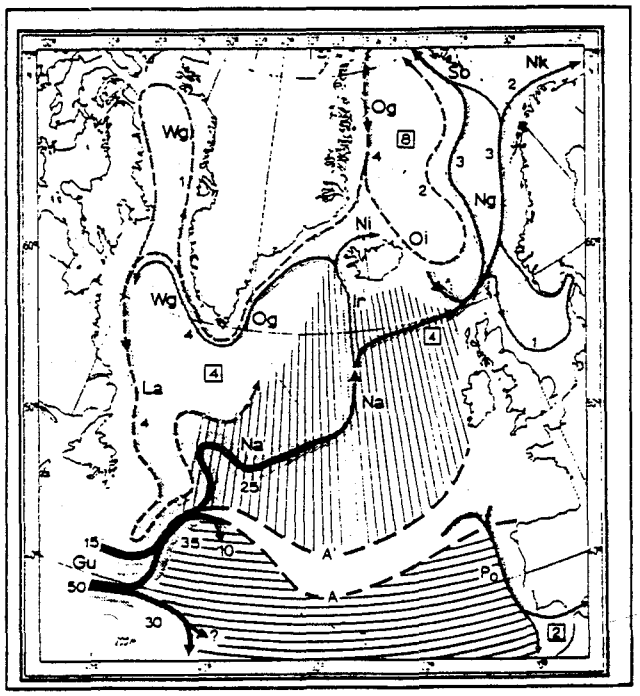

Figure 1. Path of the North Atlantic Current (Krauss)

* Krauss, W., 1986, The North Atlantic Current, J. Geophys. Res., 91, 5061-5074.

In Figure 2 we show the dynamic sea surface height, derived from a collection of hydrographic data compiled by Joe Reid from historical files and note its similarity to Figure 1 where they overlap. The isopleths roughly trace an averaged picture of the NAC through the region where it turns away from the continental slope. The principal core of the current is shaded for future reference.

In the SW corner of the diagram, the Gulf Stream turns around the Grand Banks. The retroflection northeast of the Flemish Cap (47°N-45°W) is the next major feature and then, at 38°W, the axis of the NAC is seen at about 50°W.

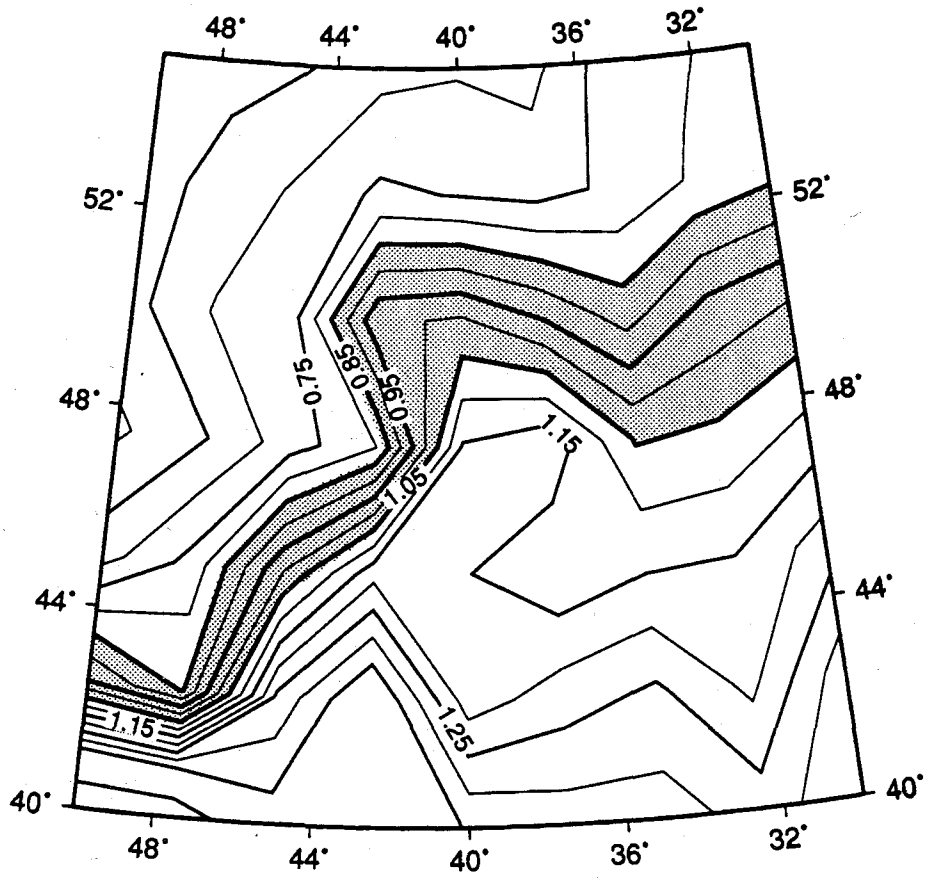

Figure 2. Dynamic Height (0 re 1500 dbars). The data are not uniform in either season or year.

Ten altimeter tracks will provide a spatially dense coverage of the NAC as it passes the Flemish Cap and begins its transit across the Atlantic. These are identified in Figure 3, superimposed on the shaded NAC of Figure 2.

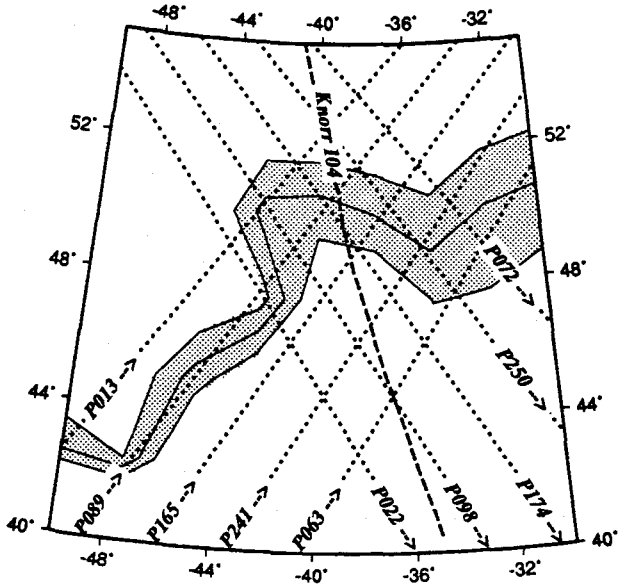

Figure 3. Tracks of T/P Altimeter To Be Analyzed. Also shown is the location of the KNORR hydrographic section to be discussed below.

II. Altimetry

A preliminary analysis of early TOPEX/POSEIDON altimeter data has been performed and Figure 4 reports the mean sea surface height along 4 central tracks from a subsample of the first 200 days (20 cycles) of the mission, Sept. 1992-Feb. 1993. After removal of tides and the geoid model, the two descending paths (even numbered) show a sea surface height change of 80 cm. While this is larger than the non-synoptic topographic map derived from Reid's data collection (Fig. 2), the magnitude and location is consistent with a synoptic section through this area by McCartney in 1983, located in Fig. 3 and shown in Fig. 5.

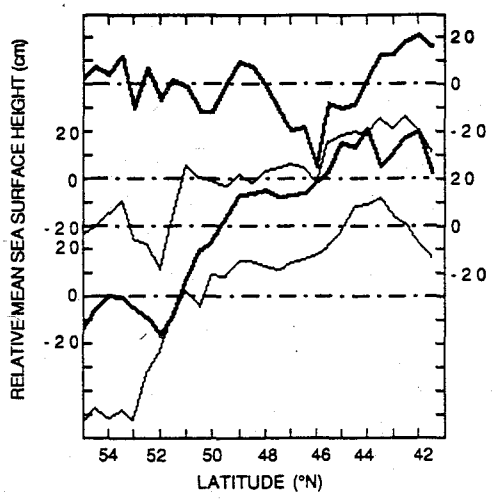

Figure 4. Relative Mean Sea Surface After 200 Days.

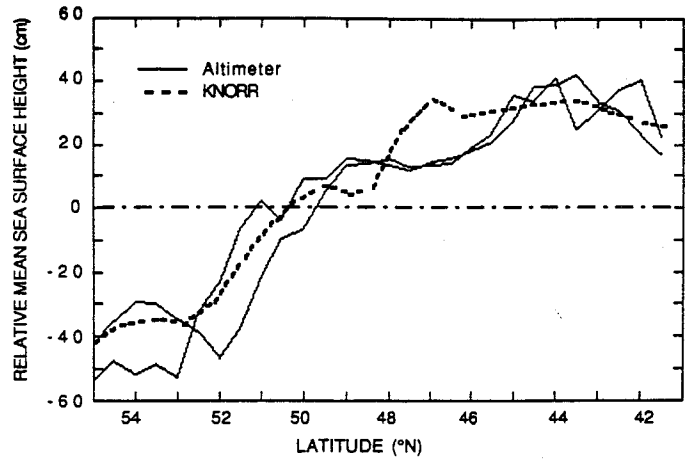

Figure 5. Comparison Between Two Altimeter Mean Sea Surfaces and an Historical Hydrographic Section. Both are smoothed over one deg. bands.

The averaging to arrive at the mean has of course removed much information of interest. The time variability at a given latitude, shown in Figure 6, is presumably caused by a combination of lateral movement of the current and variable transport, and is as large as ±40 cm in the vicinity of the NAC.

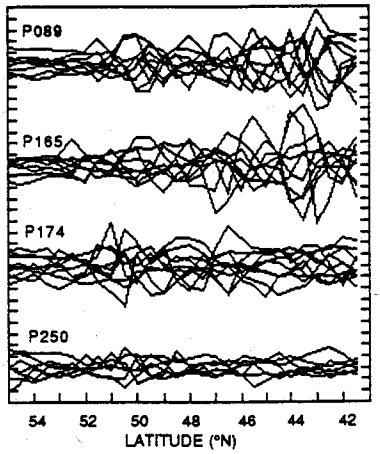

Figure 6. Anomalies of Each Cycle About Its Mean. Ordinate tics are 10 cm.

III. Supporting Role Of The Sounder Array

While the comparison shown in Figure 5 is very encouraging (especially since both the data period is still short and the precision orbits are yet to be provided), further measurements are clearly necessary to validate the result. For example, the persistent spread shown in Figure 6 in even "quiet" regions is likely due to uncertainties in satellite altitude which may only be partially corrected for in a later precision orbit determination. To remove definitively this uncertainty we propose to deploy an array of five inverted echo sounders as shown in Figure 7 to provide a "ground truth". The six interior tracks are each monitored by one or two sounders. (Some duplication is planned, as this will be one of the first attempts at such a comparison and it will be important to demonstrate reproducibility and provide an estimate of uncertainty). The four exterior tracks are indirectly monitored from their three intersections with interior tracks. Furthermore, the

sounder array will independently provide unique coherence frequency spectra at two meridional and latitudinal spatial scales.

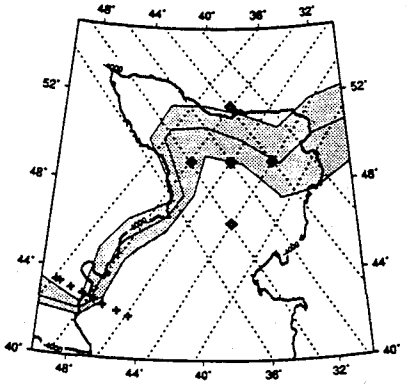

Figure 7. Location of Inverted Echo Sounders (diamonds) re Altimeter Tracks and NAC. + signs locate the Bedford Institution current meter moorings discussed in the text. Also shown is the 4000 meter depth contour.

The two modes of observation provide an interesting comparison. The altimeter measures sea surface height (after determining altimeter height over the geoid and removing tides and atmospheric variables), while the sounder measures the mean water column temperature (to a very good approximation) from an unknown but fixed distance from the geoid (i.e., its position on the ocean bottom). The value of sounder measurements has derived from the high correlation beween mean temperature and dynamic sea surface height (as seen in Figure 8) which results from (a) the strong and well-documented correlation between temperature and salinity in the ocean and (b) the baroclinic adjustment implied in the computation of dynamic sea surface height. Nonetheless, one has to demonstrate empirically, for each proposed area of deployment, that the correlation between acoustic travel time through the water column and the dynamic height is well defined. We do this in the next section, again using the Reid Atlas data, and conclude that the sounder will be able to monitor changes in dynamic height at each site with a standard error of 5.5 cm.

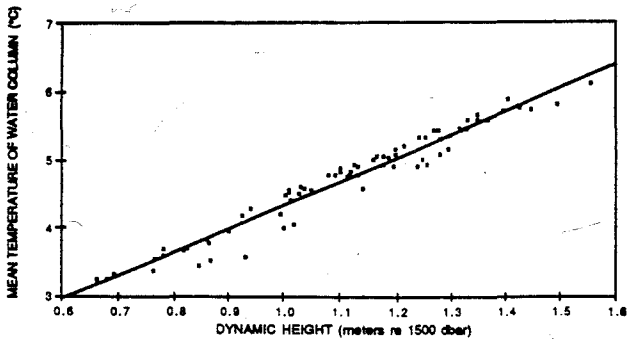

Figure 8. Correlation Between Mean Temperature and Dynamic Height in the Study Area. The computation is made again from the data in the Reid Atlas.

IV. Contemporaneous Upstream Observations

Adding significantly to the interpretation of the observations being proposed are two contemporaneous field programs which will be monitoring the NAC off the Grand Banks. The first of these is a series of eight current meter moorings, with meters throughout the water column, extending from the 1500 meter depth contour into deep water. (Locations are shown in Figure 7). These are to be deployed in August 1993 by the Bedford Institute of Oceanography and recovered in either the fall of 1994 or spring of 1995.

Supplementing this array is a mix of inverted echo sounders and horizontzal electrometers that the University of Rhode Island and Scripps Institution of Oceanography are scheduled to deploy in the same time frame as the moorings. They will both partially overlap and also extend seaward the BIO mooring line.

These observations will strongly complement ours. They will provide a quantitative and synoptic picture of the time variable flow of the NAC into our observation area and afford us the opportunity to investigate how changes upstream are propagated downstream.

Key Transects to Determine the Circulation in the Newfoundland Basin

D. Randolph Watts
University of Rhode Island
Graduate School of Oceanography
Narragansett, RI 02882

Despite extensive study and a superficial impression that the North Atlantic circulation is well understood, fundamental disagreement remains about the currents and their recirculations east of the Grand Banks. This is not surprising as the Newfoundland Basin is a crossroads of currents, surface to bottom, including essential and controlling components of the wind-driven and thermohaline circulation. The underlying reasons that the sources, transports, and structure of the flow are not understood is that the interpretation of historical hydrographic measurements is uncertain regarding an absolute reference velocity. Moreover this region has particularly strong eddy variability, complicating the float trajectories as well as the dynamic topography, even for extensive surveys.

Considerable disagreement and puzzles remain regarding several aspects of the circulation. The patterns of near-surface circulation are conflicting: Krauss shows surface drifters that all cross the Newfoundland Basin eastward, whereas Schmitz and McCartney indicate a southward recirculation gyre from the baroclinic shear and watermass properties. There are additional puzzles regarding the circulation of the intermediate waters. In particular, Labrador Sea Water has been shown to primarily flow into the Eastern North Atlantic, based upon pycnostad properties and its low salinity core. Furthermore, waters of LSW temperatures flowing along the continental slope from 55°W southward to Cape Hatteras carry a relative deficit of Freon compared to both deeper (NADW, with T <3.1°C) and shallower (SAIW, with 4°C<T<7°C) components of the subsurface southward flowing Western Boundary Current. Consequently the vertical structure of waters passing westward south of the Grand Banks is puzzling: from surface-to-bottom, near-surface Labrador Current waters mainly retroflect back northward, SAIW (6-7°C) waters apparently round the Banks readily, LSW does not, and deeper NADW and AABW do.

Figure 1 sketches the circulation in the Newfoundland Basin and indicates some key transects for time-series measurements of the currents. The objectives for these measurements are:

(1) to determine the baroclinic and barotropic transports and variability of the Western Boundary Currents throughout the water column in the Newfoundland Basin, in particular on transects at

(a) 50°W at the tail of the Grand Banks to measure the inflow from the Gulf Stream and the inshore exchanges back to the west;
(b) from the Grand Banks southeastward across the strongest, steadiest part of the North Atlantic Current; and
(c) from Flemish Cap to Milne Seamount, which is a topographic choke point for the deep circulation and which transects the NAC just before it bifurcates; all the warm saline waters that pass beyond this transect are thought to continue to the higher latitude North Atlantic rather than turn back southward.

(2) to determine the watermass characteristics and the properly referenced geostrophic current structure.

(3) to determine closed budgets for volume, heat, salt, and freshwater fluxes being carried to higher latitudes.

Along section B, Bedford Institute of Oceanography and the Univesity of Rhode Island will cooperatively deploy eight moorings with current meters at 7 levels, plus five Inverted Echo Sounders (IES), for 20 months from August 1993 to March 1995. The planned instrument locations are indicated in Figure 2. Hydrographic sections will also be taken by BIO along these three plus other connecting transects along the western boundary of the Newfoundland Basin in four cruises to the region during the same time period.

It is hoped that a planned trans-Atlantic hydrographic transect (by Peter Koltermann in upcoming European-WOCE work), will connect to and follow the mooring line B for its western section.

At the right side of Figure 1 is a sketch of a vertical profile of velocity and how it could be measured by a combination of Inverted Echo Sounders (IES), Horizontal Electrometers (HEM), and bottom current meters and bottom pressure recorders. The IESs are used to determine the dynamic heights at a profile of pressure levels above the main pycnocline, from which horizontal gradients determine the baroclinic velocity profile. The HEMs are used to determine the vertically averaged barotropic velocity. The bottom current meters and bottom pressure sensors are used to determine the bottom currents. Alternating the P/IES and HEM/bottom CM sites along a transect, as sketched at the lower right corner, is a suggested arrangement of instruments along these transects to achieve the above listed objectives.

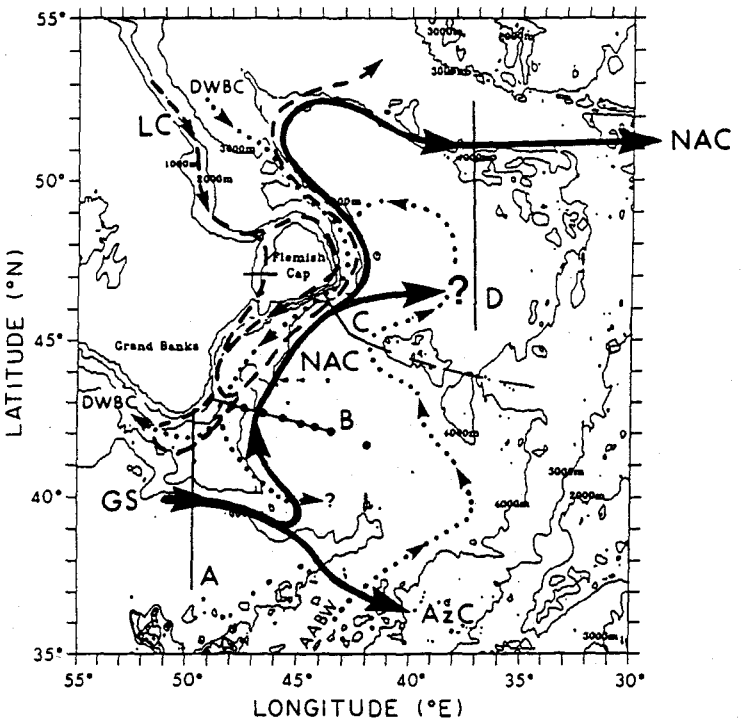
55°
50°
45°
40°
35°
LATITUDE (°N)
55°
50°
45°
40°
35°
30°
LONGITUDE (°E)
DWBC
LC
NAC
Flemish Cap
?
D
C
Grand Banks
NAC
DWBC
B
GS
?
A
AzC
AABW

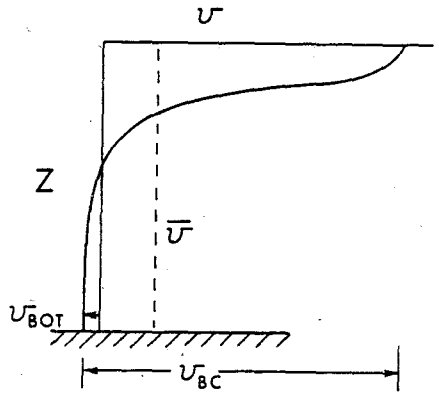
Z
$\bar{v}$
v_{BOT}
v_{BC}

FIGURE 1

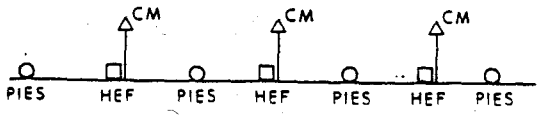
CM
CM
CM
PIES
HEF
PIES
HEF
PIES
HEF
PIES

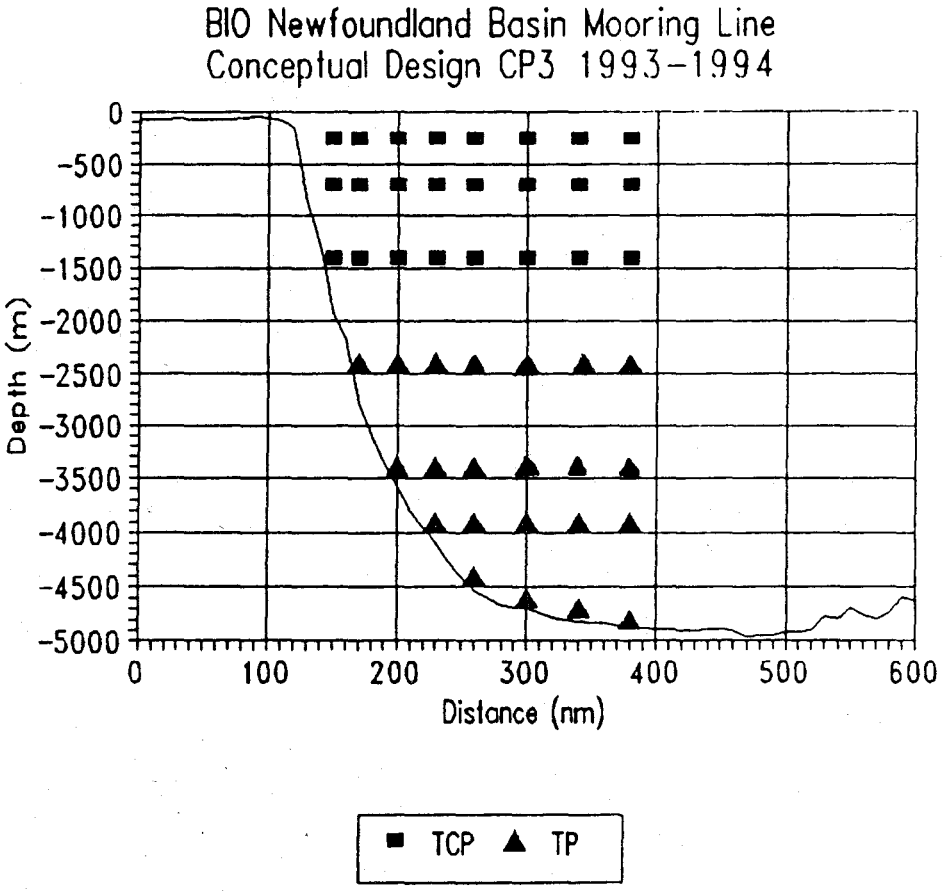
BIO Newfoundland Basin Mooring Line
Conceptual Design CP3 1993-1994
Depth (m)
0
-500
-1000
-1500
-2000
-2500
-3000
-3500
-4000
-4500
-5000
0
100
200
300
400
500
600
Distance (nm)
TCP
TP

FIGURE 2

Measuring NAC Volume and Heat Transports From the Sea Floor

Douglas S. Luther
Department of Oceanography, School of Ocean and Earth Science and Technology
University of Hawaii at Manoa, Honolulu, Hawaii 96822

Alan D. Chave
Department of Geology and Geophysics, Woods Hole Oceanographic Institution
Woods Hole, Massachusetts 02543

Jean H. Filloux
Physical Oceanography Research Division, Scripps Institution of Oceanography
La Jolla, California 92093

The combination of horizontal electrometers (HEMs) and Inverted Echo Sounders (IESs) offers great potential for economically observing the following dynamically and climatologically significant quantities from the seafloor: (1) volume transport per unit width (TUW), (2) the gravest vertical structure of the horizontal currents, and (3) the total unnormalized heat flux.

Evidence continues to accumulate demonstrating the validity of the theoretical relationship between the horizontal electric field and water currents. The horizontal electric field is directly proportional to the TUW plus a small correction due to the vertical variation of electrical conductivity and water currents. The correction term is dominated by the 1st internal mode of water current.

Seafloor to sea surface travel times measured by IESs have been shown to be directly related to the 1st mode of vertical displacement. The mode amplitudes can be used to generate the time variability of the gravest vertical structures of hydrographic quantities such as temperature, salinity, conductivity, etc. Furthermore, the horizontal gradient of the travel times (from an array of IESs for instance) can be related, under the usual oceanographic assumptions of geostrophy and hydrostasy, to 1st mode amplitudes of horizontal currents.

Consequently, IES measurements of 1st mode current and conductivity variations can be used to correct the HEM measurements, yielding TUW. The gravest vertical structure of the horizontal currents is then the sum of TUW (divided by the total water depth) plus the 1st mode amplitude of horizontal current. The total heat flux is obtained from the vertical integral of this gravest vertical structure of the horizontal currents multiplied by the temperature profiles reconstructed from the IES measurements.

If the vertical structure of the horizontal currents contains variations that are not well described by barotropic plus 1st baroclinic mode structures, as is possible in the North Atlantic Current System with its various distinct surface, intermediate and bottom flows, ancillary information must be obtained to resolve the additional current structure. For instance, bottom pressure gauges, that are already integrated into the IESs, can be used to estimate bottom geostrophic velocities, or near-bottom currents could be directly observed with point current meters or ADCPs.

The existence of short-vertical-scale current structure, even if unmeasured, does not invalidate the estimation procedure for transport (TUW) described above, nor the estimation of heat flux if the vertical temperature profile has only a trivial projection onto the baroclinic modes of number 2 or higher. Furthermore, we suggest that the HEM

observations provide a more accurate estimate of transport than is obtainable from some typical moored current meter configurations.

Horizontal Electric Fields

Motional electromagnetic induction is now theoretically well understood in certain idealized settings (e.g., Sanford, 1971; Chave and Luther, 1990). Assuming distant continental boundaries and a flat seafloor with laterally homogeneous conductivity, then for the low-frequency limit where the aspect ratio of ocean currents is small, where the effect of self induction is weak, and where the vertical velocity can be neglected in comparison with the horizontal velocity, it can be shown that the point horizontal electric fields (HEFs) in the northern hemisphere are related to horizontal water velocity (after ignoring some minor noise terms; e.g., Chave and Luther, 1990; Luther and Chave, 1993) by

$$\frac{E^{u}_{-y}(t)}{C|F_z|} = < u(t) > + \frac{1}{H} \int_{-H}^{0} \frac{\hat{\sigma}(z,t)}{< \sigma(t) >} u(z,t) dz, \qquad (1a)$$

$$\frac{E^{v}_{x}(t)}{C|F_z|} = < v(t) > + \frac{1}{H} \int_{-H}^{0} \frac{\hat{\sigma}(z,t)}{< \sigma(t) >} v(z,t) dz, \qquad (1b)$$

where the horizontal water velocity, $\vec{v}_h(z,t) = \{u(z,t), v(z,t)\}$ and seawater electrical conductivity, $\sigma(t)$, have been decomposed into vertical average, $<( )>$, and depth-dependent, (^), parts. The subscript on the electric field, E, denotes the direction in which that term is positive and the superscript indicates the horizontal water velocity component to which it is proportional. F_z is the vertical component of the geomagnetic field; and H is ocean depth. C is a scale factor that depends on $\sigma(z \leq -H)$; C can be estimated by intercomparisons, but extensive geophysical evidence suggests that C= 0.95±0.05 almost everywhere in the deep oceans (e.g., Chave and Luther, 1990).

The first term on the right hand side (RHS) of Eq. (1) is just the vertical average of horizontal water velocity (or, depth-normalized transport per unit width). The second term on the RHS is a small "correction" due to the fact that seawater conductivity is a weak function of depth. The conductivity correction is negligible if conductivity is independent of depth (as it is at very high latitudes) or if the horizontal water velocity has little vertical shear (as frequently occurs at mid- to high-latitudes). To a good approximation, $\sigma(z,t) = 3.0 + 0.09T(z,t)$ Siemens m^{-1}, where T(z,t) is temperature in °C, so that $|\hat{\sigma}(z,t)| << < \sigma(t) >$.

Projection of the current and conductivity profiles onto the vertical modes (e.g., Chave and Luther, 1990) indicates dominance of the 1st baroclinic mode in the conductivity correction of Eq. (1). Therefore, the conductivity correction can be derived from estimates of 1st mode current and conductivity estimates, such as can be obtained with IESs.

In deployments of seafloor HEMs to date, where comparison of HEM versus mooring estimates of the vertically averaged horizontal water velocity have been possible, the HEM estimates have proven to be more accurate. Such accuracy has significant importance to climate studies that rely on estimates of transport for determining the world ocean's role in climate fluctuations. The first HEM vs. mooring comparison was produced by Luther et al. (1991) from data collected during BEMPEX,

an experiment that deployed a large number of HEMs and pressure gauges in the North Pacific to study direct atmospheric forcing of gyre-scale eddies (Luther et al., 1990; Chave et al., 1992). The accuracy of the HEM estimates of $< \bar{v}_h(t) >$ was corroborated by current estimates made by reciprocal tomography, which is based on measuring reciprocal acoustic travel time differences. The inaccuracy of the current meter mooring estimates was attributed primarily to stalling of the current meter rotors in the weak flows below 1000 meters depth. Another electrometer-mooring comparison presented below comes from the opposite extreme for oceanic flows, i.e., from the Gulf Stream which has strong currents at all depths so that rotor stalling is not expected to be a problem.

Using HEM data collected during the last year ('89-'90) of the Synoptic Ocean Prediction (SYNOP) experiment, the LHSs of Eqs. (1a) & (1b) were calculated with C=0.95, as per estimates of C made by Sanford et al. (1985) in the western North Atlantic, and using an appropriate value for F_z for the time and location of the experiment, while the RHSs were estimated from nearby mooring data. The latter estimation included extrapolation of currents, temperature and pressure to a fictitious nominal 100 m depth, conversion of pressure to `depth', and estimation of conductivity using temperatures and a climatological T/S relation in an empirical formula. The currents and conductivities at the four real and one "fictitious" instruments were trapezoidally integrated, taking into account the time dependence of the depths of the instruments. The time series thus obtained, representing opposite sides of Eq. (1), are highly coherent, as shown in Figure 1.

Figure 1. Coherence amplitudes between electrometer and mooring estimates of conductivity-weighted, vertically-averaged water velocity (left and right hand sides of Eq. (1), as described in the text). Top is for zonal currents (Eq. (1a)). The 95% level of no significance is indicated. Every other point plotted is independent due to a 50% overlap of frequency band-averaging.

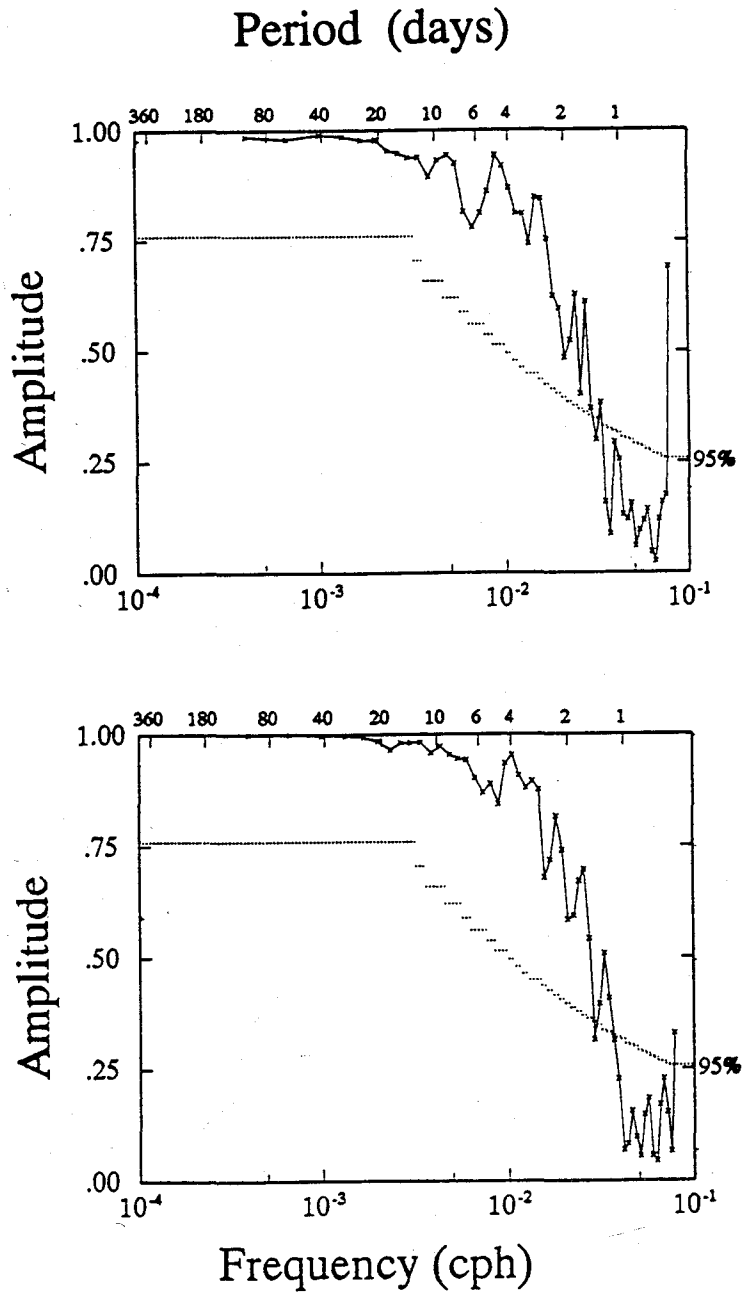

While the coherence in Fig. 1 is very encouraging, and the rms differences between the estimates of the LHS and RHS of Eq. (1) are no larger for instance than what has been considered very good agreement for testing schemes to remove the effects of mooring motion from current meter data (e.g., Hogg, 1991; Cronin, 1991), examination of the individual time series (not shown) indicates that the LHS of Eq. (1) consistently has a greater magnitude than the RHS. That there is a systematic under-estimation of current by the mooring data, or an over-estimation by the HEM data, is most easily seen by casting the data in terms of a Gulf Stream coordinate system, rather than a geographic coordinate system, since the Gulf Stream position and direction vary with time.

Daily locations of the temperature front (the north wall) of the Gulf Stream (provided by R. Watts and W. Johns) were determined from an array of IESs. These locations permitted estimation of the cross-stream positions of the moorings every day. Gulf Stream directions at each mooring were determined from the 400 m-1000 m shear. Daily estimates of Eq. (1) were then rotated into these Gulf Stream coordinates.

To put the problem in a more interesting context, the conductivity correction term on the RHS of Eq. (1) was moved to the LHS. Now we can compare mooring estimates of vertically averaged water velocity, $<\bar{v}_h(t)>$, with HEM estimates of the same quantity (that incorporate a small mooring-derived conductivity correction), all cast in terms of Gulf Stream coordinates. The results for a single mooring are shown in Figure 2, along with the differences (errors) between the two estimates. (Note that the error is not dependent upon which side of Eq. (1) we place the conductivity correction term.) The results in Fig. 2 typify the comparisons made at other HEM locations. Integrating the estimates in Fig. 2 across the stream results in a ~30% higher estimate of total transport from the HEM than from the mooring. This is certainly non-trivial

Figure 2. Two estimates of vertically-averaged water velocity in the Gulf Stream for the same time period at nominally 68°W. The estimates employ electrometer and mooring data (see text), and are plotted versus cross-stream distance. The differences between the estimates are also plotted.

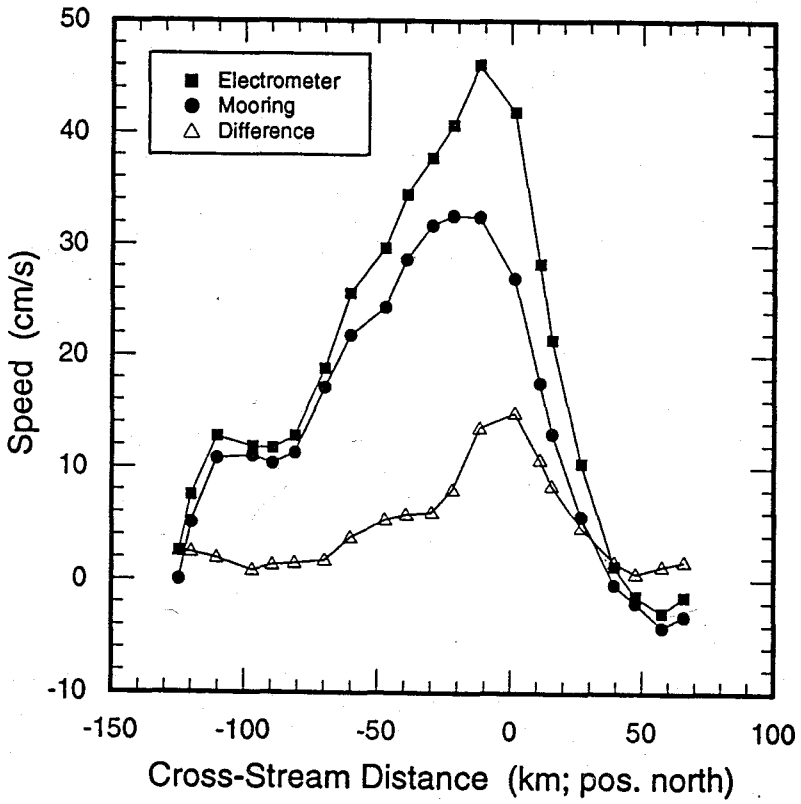

Fig. 2 shows good agreement between the estimates at distances farther "south" than -60 km and farther "north" than 30 km from the north wall of the Gulf Stream. The percentage difference between the estimates is not constant across the stream, implying that the difference is not due to a calibration error of the HEM. While there are several possible noises and small errors in the HEM data, none can result in an overestimate of velocity. We believe the error arises in the current meter data and/or its trapezoidal integration, but to date we have clearly identified only one source of error, which by itself is insufficient to account for all of the error in Fig. 2. CTD data taken at this longitude by M. Hall indicate that the extrapolation of currents to the near-surface underestimates the upper ocean geostrophic velocities (at and north of the maximum current) and the trapezoidal integration, which implies linear interpolation, underestimates the transport between the current meters at 1000 m and 3500 m (again, at and north of the maximum current). Error from the trapezoidal integration is further suggested by the high coherence (not shown) between the error time series and currents measured at 1000 m.

Combining HEM & IES Measurements

We will demonstrate here the great potential of combining HEM measurements of horizontal electric fields (HEFs) with IES measurements of vertical acoustic travel times (VATTs) to provide estimates of (1) volume transport per unit width, (2) the gravest vertical structure (i.e., barotropic and 1st baroclinic modes) of the horizontal currents, and (3) the total unnormalized heat flux (using the gravest vertical structures of the currents and temperature).

The VATT measured by an IES is

$$\tau = 2 \int_{-H}^{0} \frac{dz}{c}, \tag{2}$$

where c=c(z,t) is the speed of sound. Potential small errors in the interpretation of VATT in terms of the simple relation in Eq. (2) have been enumerated by Watts and Rossby.

Following Pickart and Watts (1990), an empirical relationship between τ and the amplitude of the 1st baroclinic mode of displacement, q_1, can be obtained by idealizing variations in the state variables T and S as perturbations on a base profile which varies only with z (pressure is not perturbed since it is essentially the integration variable), so that sound velocity can be written

$$c(z,t) = c[\overline{T}(z+\zeta(z,t)), \overline{S}(z+\zeta(z,t)), P(z)], \tag{3}$$

where $|\zeta|<<|z|$ by assumption. We now expand ζ in terms of displacement modes (e.g., Gill and Clarke, 1974), such that

$$\zeta(z,t) = \sum_{i=1}^{\infty} q_i(t)\theta_i(z), \tag{4}$$

where the amplitudes q_i are non-dimensional and the displacement structure functions θ_i have dimensions of length. Eq. (4) is truncated after mode 1 and substituted into the perturbation forms of T and S in Eq. (3), to produce the desired relation between τ and q_i.

After the basic state profiles are chosen, numerical evaluation of c based on its empirical dependence on T, S and P, using different values for q_i, leads to a functional relationship between τ and q_i (Pickart and Watts, 1990) which can be inverted to yield the amplitude of the 1st baroclinic displacement mode for any measured VATT. In practice, since the depth is never known precisely enough, in situ profiles of T and S must be taken (by CTD or XBT) while the IES is deployed in order to calibrate the VATT. Pickart and Watts (1990) have shown evidence that the relationship between τ and q_1 is not sensitive to the choice of basic state profile of S, but they do note that the choice of basic state T profile is important, and a climatological mean T profile is inadequate in frontal regions such as the Gulf Stream and North Atlantic Current..

The strong (weak) dependence of VATT on the 1st (other) baroclinic mode for mid-latitude hydrographic profiles has been documented by Watts and Rossby (1977) and Pickart and Watts (1990). (Also, Hall, 1986, and Pickart and Watts, 1990, have shown with current meter data that the 1st baroclinic mode dominates the vertical velocity, hence also the vertical displacement, in the Gulf Stream.) In the tropics, however, 2nd baroclinic mode variability makes a non-trivial contribution to the VATT and cannot be ignored (Garzoli and Katz, 1981). In what follows, we assume the application is at mid- to high-latitudes where isopycnal displacements can be described as dominated by 1st baroclinic mode variations.

Departing from previous authors, we develop an expression for the amplitude of the 1st baroclinic mode of current as follows. Under the hydrostatic and geostrophic approximations, and assuming perturbations of density can be described as perturbations on a base profile like T and S above, then

$$\frac{\partial \vec{v}_h}{\partial z} \approx \frac{g}{f\rho_*}\frac{d\bar{\rho}}{dz} k \times \nabla_h \zeta, \tag{5}$$

where $\rho = \rho_* + \bar{\rho}(z+\zeta(z,t))$, and k is the local upward unit vector. Substituting the modal expansion for ζ (Eq. (4)), and a corresponding modal expansion for $\vec{v}_h = \sum_{i=0}^{\infty} \vec{a}_{h,i}\phi_i(z)$ into Eq. (5), applying the relationship between displacement and horizontal current structure functions, $\frac{d\phi_i}{dz} = -\frac{N^2}{\gamma_i^2}\theta_i$ and truncating after mode 1 yields an expression for the amplitudes of the 1st baroclinic current modes, viz.

$$\vec{a}_{h,1} = \frac{\gamma_1^2}{f} k \times \nabla_h q_1, \tag{6}$$

where γ_1^2 is the 1st baroclinic mode eigenvalue. Note that none of the physical assumptions leading to Eq. (6), except the space modal truncation, is more severe than is typically used to estimate relative or absolute (β spiral) currents from hydrographic data, or to estimate cross-Gulf Stream profiles of current (and transport, after upward extrapolations) from single moorings (e.g., Hogg, 1992).

Analysis of the combined HEF and VATT datasets from the SYNOP experiment is in its early stages, but we can show a simple preliminary comparison of two derivations

of one horizontal component of $\bar{a}_{h,1}$ in Figure 3a. Rather than using Eq. (6) to estimate 1st mode displacement, we assumed for simplicity that the difference of the measured VATTs from two IESs is proportional to the 1st mode current amplitude, then estimated the constant of proportionality by least squares. The result is the dotted curve in Fig. 3a. The solid curve in Fig. 3a is an average of the 1st mode current amplitudes from three moorings, two at the endpoints and one close to the center of (but off of) the line running between the two IESs. The agreement between the curves is certainly encouraging.

Volume Transport Per Unit Width

Expanding the conductivity perturbations in Eq. (1) in terms of horizontal current modes, $\frac{\hat{\sigma}(z,t)}{<\sigma(t)>} = \sum_{i=1}^{\infty} s_i(t)\phi_i(z)$, and incorporating the horizontal current mode expansions (all expansions being truncated after mode 1) yields

$$\frac{E^u_{-y}(t)}{C|F_z|} \approx a_{x,0} + s_1 a_{x,1}, \tag{7a}$$

$$\frac{E^v_y(t)}{C|F_z|} \approx a_{y,0} + s_1 a_{y,1}, \tag{7b}$$

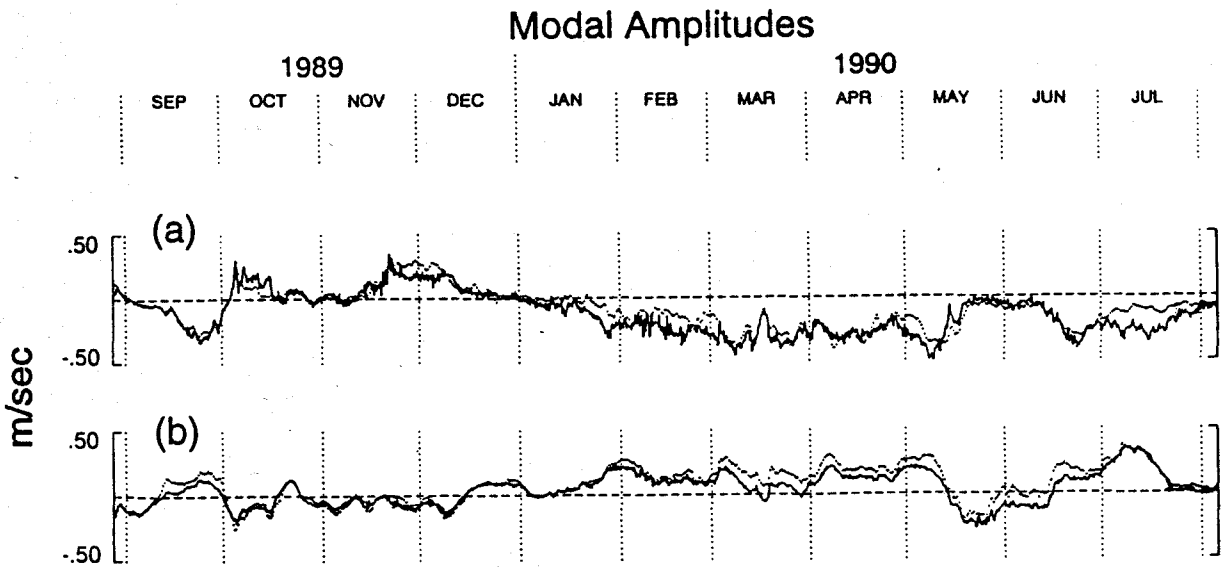

Figure 3. (a) IES (dotted curve) and mooring estimates (see text) of one component of the vector amplitude of the 1st baroclinic mode of horizontal current, $\bar{a}_{h,1}$. (b) HEM/IES (dotted curve) and mooring estimates (see text) of one component of the vector amplitude of the barotropic mode of horizontal current, $\bar{a}_{h,0}$. Data for both plots were collected during the SYNOP experiment in the Gulf Stream at nominally 68°W. Ordinate units are m/sec.

Our estimate of volume transport per unit width is simply $\bar{a}_{h,0}$ from Eq. (7) times the depth H. To solve Eq. (7) we need estimates of s_1 and $\bar{a}_{h,1}$. The latter are obtained from the IESs by Eq. (6). The former are obtained by reconstructing a time-dependent conductivity profile (using IES-derived estimates of q_1 in $\sigma(z,t) = \overline{\sigma}(z + q_1(t)\theta_1(z))$,, which is then decomposed in terms of horizontal current modes, as above.

In the same vein as Fig. 3a, a rough estimate of that component of $\bar{a}_{h,0}$ parallel to $\bar{a}_{h,1}$ shown in Fig. 3a, is presented as the dotted curve in Fig. 3b. The IES-derived estimate of $\bar{a}_{h,1}$ in Fig. 3a was used in Eq. (7) with a climatological mean s_1. An average of the data from two HEMs (deployed near the IESs) was used in Eq. (7) as well. The only calibration employed was that for the 1st mode amplitude described above. The solid curve in Fig. 3b is an average of barotropic mode current amplitudes from the same three moorings used in Fig. 3a.

[Note that the comparison in Fig. 3b is not directly relatable to the HEM-mooring comparison of transport estimates discussed previously, and evidenced by Figs. 1 and 2, because Fig. 3b only shows one of the two horizontal components of $\bar{a}_{h,0}$, and Fig. 3b is necessarily derived from data spanning about 50 km, whereas the data for the prior comparison were all obtained at a single geographic location.]

Current Profiles and Heat Flux

The large vertical scale currents, $\bar{v}_h(z,t)$, are reconstructed by adding $\bar{a}_{h,0}$ and $\bar{a}_{h,1}\phi_1(z)$. The heat flux is readily obtained from this reconstructed current profile and a reconstructed potential temperature profile, $T_p(z,t) = \overline{T}_p(z + q_1(t)\theta_1(z))$.

Summary of Some Oceanic Variables Derivable from HEFs and VATTs

An ideal array would result in at least 3 IESs situated around each HEM. (Note that this does not mean that 3 times as many IESs are deployed as HEMs.) After choosing appropriate basic state temperature, $\overline{T}(z)$, and salinity, $\overline{S}(z)$, profiles, preferably from coincident CTD profiles rather than climatological mean profiles, the following are estimated:

$q_1(t)$, for each IES (see Eq. (3) and subsequent discussion);

$$\tilde{q}_1(t) = \frac{1}{m}\sum_{j=1}^{m} q_1^j(t) \text{ for the m IESs;}$$

$\overline{T}_p(z)$, the basic state potential temperature profile, from the equation of state;

$T_p(z,t) = \overline{T}_p(z + \tilde{q}_1(t)\theta_1(z))$;

$\overline{\sigma}(z)$, the basic state conductivity profile, from the equation of state; and

$\sigma(z,t) = \overline{\sigma}(z + \tilde{q}_1(t)\theta_1(z))$.

Then the amplitudes of the 1st baroclinic modes of horizontal current are estimated from Eq. (6). The barotropic modal amplitudes follow from Eq. (7), viz.

$$a_{x,0} = \frac{E^{u}_{-y}(t)}{C|F_z|} - s_1 a_{x,1},$$

$$a_{y,0} = \frac{E^{v}_{x}(t)}{C|F_z|} - s_1 a_{y,1},$$

where s_1 is obtained from $\sigma(z,t)$ above.

Finally, we arrive at estimates of the following oceanic quantities:

- Volume Transport Per Unit Width = $H\vec{a}_{h,0}$;;
- Horizontal Current Profiles, $\vec{v}_h(z,t) = \vec{a}_{h,0} + \vec{a}_{h,1}\phi_1(z)$;
- Un-normalized Heat Transport Per Unit Width = $\int_{-H}^{0} \rho_* C_p \vec{v}_h(z,t)\overline{T}_p(z,t)dz$, where C_p is the specific heat of seawater at constant pressure.

References

Chave, A.D., and D.S. Luther, 1990: Low-frequency, motionally induced electromagnetic fields in the ocean, 1, theory. J. Geophys. Res., 95, 7185-7200.

Chave, A.D., D.S. Luther, and J.H. Filloux, 1992: The Barotropic Electromagnetic and Pressure Experiment, 1. Atmospherically-forced barotropic currents, J. Geophys. Res., 97, 9565-9593.

Cronin, M., 1991: How good is the mooring motion correction? Tests using the Central Array current meter data. SYNOPtician, 2, 5-6 & 20-23.

Garzoli, S., and E.J. Katz, 1981: Observations of inertia-gravity waves in the Atlantic from inverted echo sounders during FGGE. J. Phys. Oceanogr., 11, 1463-1473.

Gill, A.E., and A.J. Clarke, 1974: Wind-induced upwelling, coastal currents and sea-level changes. Deep-Sea Res., 21, 325-345.

Hall, M.M., 1986: Horizontal and vertical structure of the Gulf Stream velocity field at 68°W. J. Phys. Oceanogr., 16, 1814-1828.

Hogg, N.G., 1991: Mooring motion revisited. J. Atmos. Ocean. Technol., 8, 289-295.

Hogg, N.G., 1992: On the transport of the Gulf Stream between Cape Hatteras and the Grand Banks. Deep-Sea Res., 39, 1231-1246.

Luther, D.S., Chave, A.D., J.H. Filloux, and P.F. Spain, 1990: Evidence for local and nonlocal barotropic responses to atmospheric forcing during BEMPEX. Geophys. Res. Lett., 17, 949-952.

Luther, D.S., J.H. Filloux, and A.D. Chave, 1991: Low-frequency, motionally induced electromagnetic fields in the ocean, 2, Electric field and Eulerian current comparison from BEMPEX. J. Geophys. Res., 96, 12797-12814.

Luther, D.S., and A.D. Chave, 1993: Observing "integrating" variables in the ocean. Proc. 7th 'Aha Huliko'a Hawaiian Winter Workshop, Univ. Hawaii, 12-15 January, 1993.

Pickart, R.S. and D.R. Watts, 1990: Using the Inverted Echo Sounder to measure vertical profiles of Gulf Stream temperature and geostrophic velocity. J. Atmos. Oc. Tech., 7, 146-156.

Sanford, T.B., 1971: Motionally-induced electric and magnetic fields in the sea. J. Geophys. Res., 76, 3476-3492.

Sanford, T.B., R.G. Drever, and J.H. Dunlap, 1985: An acoustic Doppler and electromagnetic velocity profiler. J. Atmos. Ocean. Technol., 2, 110-124

Watts, D.R. and H.T. Rossby, 1977: Measuring dynamic heights with inverted echo sounders: Results from MODE. J. Phys. Oceanogr., 7, 345-358.

Subtropical/Subpolar Gyre Property Exchanges in the North Atlantic Current: A Lagrangian Observational and Numerical Analysis/Modelling Experiment

Thomas Rossby and Lew Rothstein
University of Rhode Island
Graduate School of Oceanography
Narragansett, RI 02882

The region east of the Grand Banks and Newfoundland is a broad meridional swath where warm waters from the Gulf Stream make their way east, in part as zonal currents, the Azores Current and the Polar Front, and in part as a broad eastward drift across the Newfoundland Basin. The cold Labrador Current (LC) flows south towards the Tail of the Grand Banks, but much of its transport is returned to the north just inshore of the North Atlantic Current (NAC). The hydrographic and potential vorticity contrast across the LC/NAC front is enormous south of Flemish Cap and weakens following the current downstream, but it is still quite discernible even where the Polar Front crosses the Mid-Atlantic Ridge. On the one hand the front imposes a significant constraint to intergyre exchange, on the other hand it is evident from water mass analysis that some degree of stirring and mixing is taking place. The focus of this research program is to investigate the issues of transport, cross-frontal exchange and eddy processes throughout the region.

The observational component of this program starts in July 1993. It is a Lagrangian study of fluid motion on two density surfaces, σ_t 27.2 and 27.5, the deeper one because it is about the shallowest density surface that does not feel seasonal change throughout the region between the Azores Current in the south and the Polar Front in the north. The shallower surface is subject to seasonal change, but does not outcrop south of the Polar Front in the Western North Atlantic. The floats are designed to measure stratification as a first difference in pressure of two density surfaces. The objective is to examine potential vorticity (PV) changes as the (isopycnal) floats move through the eddy field and across the NAC/Polar Front where the contrast in stratification is enormous. It will be assumed that PV is conserved, at least for short periods of time. By measuring layer thickness directly and computing the product of trajectory curvature and float speed as a proxy for curvature vorticity, the shear vorticity and its change with time can be estimated as a residual. The floats will be deployed in July and November 1993. They will be concentrated in and near the North Atlantic and Labrador Currents, mostly south of Flemish Cap. The floats are designed for missions up to one year in duration. As part of the field program, hydrographic stations (with Pogo measurements of transport) and ADCP measurements of upper ocean current variability will be taken.

Numerical modelling studies of this energetic region are very difficult due to the many different competing physical processes: wind forcing, seasonally varying mixed layers and convective overturning to varying depths, very strong topographic control; further, both the upper and lower limbs of the global thermohaline cell flow right through the region, and are plausibly the reason for warm western boundary currents at such a high latitude in the first place. It is important to begin by viewing how existing models are predicting the current structure in this region, and to question why these models may fail in some areas. From this point of view, output from the 1/3 and 1/6 degree resolution CME level model is being analyzed. However, several issues of interest in this region can be investigated using simple process oriented studies. An examination of cross-gyre exchange is planned using the Miami isopycnal model. The exchange of fluid between gyres will be considered using Lagrangian particles and the enhancement of mixing due to seasonal changes in forcing will be examined. An important feature of the Miami

isopycnal model is the inclusion of an active mixed layer, albeit a bulk mixed layer. The importance of deep mixed layers in the facilitation of cross-frontal and inter-gyre communication will be addressed and during this exchange pathways of subduction along the gyre front will be determined. The sources of potential vorticity and the distribution of passive tracers in terms of the surface fluxes will be investigated. A study of frontal mixing between the Labrador current and the NAC will be performed to examine the effect that changes in water mass characteristics by mixing might have on the energetics of the system. The actual float trajectories obtained from the observational portion of this experiment will prove invaluable.

Observations of the Structure and Dynamics of Flow Around the Grand Banks

Thomas B. Sanford
Applied Physics Laboratory
and School of Oceanography
University of Washington
1013 NE 40th Street
Seattle, WA 98105

Introduction

A comprehensive study is being planned of the multiple currents in the vicinity of the Grand Banks. This region is important for a number of reasons: large meridional heat flux, strong air/sea interaction, deep undercurrents, topographic interactions, vertical and lateral mixing, etc. Of particular interest, is the response of the Gulf Stream (GS) as it passes by the southern tip of the Grand Banks. The traditional view is that the Stream splits into several distinct fronts or currents (e.g., Azores and North Atlantic Currents). An international group of investigators are planning to conduct field, numerical and remote sensing studies of the Gulf Stream/North Atlantic Current system. Our contribution would be to conduct a vessel survey of the Gulf Stream as it evolves using towed, dropped and floating instruments.

Program Description

The scientific challenge and opportunity is to observe the complex dynamics and responses of the Gulf Stream as it encounters and navigates around the southern and eastern flanks of the Grand Banks where the current undergoes strong shifts in direction and bifurcations. These phenomena present opportunities to investigate the dominant physics at work. For example, pertinent questions are what causes the Stream to split into the North Atlantic and Azores Currents at the tail of the Grand Banks and what causes the NAC to turn northward at this point or turn eastward further north? The consequences of the GS/NAC behavior are significant dynamically and climatically.

Many oceanographers have exhibited their interest and intentions in the Gulf Stream/North Atlantic Current. Likely components include tomographic arrays, inverted echo sounders combined with horizontal E-field instruments, float deployments, current meter arrays, synoptic field studies and others. It should be emphasized that significant projects are already underway, such as the RAFOS float deployments of Tom Rossby and the current meter and hydrographic work of Clarke, Hendry and Lazier (BIO).

This project intends to conduct a comprehensive, synoptic study of the currents and water masses in the area. It is likely that our program could be combined with others needing to survey the currents, such as hydrographic and tracer projects. Our approach is to conduct observations of barotropic flow from a ship underway, to deploy a few Lagrangian (RAFOS) drifters and conduct velocity and water property profiling. We intend to track the transport function (i.e., barotropic velocity) as the Gulf Stream approaches the Grand Banks. Mapping the kinematics and dynamics of the region of NAC/Azores current bifurcation is one goal. Another is to explore the dynamics of NAC as it turns cyclonically toward the north. Finally, it turns sharply anticyclonically in the vicinity of the Flemish Cap and flows to east or northeast. These changes are accompanied by major water mass and potential vorticity changes. In addition there is much eddy variability.

In the face of this variability, we propose to focus on the transport function and expect that this function will be more easily mapped than more surface-intensified structures, such as baroclinic eddies. Fortunately, technological advances have made it easier to make these observations of current and water properties in the area. In particular, we intend to focus on the barotropic or depth-averaged pattern of flow using freely drifting and towed instruments. We plan to deploy EM RAFOS floats (a.k.a. EFF, funded by NSF) in the Gulf Stream as it approaches the tail of the Grand Banks. The EFFs (Fig. 1A) will follow the water at its deployment depth but also will provide determination of barotropic velocity, a quantity much more pertinent to the kinematics of the Stream. The Towed Transport Meter (TTM) will be towed from the ship on multiple transects of the GS/NAC to map the kinetic structures. TTM (Fig. 1B) should be able to sort out the matter of narrow versus diffuse currents east of the tail of the Grand Banks based on actual transport. Finally, the Absolute Velocity Profiler (AVP), now fitted out with WOCE quality CTD sensors, will be used to obtain direct measurements of velocity and density. The AVP (Fig. 1C) would provide transport measurements for correlation with the TTM observation and will determine bottom velocities in relation to the bottom topography. A conventional CTD will be used to obtain additional density profiles.

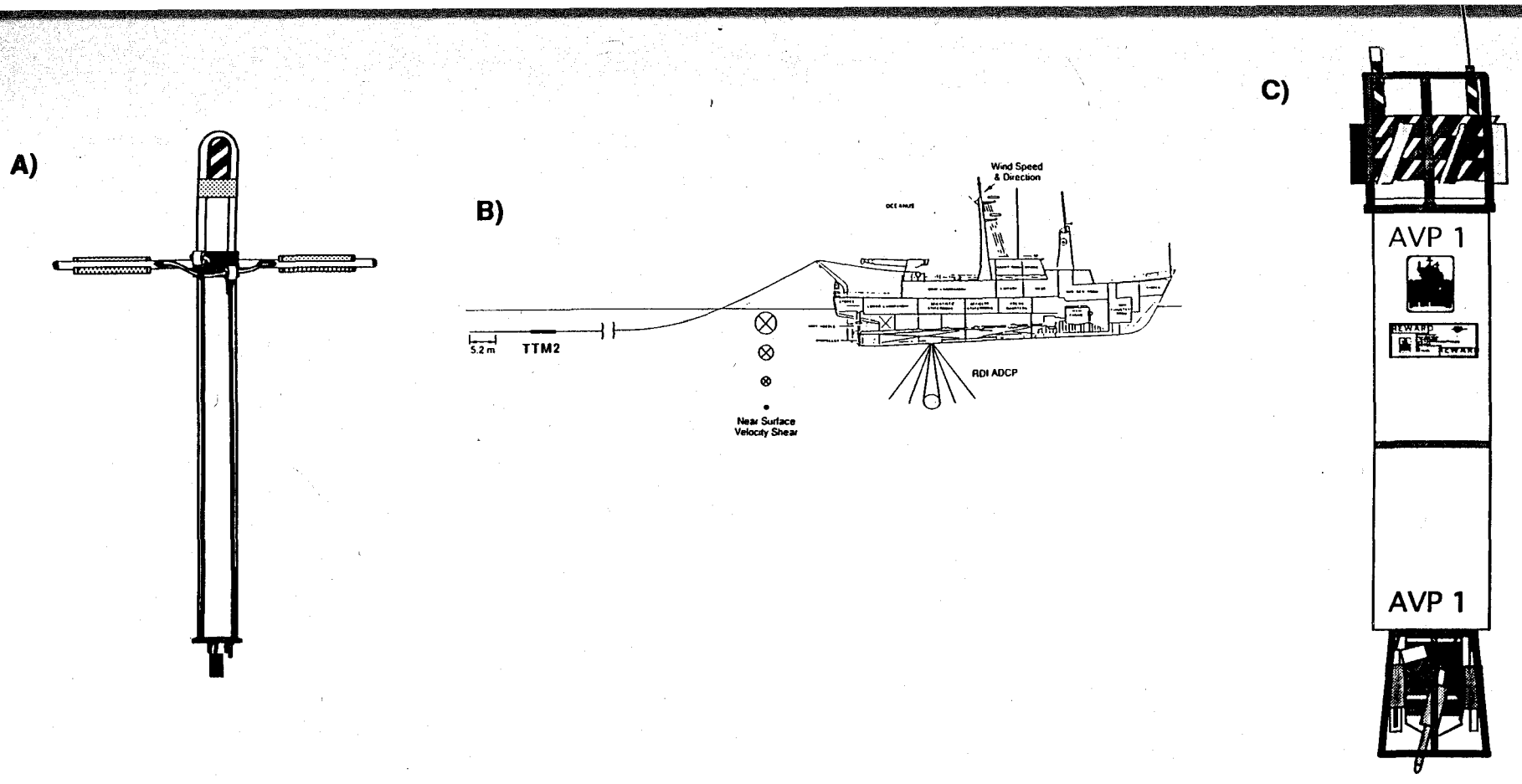

Fig.1 A) The Electric Field Float (EFF) is shown with collar, arms and vanes. The electric fields are observed as voltages between the ends of opposing arms. The whole assembly rotates as water flows vertically past the vanes. The electric field yields $\mathbf{v}-\bar{\mathbf{v}}^*$, and the RAFOS tracking provides $\mathbf{v}$. The combination yields $\bar{\mathbf{v}}^*$, a quantity that is very nearly the depth-averaged or barotropic velocity. B) The Towed Transport Meter (TTM2) in towing configuration. The TTM2 also observes $\mathbf{v}-\bar{\mathbf{v}}^*$. The vessel set and drift determines $\mathbf{v}$ (the surface velocity), and the combination yields $\bar{\mathbf{v}}^*$ from a ship under way. C) The Absolute Velocity Profiler (AVP). The lower end of the instrument houses the SBE CTD functions (pumped and ducted T/C pair and O_2), two dissipation sensors, an optical backscatter device, the acoustic Doppler transceiver array and the 10 kHz tracking pinger. The dark band part way up the skin houses a two-axis electric field array which provides the information for constructing a relative velocity profile throughout the water column. The acoustic Doppler information provides the offset needed to convert the relative velocity profile into an absolute one. The blades at the upper end of the instrument cause the AVP to rotate at a period of about 10 seconds while falling or rising at 1 m s^{-1}. The upper end also contains the mechanism for releasing the beach ball used to keep AVP on the surface while the ship moves away. Other elements there are the VHF radio transmitter and Xenon flasher used for instrument location on the sea surface.

VI. KEY LECTURES

The North Atlantic Current: At the Crossroads of the Wind-driven and Thermohaline Circulations

Thomas Rossby
University of Rhode Island
Graduate School of Oceanography
Narrangsett, RI 02882

Introduction

The North Atlantic Current (NAC) is the name given to the northern branch of the Gulf Stream after it bifurcates near the Tail of the Grand Banks (TGB). The current flows northeast along the continental rise, past Flemish Cap and to the northwest to about 52°N where it retroflects and turns east towards the Charlie Gibbs Fracture Zone on the Mid-Atlantic Ridge (MAR). This eastward flowing front is also known as the Polar Front. Inshore of the NAC along the continental shelf edge, the Labrador Current (LC) flows south towards the Tail of the Grand Banks where it splits, with some waters continuing to the west and the remaining if not most waters turning northeast and following along just inshore of the NAC. This simple description, however, glosses over what appears to be an extraordinary system of currents and eddy variability about which not very much is understood.

One might even say that the current must take a tremendous 'beating'. It is subject to enormous heat and water vapor losses to the atmosphere while the remaining reservoir of heat in the current is much less than in the Gulf Stream farther south. Thus, the heat losses may have a proportionally larger impact on the current and circulation in the region than in the Western Sargasso Sea. Further, the close proximity of the NAC to the cold waters of the subpolar gyres exposes the current to heat losses through intergyre exchange. The wind stress curl changes sign between summer and winter making the region part of the subtropical and subpolar gyres at different times of the year. We know very little about the stability of the current: Can it, or should it be viewed as a simply connected flow subject to instability, or should it be viewed as a 'turbulent jet'? Our knowledge of the eddy field is fragmentary, but it is clear that there is considerable variability, spatially, temporally as well as structurally. Substantial changes on interannual timescales have been documented in several recent studies. In the following sections I try to highlight and discuss some of these issues.

Why does the Gulf Stream turn the corner at the Tail of the Grand Banks?

The assumption is that the northward flow of the NAC is intimately connected to the thermohaline circulation. A decreasing yet important fraction of the transport makes its way into the Eastern North Atlantic and into the Norwegian Sea. We know that deep and bottom waters are regularly produced there although there is evidence for recent slowdown in the amount of deep water produced in the Greenland Sea (Schlosser et al., 1991). The extreme case would be when no new deep waters are produced, and consequently the thermohaline mode is turned off. This would almost certainly have an enormous impact on the upper ocean circulation: According to a reconstruction of sea surface temperatures during the last glacial maximum (CLIMAP), the North Atlantic looked rather 'Pacific' with a comparatively zonal flow from west to east between 35 and 45°N, Fig. 1. Studies of paleoclimatic change indicate that this switch can take place on

<100 year timescales (e.g. Keigwin and Boyle, 1992). It would be interesting to know to what extent this timescale is determined by data resolution. I make this point for we are moderately certain that there have been quite large and rapid changes in baroclinic transport in Gulf Stream in recent years (Greatbatch et al., 1991; Sato and Rossby, 1993).

The Gulf Stream is much different at 50°W than at Cape Hatteras where it first separates from the coast. Its waters have lost much heat to the atmosphere; it is less baroclinic and more barotropic. The transports may be comparable (65 Sv at Cape Hatteras, Richardson and Knauss, 1971; 65 Sv at 50°W, Krauss, 1986), but down from a maximum of 150 Sv near the New England Seamounts (Hogg, 1992). When the current passes the Tail of the Grand Banks, two factors may come into play in governing its subsequent course. First, the Gulf Stream has the very cold waters of the LC on its left side. The decrease in dynamic height can support an increase in surface transport (which seems to manifest itself as the 'retroflected' Labrador Current). It is also tempting to speculate that a decrease in sea level is responsible for inducing the north- or leftward turn of the current. Second, the increasingly barotropic character of the Gulf Stream may make it more sensitive to topographic control. The southeast extending Newfoundland Ridge is a major topographic feature of the region. What happens as the Gulf Stream approaches and flows over it? Could this impose a cyclonic curvature to the path of the current?

The NAC extends much farther poleward than any other WBC

In part this is no doubt due to the 'demands' of the thermohaline circulation. But the latitude at which the current separates is also due to the windstress patterns over the northern North Atlantic. But these, in turn, must be influenced by the presence of the warm waters, so this may be a region where the atmospheric and oceanic circulation patterns are particularly closely coupled. The seasonal change in the wind stress is enormous, from < 10 Nm^{-2} to 30 Nm^{-2}. But perhaps more important, the zero wind stress curl line migrates from 50°N in September to about 36°N in March (Isemer and Hasse, 1987), Fig. 2. Thus, the wind stress curl switches sign over a wide range of latitudes such that the Newfoundland Basin (and more) is forced both anticyclonically and cyclonically. This north-south shift is much larger on the western side of the ocean than farther east where the zero-windstress curl line is located near Ireland most of the year. It is not difficult to imagine that a modest change in the prevailing westerlies could have a profound impact on the forcing of this region and hence the circulation and poleward transport of heat . The heat losses to the atmosphere are enormous during the winter months, Fig. 3. While they are not quite as large as farther west east of Cape Hatteras it must be remembered that the reservoir of heat in the upper ocean is also much less: the thermocline shoals substantially towards the north, and the upper ocean temperatures are lower. The depth of the mixed layer depends on the balance between heat losses to the atmosphere and the advective maintenance of upper ocean heat storage both of which may undergo significant interannual change. The water vapor fluxes associated with the high heat losses may be important to the upper ocean salt balance. In short, to what extent might surface fluxes in this region precondition or control deep convection elsewhere?

Unlike other WBC's the NAC transport decreases downstream

We normally think of boundary currents as the result of imposed external conditions, such as inflow, leading to increased transport in the boundary current. The boundary layer breaks up when it goes unstable, or separates from the boundary, which

seems to be the case with all WBC's. At first glance the NAC seems distinctly different from the typical boundary current in that its transport decreases downstream, 35 Sv where it starts at the Tail of Grand Banks and 25 Sv in the Polar Front (Krauss, 1986). But the 10 Sv decrease may not be gradual, but concentrated at a point near 47°N where a second zonal flow emanates from the NAC. For future reference, we call it the 47°N jet. It is very likely that this jet is forced by the special topography of the Flemish Cap. Clearly the NAC does not want to separate for it continues farther north until it retroflects at a nearly permanent site at 52°N. Indeed, to maintain a stable western boundary current (if that is what we have), it may be necessary for a certain amount of return- and inflow to be present elsewhere along the current.

Stability and continuity of the NAC and LC

A striking characteristic of the Gulf Stream is its structural stability, by which we mean that regardless of how it is meandering, the downstream velocity can be pretty well anticipated. Further, except at times when meanders are actually pinching off or rings are being reabsorbed, the current can be viewed as a simpled connected flow extending for several thousand kilometers, from the Yucatan Straits to the New England Seamounts and beyond. Can this picture or description of a reasonably laminar flow be extended to include the NAC and Polar Front as well? The hydrographic sections I have seen would seem to suggest so. Satellite imagery, on the other hand, are more suggestive of a turbulent jet, but the thermal contrast is often poor making them difficult to interpret. Cyclonic eddies are formed along the NAC, so clearly it is unstable at times. But are anticyclonic (WCR) eddies formed on the LC side? Anticyclonic eddies are also observed in the Newfoundland Basin (see below). Fig. 4 shows the location of a hydrographic section across the LC and NAC just south of Flemish Cap. The panels in Fig. 5 show temperature and density as a function of pressure (top panels) and temperature and potential vorticity (f/h) as a function of σ_t (bottom panels). Fig. 6 shows the corresponding fields along the topogulf section west of the MAR.

(One exception to the simply connected current might be the region just west of the Tail of the Grand Banks where the transport of the Gulf Stream is rapidly decreasing due to the recirculation of waters to the west, both north and south of the current. Is the current sufficiently stable that it can maintain its identity as a continuous jet while it is diminishing in transport? Or does it break down into a population of eddies which perhaps regroup or reform into a jet after they pass the Tail of the Grand Banks?)

'Retroflection' of both the NAC and the LC

What causes the western boundary currents (particularly the LC) to overshoot so far into the 'the other gyre' before retroflecting? The LC, instead of turning east along the Polar Front continues south to the southern tip of the Grand Banks before it turns north and apparently flows along side of the NAC back towards the north, past Flemish Cap and the retroflection of the NAC near 52°N. It is very hard to imagine that this long southward extension is 'inertial', so to call this a retroflection may be misleading. But the loop to the northwest by the NAC and LC together may be more characteristic of a retroflection. The available evidence suggests that this northwestern corner of the NAC is spatially stable, i.e. it does not meander about much (Lazier, personal comm.). There are some indications it may break off and form an anticyclonic eddy at times (and presumably remains fairly stationary).

Formation of zonal jets

The three zonal jets are the Azores Current, the 47°N jet, and the Polar Front. The Azores current appears to be the shallowest of the three and this may be significant in understanding its formation, while the other two seem to extend well below the main thermocline (Harvey and Arhan, 1987). How the Azores Current comes into being where the Gulf Stream 'bifurcates' is a mystery. I believe it is fair to say that the current, as a front, has not been observed at the TGB, but emerges as such only farther to the southeast. This would be consistent with a Gulf Stream that is no longer a 'simple' current by the time it reaches the TGB, but a turbulent mixture of meandering jets and eddies. At the TGB a sorting process takes place with only the shallower eddies or upper waters that do not feel the bathymetry continuing off to the southeast, and the rest 'reforming' into the NE flowing NAC, if, as mentioned earlier it can be described as a simply connected flow.

The 47°N jet is intriguing for it appears to be so tightly locked to the topography of Flemish Cap. It appears to form by peeling off the warm waters on the anticyclonic side of the current. While the details are unclear, I think it is due to these waters having so much negative shear vorticity that as they begin to curve around Flemish Cap and the curvature vorticity increases, parcels can't adjust with increasingly negative curvature vorticity without inducing a return flow, which cannot be done without increasing the layer thickness. But increasing the layer thickness means a deeper thermocline going north, and this is not possible unless we want to rearrange the interior density field. The result is that parcels are expelled before they reach the point of maximum positive curvature. The waters that continue north probably have very sharp anticyclonic shear on the right side of the current and weaker cyclonic shear on the left side. The expelled waters can either continue east as a zonal baroclinic jet or they may have so much negative vorticity that they curve back on themselves as anticyclonic vortices (see below). The 47°N jet seems to form a northern boundary to the waters in the Newfoundland Basin (Harvey and Arhan, 1988), which suggests that the jet should be seen as a permanent (meandering) feature of the region.

The Polar Front

The Polar Front seems to be the most well-defined and stable of all three zonal flows. It emerges from the loop at about 51°N and continues east and crosses the MAR at the latitude of the CGFZ, 52-53°N. This is borne out very nicely by the ensemble of surface drifters deployed by the Institut für Meereskunde (IfM) over the last ten years. The latitudinal constraint of the CGFZ on the position of the Polar Front in the vicinity of the MAR seems to be very strong. It is interesting to note that there seems to be little intergyre exchange along the front. The CGFZ is also the principal route by which deep waters make their way into the western basin. A few degrees farther south the Topogulf program maintained an array of current meter moorings across the MAR in four clusters. They noted that there was an upgradient heat flux at the westernmost site (west of the ridge) and a downgradient flux at the other sites. The tentative conclusion was that 'west of the ridge the mesoscale eddy energy appears ... to feed the mean flow, while east of the ridge local baroclinic energy transfer would enhance the mesoscale' (Colin De Verdiere et al., 1989).

Intergyre Exchange

The physical properties of the waters in the Newfoundland Basin are due to the admixture of waters of subpolar origin. How mixing takes place across the

NAC/LC/Loop current/Polar Front is not at all known. Even less do we know where exchange is most likely or whether the frontal system is more 'permeable' in one direction or the other. From our experience in the Gulf Stream, we can postulate certain pathways associated with the meandering of the current, namely submesoscale stirring and ring formation. But I am not aware of any attempt to quantify exchange rates, for example in a spirit similar to the Bower et al. study (1985). The Topogulf sections show weak meridional property gradients in the main thermocline. Further, north-south sections of Tritium show a sharp decrease in concentration between the Polar Front and Azores Current. Thus, even though there is considerable eddy energy in the region, it is clearly not fully homogenized. Perhaps the predominantly eastward scattering of the IfM surface drifters (drogued at 100 m) are an indication why. It is noteworthy that none of the IfM drifters dispersed into the Labrador Current, and from what I have seen of the trajectories of drifters released by the International Ice Patrol in the Labrador Current (to study iceberg movements), many of them drift quite far south before turning north again just inshore of the NAC.

Discrete Eddies

Two observations of discrete eddies are worth mention. The first one is a truly extraordinary anticyclonic eddy reported by Mann (1967). The 10°C isotherm was clearly more than 1000 m deep, or at least 300 m deeper than average than typical for the region, Fig. 7. It has a nearly 1000 m thick layer of almost uniform waters at 14.8°C. Since the observation was made in July the eddy is covered with a shallow seasonal thermocline. The T/S properties indicate that the waters in and below the eddy are of local origin. I believe this eddy is of the same kind as the very intense anticyclone reported by Worthington (1977), which was also observed on the warm side of the current where we normally expect to find CCRs. My guess is that both of these were spun off of the main current (The NAC perhaps at Flemish Cap, and a trough in the Gulf Stream, respectively) due to an excess of negative relative vorticity (Rossby, 1991).

The other eddy is an intrathermocline lens reported by Bubnov et al. (1991) and brought to my attention by Dr. Paka at the Shirshov Institute of Oceanology. The waters in this lens are slightly more saline (0.1 psu) than the surrounding waters, 8.5°C and 35.2^{+}psu, Fig. 8. It was located at 49°N, 41°W or just NE of Flemish Cap. Its central density was about 27.35 (700 m deep), a surface that outcrops in winter only a few degrees farther north. It seems likely that the lens was formed at the surface as a deep mixed layer, perhaps as a WCR. Somehow, it then got subducted into and across the NAC without getting sheared apart. It certainly is a fascinating observation! This brings to mind the deep anticyclonic lens that was observed in the POLYMODE study (Elliott and Sanford, 1985).

Colin De Verdiere et al. (1989) observed a number of intense cyclonic lenses below the main thermocline in their current meter data at the MAR. They refer to them as empty coherent vortices as their main characteristic seemed to be the absence of Labrador Sea Water!

References

Bower, A. S., T. Rossby, and J. Lillibridge, Jr.: The Gulf Stream - Barrier or Blender? J. Phys. Oceanogr., 15, 24-32.

Bubnov, V. A., V. I. Bishev, B. V. Volostnich, N. N. Golenko, V. D. Egorihin, A. B. Zubin, and V. T. Paka, 1991: A Frontal Intrathermocline Lens. Dokl. Akad. Sci., USSR

Colin de Verdiere, A., H. Mercier, and M. Arhan, 1989: Mesoscale variability from the western to the eastern Atlantic along 48°N., J. Phys. Oceanogr., 19, 1149-1170.

Elliot, B. A. and T. B. Sanford, 1986: The Subthermocline Lens D1. Part I: Description of Water Properties and Velocity Profiles. J. Phys. Oceanogr., 16, 532-548.

Greatbatch, R., J., A. F. Fanning, A. D. Goulding, and S. Levitus, 1991: A diagnosis of interpentadal circulation changes in the North Atlantic. J.Geophys. Res., 96, 22009-22024.

Harvey, J. and M. Arhan, 1988: The water masses of the central North Atlantic in 1983-84. J. Phys. Oceanogr., 18, 1855-1875.

Hogg, N. G., 1992: On the transport of the Gulf Stream between Cape Hatteras and the Grand Banks. Deep Sea Res., 39, 1231-1246

Isemer, H.J. and L. Hasse, 1987: The Bunker Climate Atlas of the North Atlantic Ocean. 2 vols. Springer Verlag, New York

Keigwin, L. D. and E. A. Boyle, 1992: Century and Millenial-Scale Changes in North Atlantic Surface and Deep Waters During the Past 80,000 years. Proc. ACCP P.I. Conf. Miami.

Krauss, W., 1986: The North Atlantic Current. J. Geophys. Res., 91, 5061-5075

Krauss, W., E. Fahrbach, A. Aitsam, J. Elken and P. Koske, 1987: The North Atlantic Current and its associated eddy field southeast of Flemish Cap. Deep Sea Res., 34, 1163-1185

Mann, C., 1967: The termination of the Gulf Stream and the beginning of the North Atlantic Current. Deep Sea Res., 14,337-359.

McIntyre, A., N. G. Kipp, A. W. H. Be, T. Crowley, T. Kellog, J. V. Gardner, W. Prell and W. F. Ruddiman, 1976: Glacial North Atlantic 18,000 Years Ago: A CLIMAP Reconstruction. Geol. Soc. America Mem., 145, 43-76

Richardson, P. L. and J. A. Knauss, 1971: Gulf Stream and western boundary undercurrent observations at Cape Hatteras. Deep Sea Res., 18,1089-1109.

Rossby, T., 1991: Anticyclonic eddies in the Sargasso Sea. The SYNOPtician, 3. (An informal newsletter of the SYNOP community.)

Sato, O. and T. Rossby, 1993: Seasonal and secular changes in dynamic height and baroclinic transport by the Gulf Stream. Deep Sea Res. Submitted.

Schlosser, P., G. Bönisch, M. Rhein and R. Bayer, 1991: Reduction of deepwater formation in the Greenland Sea during the 1980s: Evidence from tracer data. Science, 251, 1054-1058.

Worthington, L.V., 1977: The intensification of the Gulf Stream after the winter of 1976-1977. Nature, 270, 415-417.

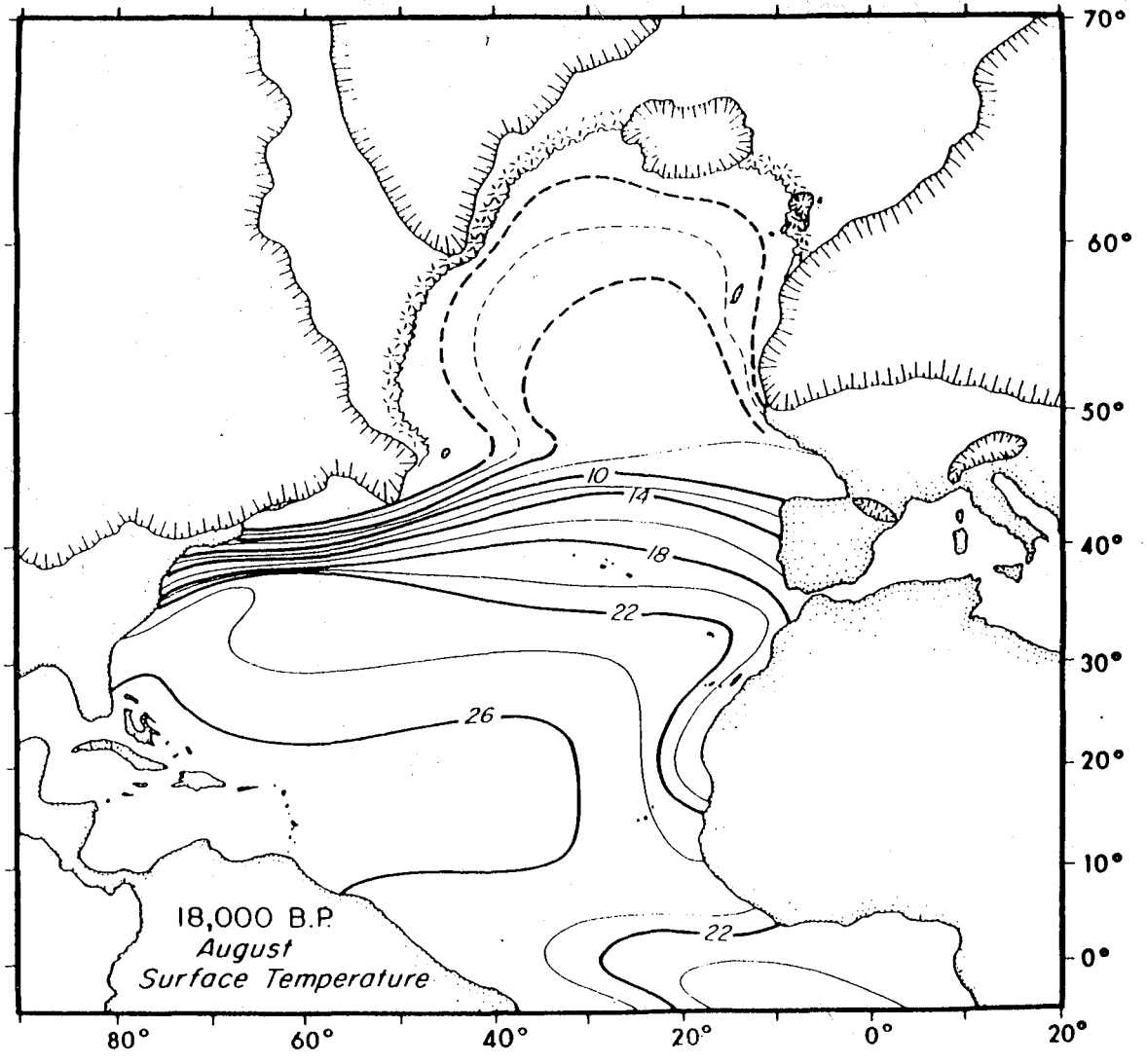

Sea surface temperature 10,000 years B.P. (McIntyre, al., 1976).

Figure 1

Chart 136

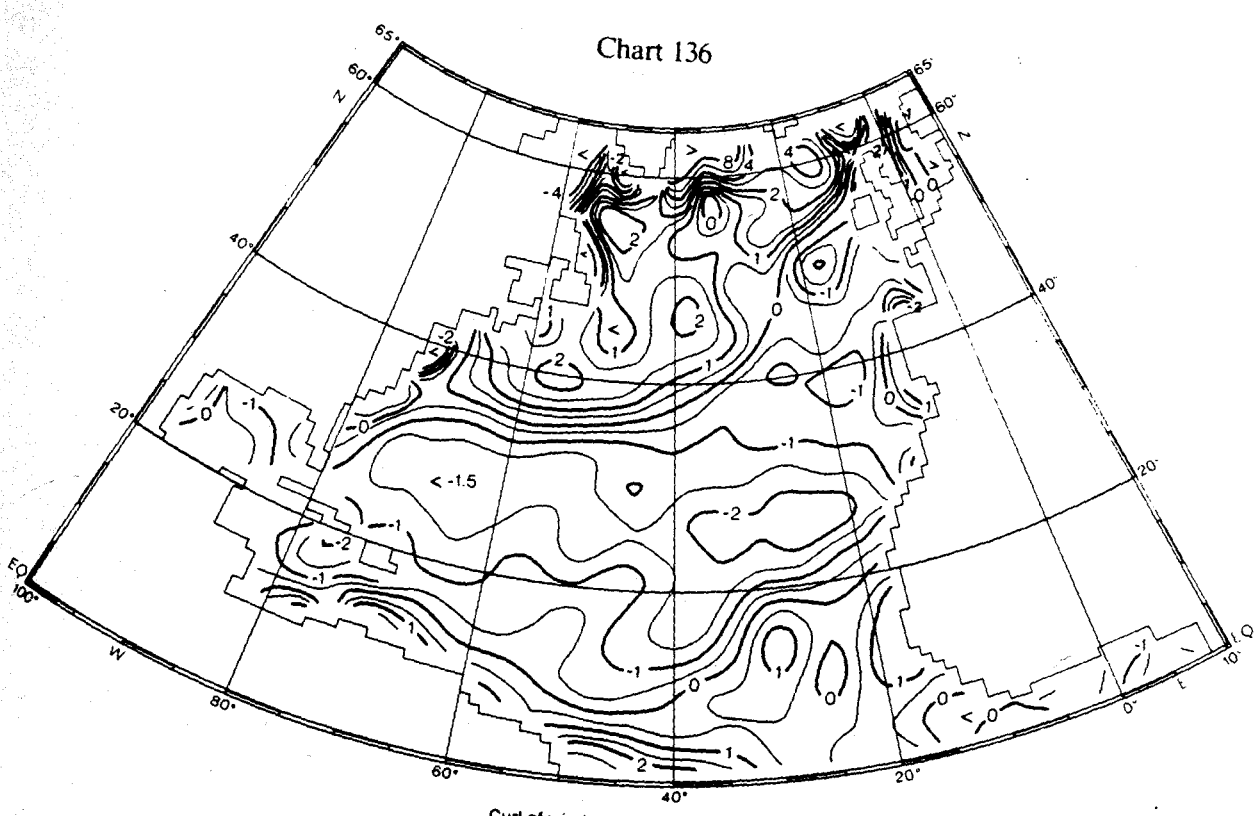

Curl of wind stress [10^{-7} N m^{-3}]
March

Chart 148

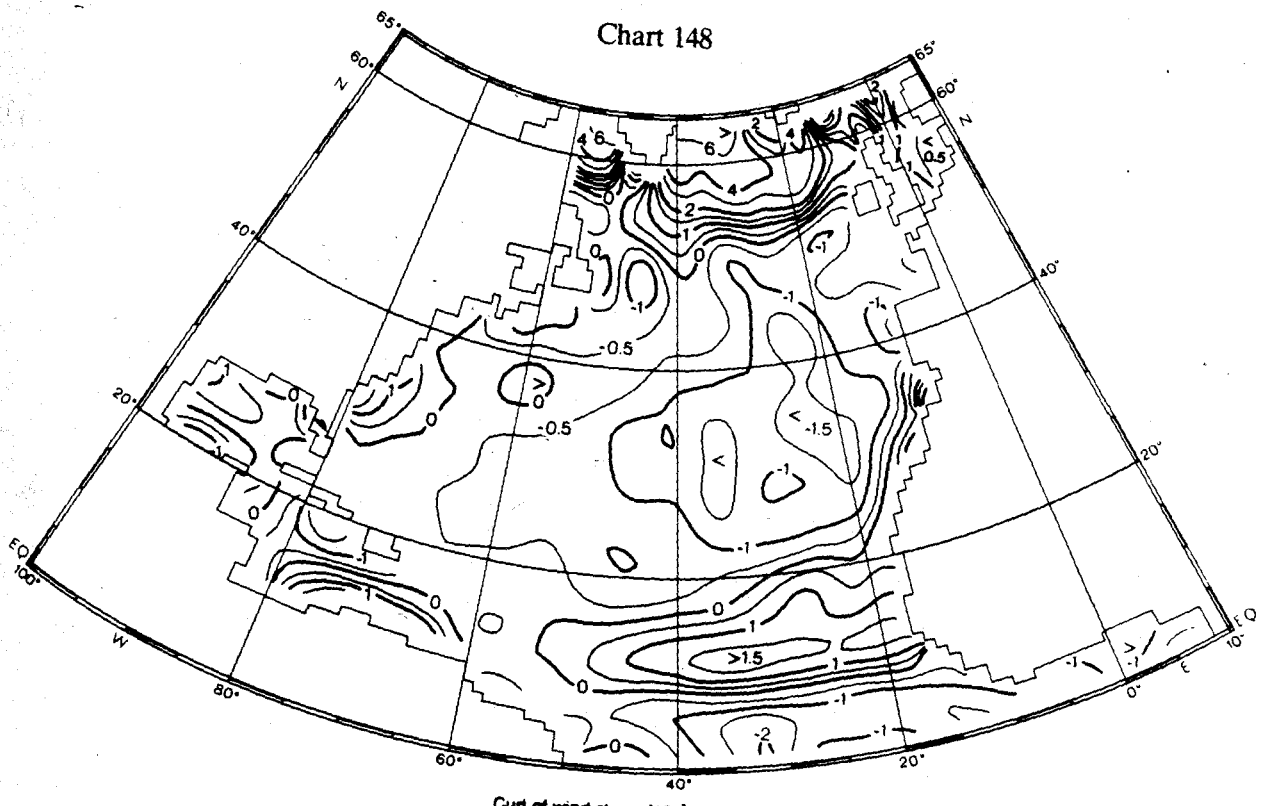

Curl of wind stress [10^{-7} N m^{-3}]
September

Figure 2

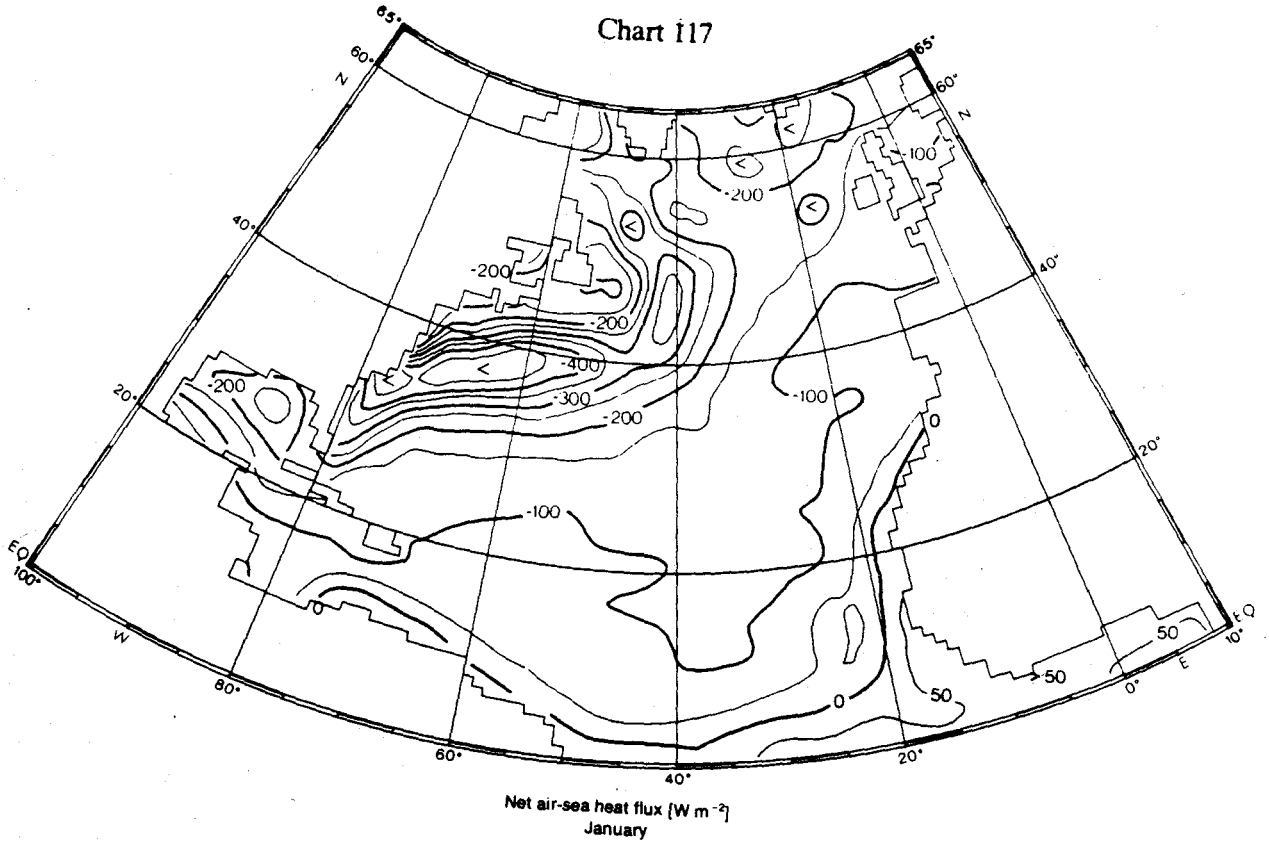
Chart 117
65°
60°
N
40°
20°
EQ
100°
W
80°
60°
40°
20°
0°
E
10° EQ
-200
-100
-400
-300
0
50
Net air-sea heat flux [W m⁻²]
January

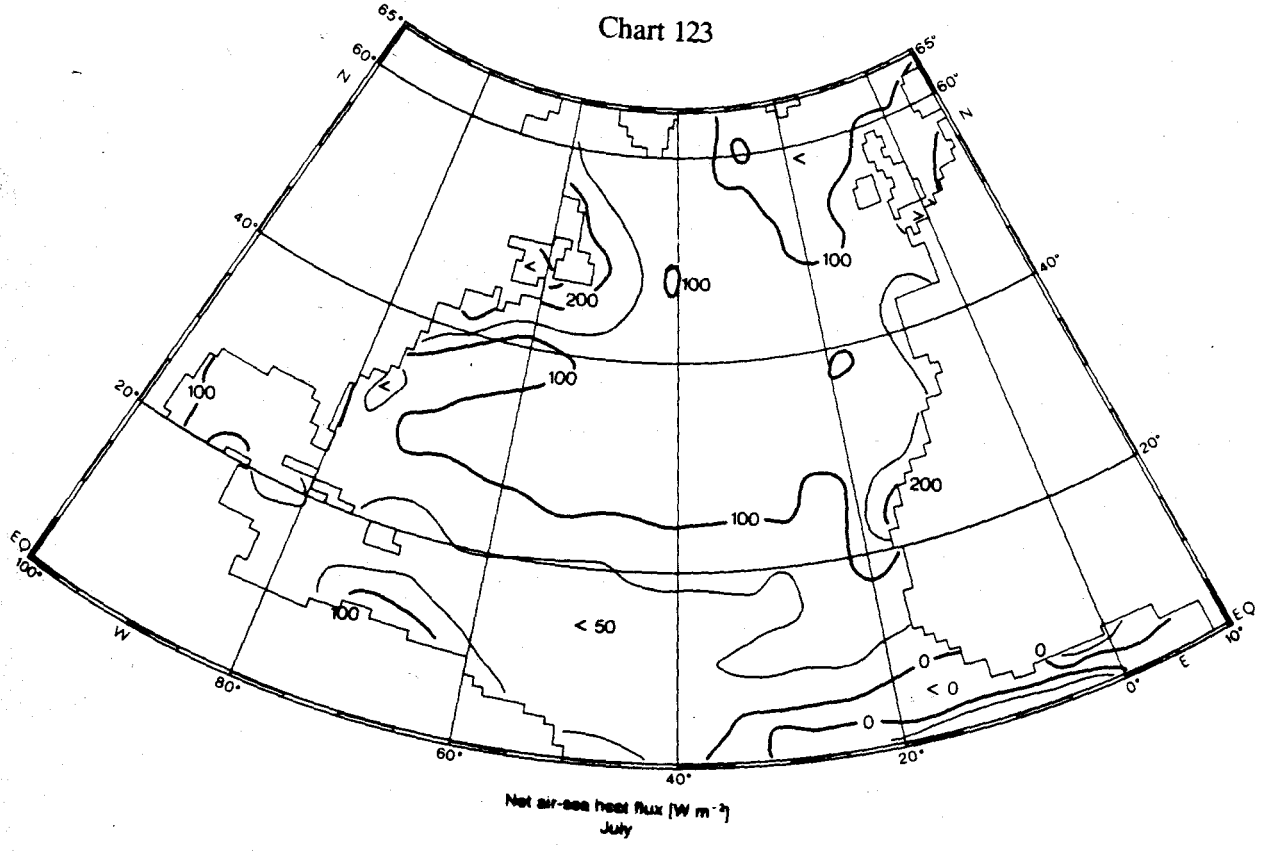
Chart 123
65°
60°
N
40°
20°
EQ
100°
W
80°
60°
40°
20°
0°
E
10° EQ
100
200
< 50
0
< 0
Net air-sea heat flux [W m⁻²]
July

Figure 3

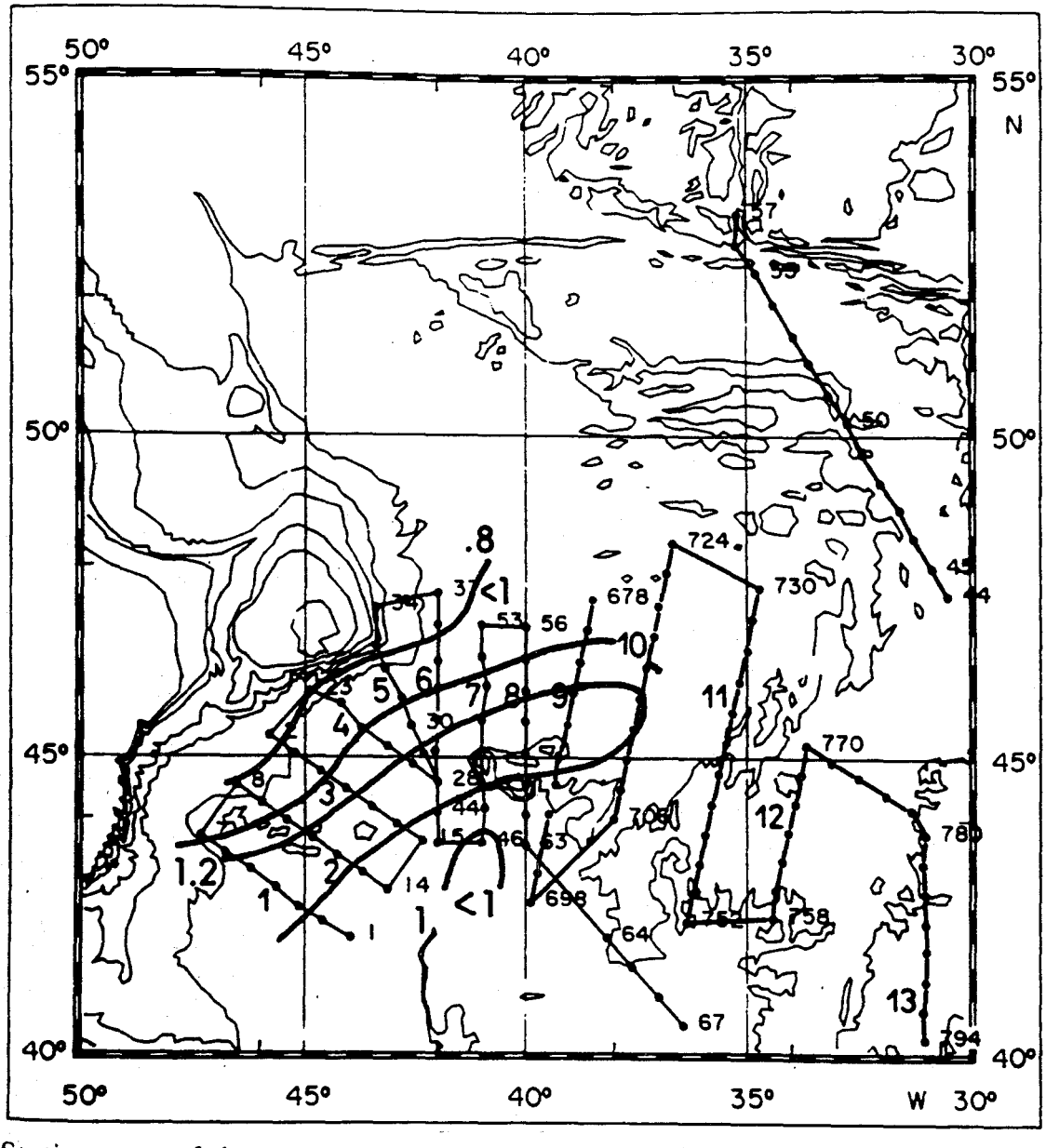

Station map of the survey area east and southeast of Flemish Cap. Large numbers are the section numbers, small numbers are station numbers.

Figure 4

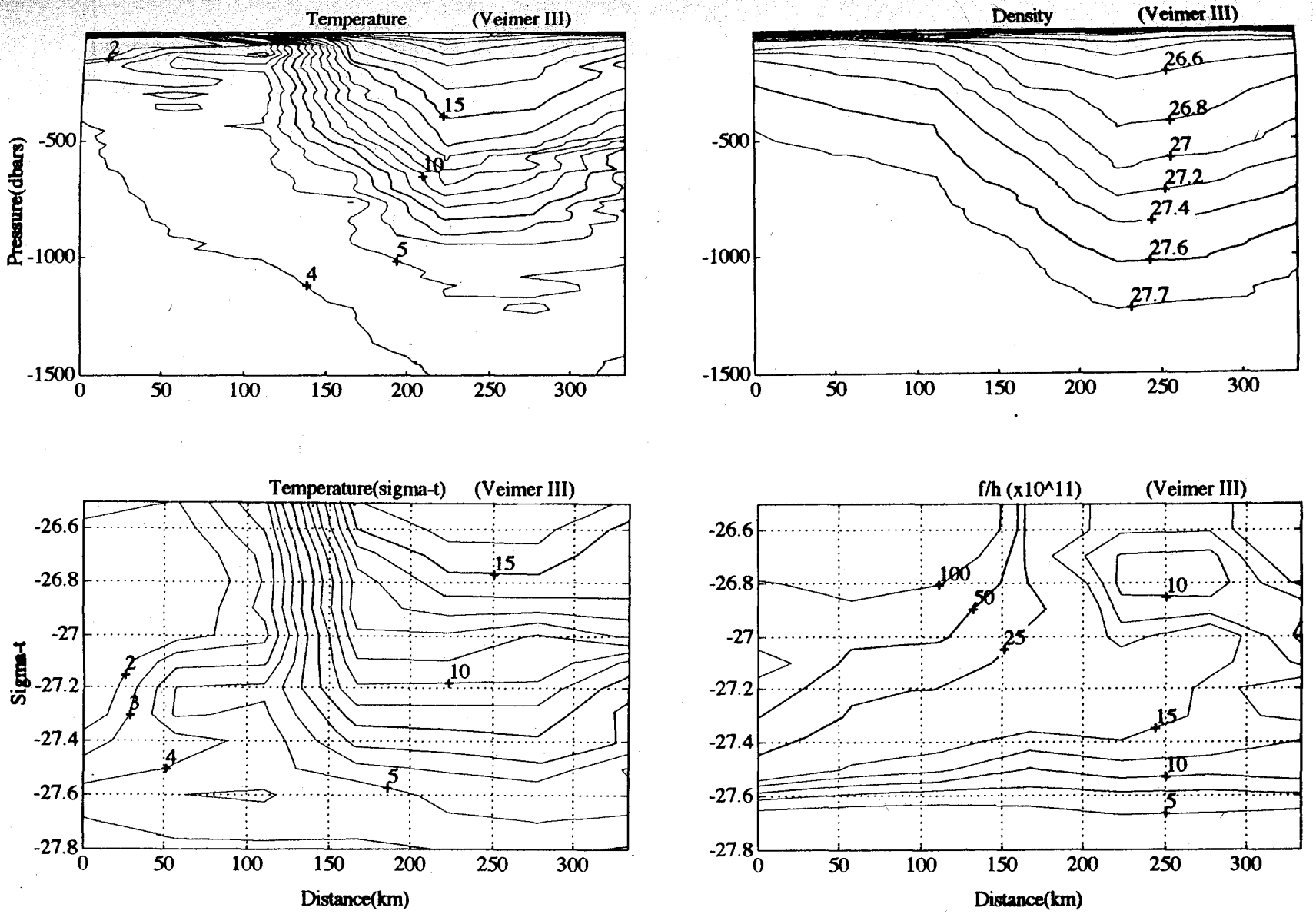
Temperature (Veimer III)
Pressure(dbars)
-500
-1000
-1500
0
50
100
150
200
250
300
2
15
10
5
4
Density (Veimer III)
26.6
26.8
27
27.2
27.4
27.6
27.7
Temperature(sigma-t) (Veimer III)
Sigma-t
-26.6
-26.8
-27
-27.2
-27.4
-27.6
-27.8
Distance(km)
f/h (x10^11) (Veimer III)
100
50
25
10
15
5
Distance(km)

Figure 5

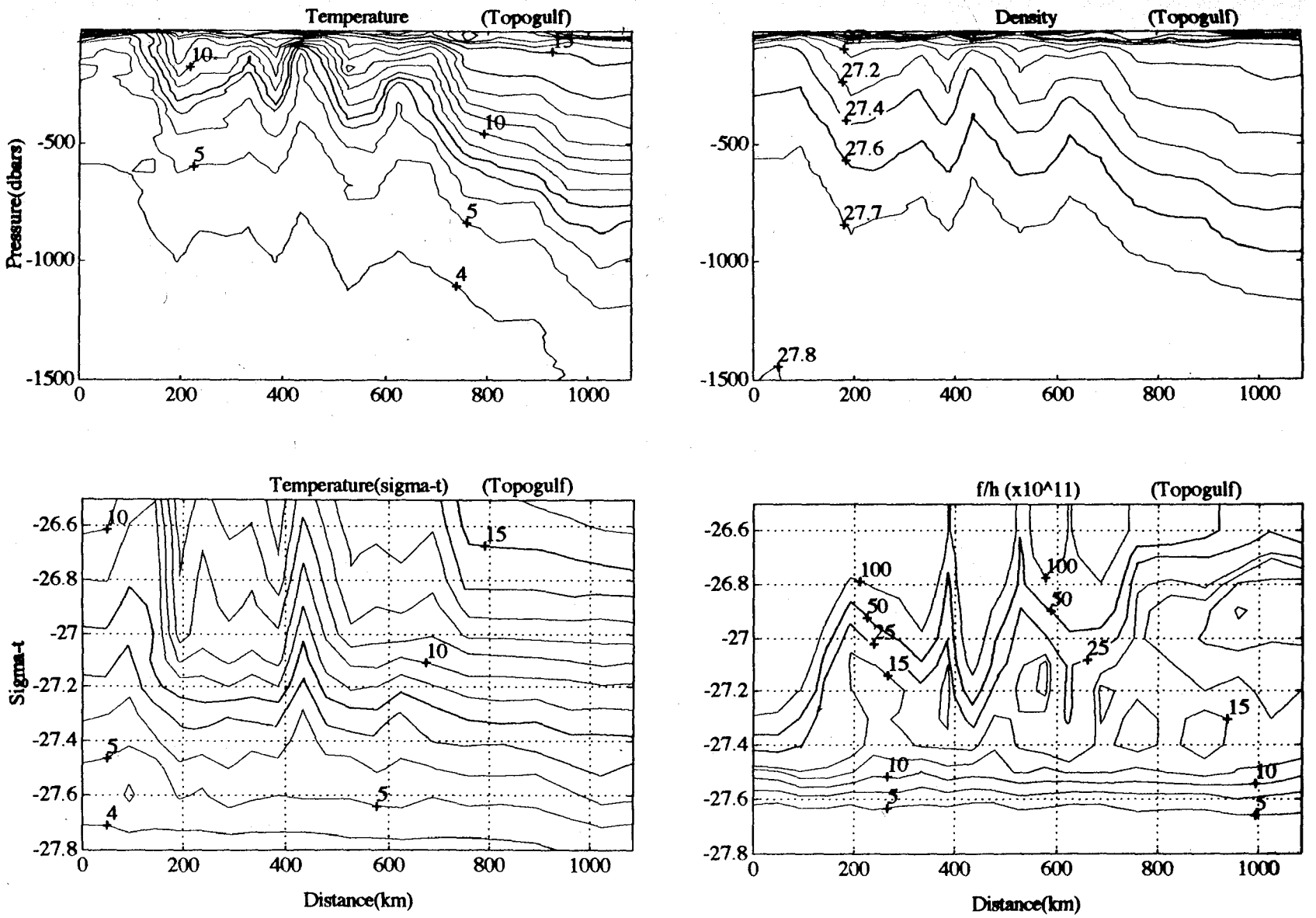
Temperature (Topogulf)
Pressure(dbars)
-500
-1000
-1500
0
200
400
600
800
1000
10
5
10
5
4
15
Density (Topogulf)
27.2
27.4
27.6
27.7
27.8
Temperature(sigma-t) (Topogulf)
Sigma-t
-26.6
-26.8
-27
-27.2
-27.4
-27.6
-27.8
Distance(km)
10
15
10
5
5
4
f/h (x10^11) (Topogulf)
100
100
50
50
25
25
15
15
10
10
5
5

Figure 6

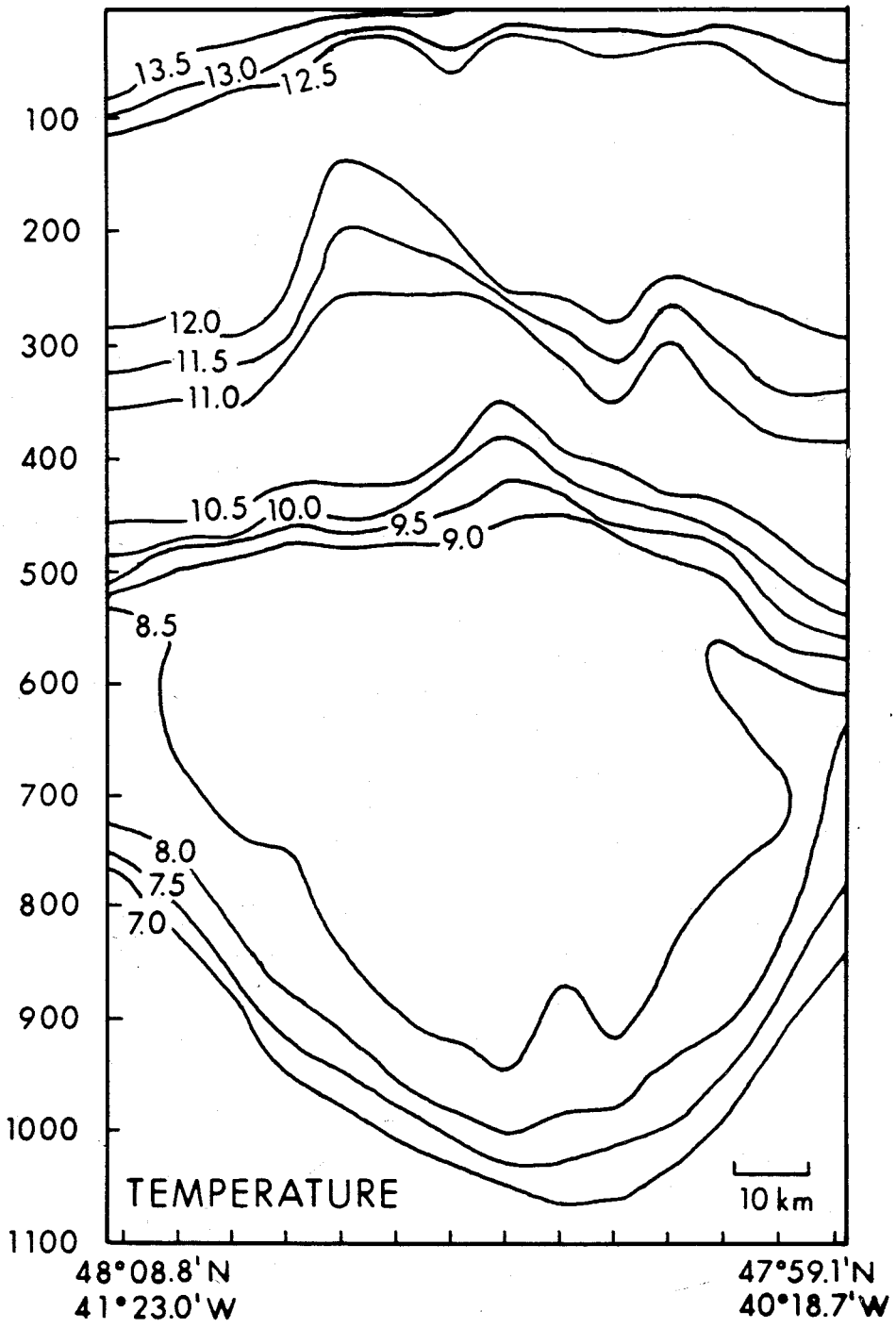
13.5
13.0
12.5
12.0
11.5
11.0
10.5
10.0
9.5
9.0
8.5
8.0
7.5
7.0
100
200
300
400
500
600
700
800
900
1000
1100
TEMPERATURE
10 km
48°08.8'N
41°23.0'W
47°59.1'N
40°18.7'W

Figure 7

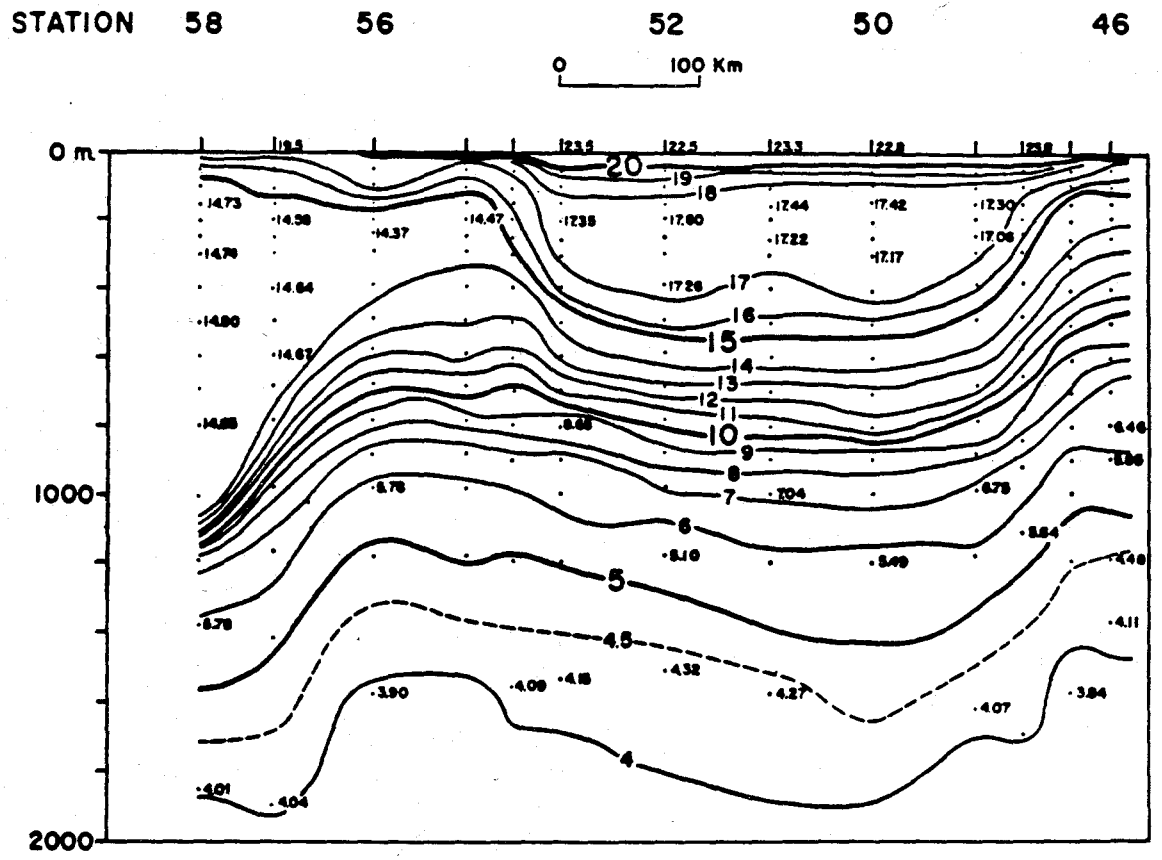
STATION 58 56 52 50 46
0 100 Km
0 m
1000
2000
20
19
18
17
16
15
14
13
12
11
10
9
8
7
6
5
4.5
4

Figure 8

Modeling the Subpolar North Atlantic

C.W. Böning, F.O. Bryan, and W.R. Holland
National Center for Atmospheric Research
P.O. Box 3000
Boulder, CO 80307

In contrast to the tropical and midlatitude Atlantic, or for the Arctic, there is not a long history of modeling of the subpolar region of the North Atlantic. Model simulations of the thermohaline circulation with grid resolutions that capture the small-scale frontal structures and eddies of the high latitudes have become possible only very recently. The discussion of problems and achievements in the simulation of the North Atlantic Current (NAC) system presented here will be based mainly on results from the "Community Modeling Effort" (CME). Following the initial model run of Bryan and Holland (1989), a series of experiments have been conducted by the groups at NCAR and in Kiel that explore the sensitivity to a variety of factors such as atmospheric forcing, model resolution, and lateral boundary conditions.

Previous evaluations of the model results and detailed comparisons with observations were focused mainly on the tropical and subtropical North Atlantic. The present, preliminary analysis of the model behavior in the subpolar North Atlantic indicates horizontal resolution and thermohaline forcing to be of critical importance to the mean circulation. Compared to the subtropics and tropics, the solution is much less sensitive to the wind stress climatology. We shall discuss the influence of these model factors following a brief outline of the model configuration, and a general overview of the model circulation in the subpolar North Atlantic.

1. Model configuration

The model of the wind- and thermohaline-driven circulation in the Atlantic Ocean is based on the Geophysical Fluid Dynamics Laboratory (GFDL) primitive equation model. The model domain extends from 15°S to 65°N (Fig. 1). There are 30 vertical levels, their spacing smoothly increasing from 35 m at the surface, to 100 m near 500 m depth, and 250 m below 100 m depth. The thermohaline circulation is driven by a relaxation of surface salinity to the monthly mean values of Levitus (1982) on a time scale of 50 days, and a linear bulk formula for the surface heat flux, i.e., a relaxation to observed "effective" air temperatures.

In what we will refer to as the "standard" configuration of the model, the northern and southern (wet) boundaries are closed to normal flow. In the last five grid cells adjacent to these boundaries, potential temperature (T) and salinity (S) are restored to the monthly mean values of the Levitus' (1982) climatology. The rationale for the buffer zones is to include the effect of water mass transformations taking place outside of the model domain. At present there is no ice model included. To prevent the occurrence of super-cooled water due to the strong winter heat losses, the water temperatures over the northern portion of the Labrador Shelf are restored to climatology.

A suite of model experiments has been carried out to explore the effect of different model factors and parameterizations and the sensitivity to various aspects of the atmospheric forcing. There are three basic versions: with a horizontal resolution (meridional x zonal) of 1° x 1.2°, 1/3° x 0.4°, and 1/6° x 0.2°. We will refer to these as the medium-resolution (MR), high-resolution (HR), and very-high resolution (VR) versions. For the HR and VR models, a biharmonic scheme is used for horizontal diffusion and

viscosity, whereas an isopycnal diffusion scheme is adopted for the MR model to account for the mixing effect of mesoscale eddies.

2. Model features in the subpolar North Atlantic

The most prominent feature of the upper-layer flow field in the HR and VR cases is the band of energetic eddy activity straddling the course of the NAC (Fig. 2). The distribution of eddy variability is similar for the HR and VR cases, but the energy is about twice as high in the VR case. The maximum energies in that case are close to the observed values of about 1000 cm^2s^{-2} in the Newfoundland Basin east of Flemish Cap, as given by drifting buoy or Geosat altimeter data (Beckmann et al., 1993). Apart from its influence on the quantitative representation of the instability processes, the different resolution of the MR and VR cases has only a minor impact on the mean circulation in the subpolar ocean. The discussion of the mean flow properties will, therefore, be based on the HR (and, in the subsequent section, MR) case.

Mean upper-layer fields are depicted in Fig. 3 for the HR case in "standard" configuration, that is with a closed boundary at 65°N and restoring to Levitus' T and S in a 1.67°-wide buffer zone. Despite the long-term averaging, the subarctic front in the northwest corner region is remarkably sharp, indicative of only little meandering in that area, and little cross-frontal exchange of the warm, salty waters in the Newfoundland Basin with the cold, fresh water of the Labrador Sea. (The eddy activity has its maximum in the Newfoundland Basin, and there is a sharp drop of eddy energy across the front in the NW corner.) An outstanding, unrealistic feature of the solution concerns the northward flowing current along the Grand Banks: it is pressed against the continental slope, with the bulk of the water carried through Flemish Pass. Possibly related to that, the Labrador Current is blocked at the northern edge of the Grand Banks and a wedge of cold, fresh Labrador Shelf water is drawn eastward along the subarctic front. The cause of these local model problems is, as yet, unknown.

Another major unrealistic feature of the mean fields depicted in Fig. 3 is the downstream course of the NAC. Instead of extending northeastward into the Icelandic Basin, the flow turns northward already at about 35°W, leaving the northeastern basin too cold and far too quiet energetically. As will be discussed below (section 4), that behavior is related to the conditions applied at the northern wall. About one half of the 22 Sv carried northward by the NAC recirculates horizontally with the cyclonic gyre of the subpolar North Atlantic, the other half is transformed to deep water and carried southward with the DWBC in the Labrador Sea (Figs. 4 and 5). However, there is no continuation of the DWBC along the Grand Banks. At about 50°N (just north of the axis of the NAC), the DWBC separates from the continental slope and is deflected eastward, eventually turning southward again near the mid-Atlantic Ridge. A similar behavior has been observed in model experiments with coarser resolution (Gerdes, 1988) and may be seen also in the 1/2° World Ocean model of Semtner and Chervin (1992). It remains to be seen whether this apparently robust model behavior is related to the local problems of the upper-layer flow in the Grand Banks area.

3. Influence of horizontal resolution

While differences in the mean flow patterns of HR and VR cases are minor, there is an important difference between the non-eddy resolving (MR) and the eddy-resolving cases, concerning the location of the subarctic front (Fig. 6). In the high resolution cases, the front is not only sharpened, it is also shifted to the north by about 5° of latitude. Consequently, surface temperatures over a large area of the Newfoundland Basin are

significantly higher than in the MR case. The shift of the front, roughly to its observed location, has a profound impact on the surface heat budget, partially remedying a typical problem of low resolution models (Fig. 7). As a consequence of their much too cold surface temperatures in the Newfoundland Basin, non-eddy resolving models like the present MR version, or the models of Sarmiento (1986) and Gerdes (1988), all show a strong heat uptake of the ocean in that area, locally exceeding 100 wm^{-2}. The dynamical mechanism of the drastically different behavior of the eddy-resolving cases has yet to be studied; this feature demonstrates, however, the importance of model resolution for an adequate representation of the mean flow properties in this area.

4. Effect of the northern boundary condition

To avoid the explicit numerical representation of the overflow processes across the Greenland-Scotland-Ridge system, a closing of the North Atlantic near the ridge has been a common practice in various models, e.g., Sarmiento (1986) and Semtner and Chervin (1992). The effect of the water mass transformations taking place north of Iceland are taken into account by buffer zones in which T and S are restored to observed values. Two problems associated with the standard use of climatological values for T and S as given by Levitus (1982) are noted here:

In spatially smoothed climatological data, the signature of Denmark Strait Overflow Water (DSOW), which is tightly pressed against the continental slope of Greenland, is almost completely lost; i.e., in the Levitus' data there is no water with temperatures less than 3°C south of the Denmark Strait. The lack of the cold (~0°C) DSOW-core in the buffer zone has important consequences for the thermohaline circulation (Fig. 8): southward transport is mostly confined to the upper NADW-range, above ~2500 m and >3°C. Using restoring temperatures based on actual section data that include the signature of DSOW south of the Denmark Strait has a damatic impact on the deep flow field and the meridional overturning (Döscher et al., 1993).

The narrowness of the buffer zone and the positioning of the northern boundary may have a deleterious effect on the upper-layer flow, i.e., the path of the NAC. Because the buffer zone does not extend south of Iceland, in order to satisfy mass conservation, the upper-layer water to be converted to DSOW must be drawn into the buffer zone between Greenland and Iceland, rather than to the east of Iceland. Thus, the buffer zone formulation, meant to help in the simulation of the large-scale thermohaline circulation, is incompatible with a large fraction of the NAC flowing into the Northeast Atlantic. Open boundary conditions may be a solution to this problem, and work is underway to test different formulations.

References

Beckmann, A., C.W. Böning, B. Brügge, and D. Stammer, 1993: Eddy variability in the central North Atlantic Ocean: Results from satellite altimetry, surface drifters, and numerical modeling, submitted to J. Phys. Oceanogr.

Bryan, F.O., and W.R. Holland, 1989: A high resolution simulation of the wind- and thermohaline-driven circulation in the North Atlantic Ocean, Special Report, University of Hawaii, 99-115.

Döscher, R., C.W. Böning, and P. Herrmann, 1993: Response of meridional overturning and heat transport in the North Atlantic to changes in thermohaline forcing in northern latitudes: A model study, submitted to J. Phys. Oceanogr.

Gerdes, R., 1988: Die Rolle der Dichtediffusion in numerischen Modellen der Nordatlantischen Zirkulation. Ber. Inst. f. Meereskunde, Kiel, No. 179, 176 pp.

Isemer, H.-J., and L. Hasse, 1987: The BUNKER Climate Atlas of the North Atlantic Ocean, Vol. 2: Air-Sea Interactions, Springer-Verlag, Berlin, 256 pp.

Levitus, S., 1982: Climatological Atlas of the World Ocean, NOAA Prof. Paper 13, U.S. Government Printing Office, 173 pp.

Sarmiento, J.L., 1986: On the North and Tropical Atlantic heat balance, J. Geophys. Res., 91, 11677-11698.

Semtner, A.J. and R.G. Chervin, 1992: Ocean general circulation from a global eddy-resolving model, J. Geophys. Res., 97, 5493-5550.

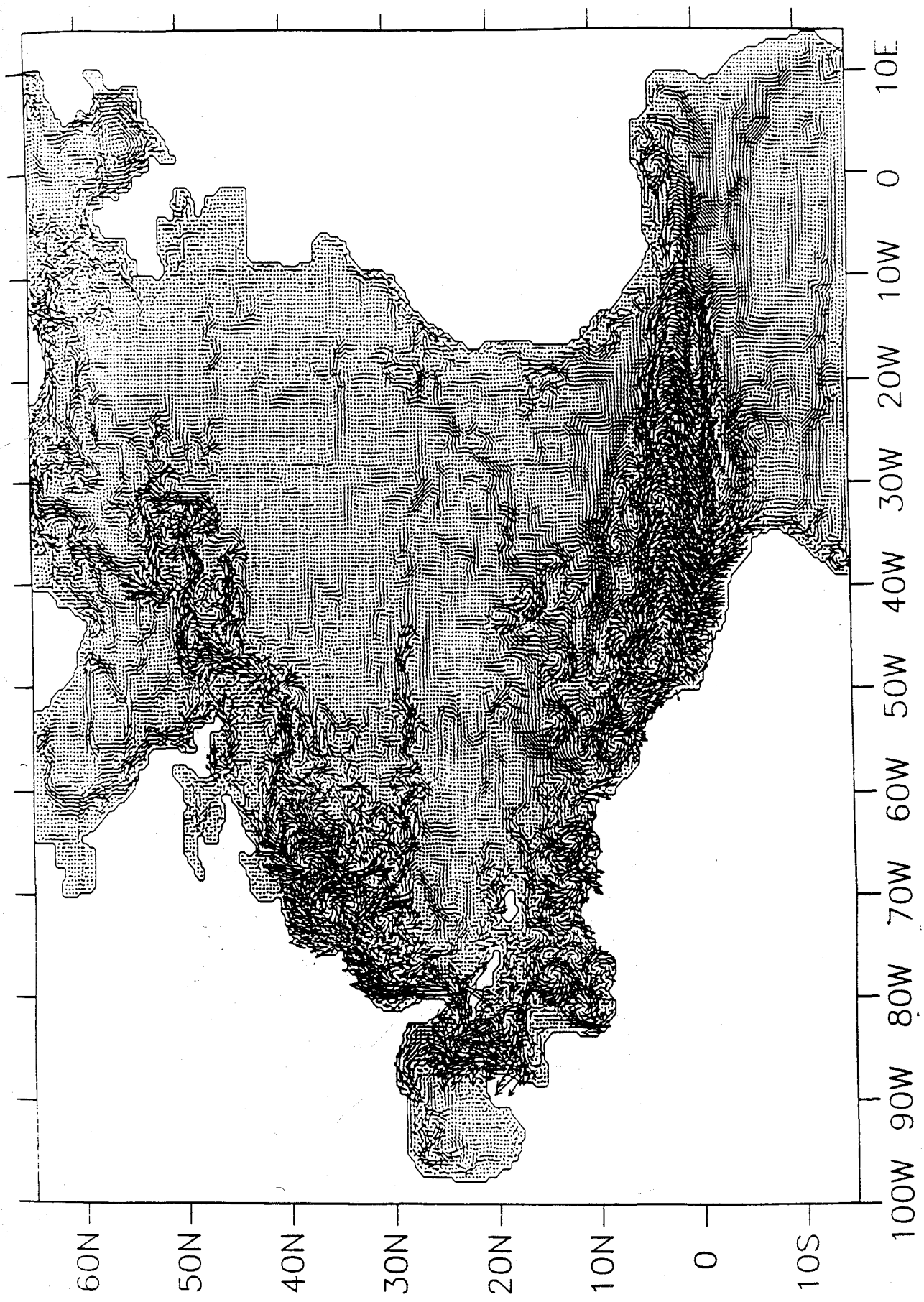

Fig. 1 Instantaneous flow field at a near-surface level (91 m), for the high-resolution version ($1/3° \times 0.4°$) of the CME.

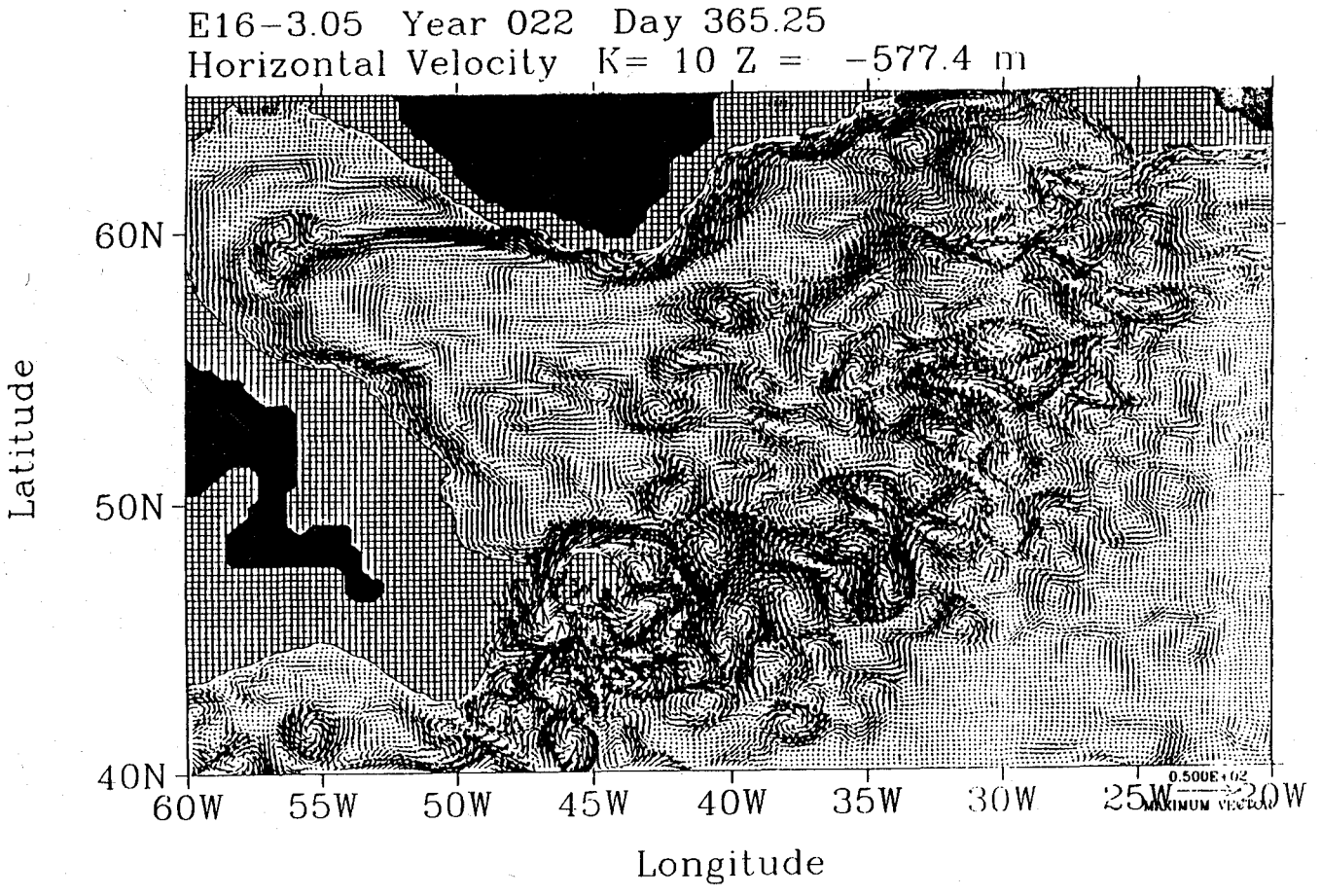

Fig. 2 Instantaneous flow field at 577 m depth in the subpolar North Atlantic, for the very-high resolution version (1/6° × 0.2°).

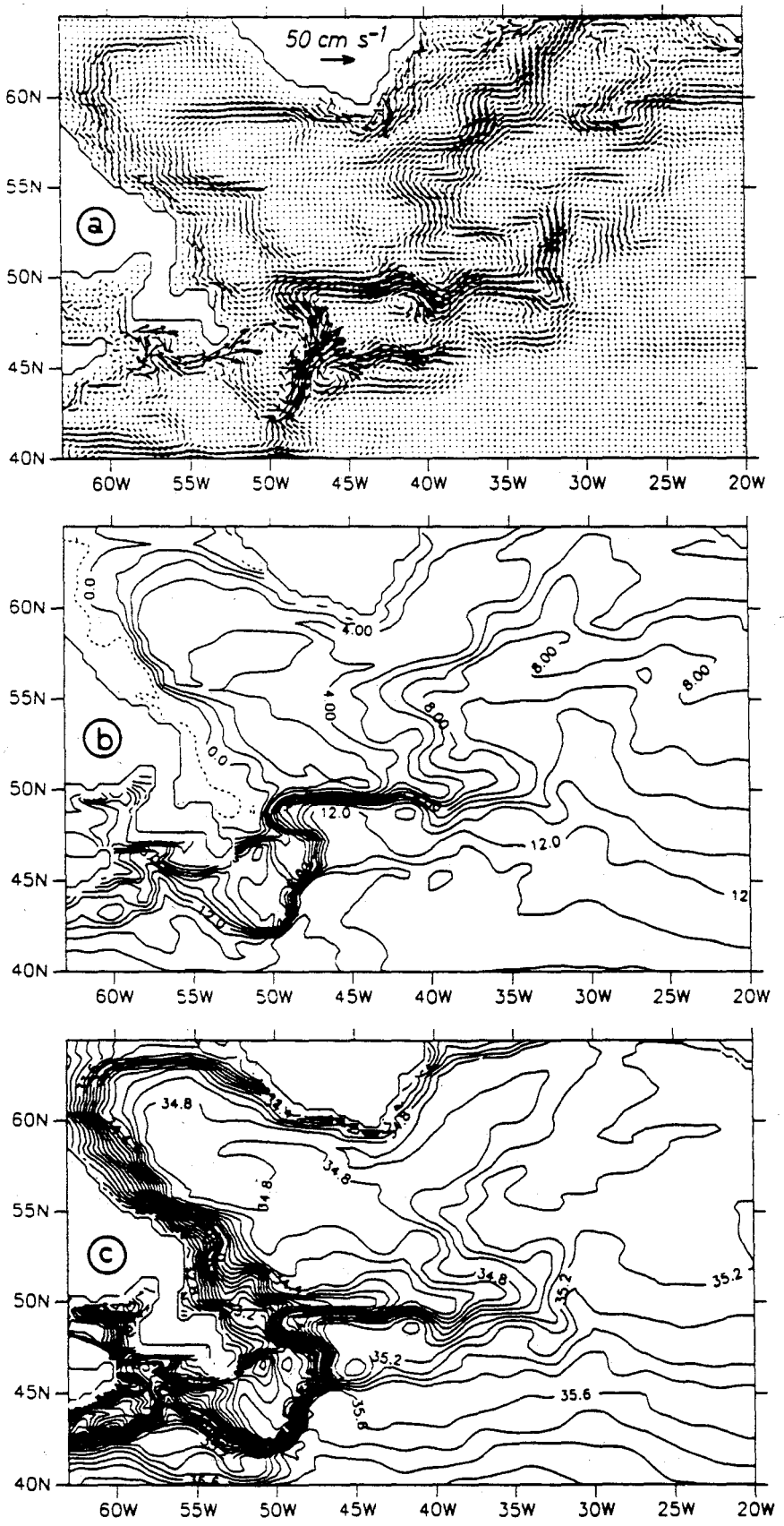

Fig. 3 Mean fields (5-year averaging) of surface velocity, potential temperature, and salinity in the subpolar North Atlantic, for the high-resolution version ($1/3° \times 0.4°$).

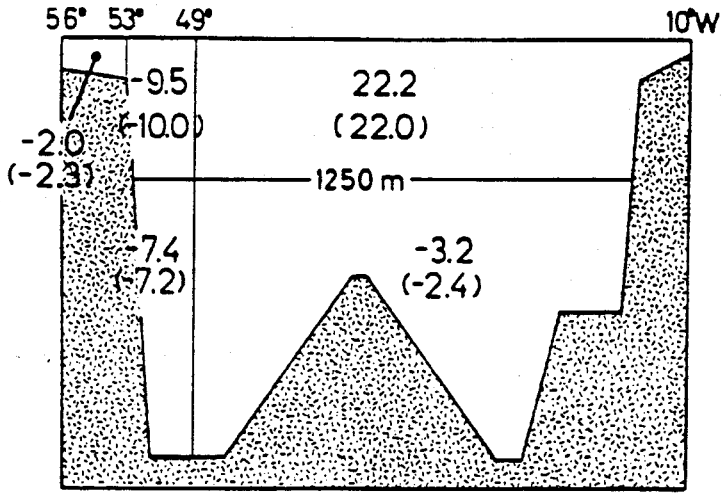

Fig. 4 Meridional volume transports (in Sv) through a cross-section along 53.5° N; HR-version with Levitus' buffer zone and forcing with Hellerman-Rosenstein wind stresses; in parenthesis: forcing with Isemer-Hasse wind stresses.

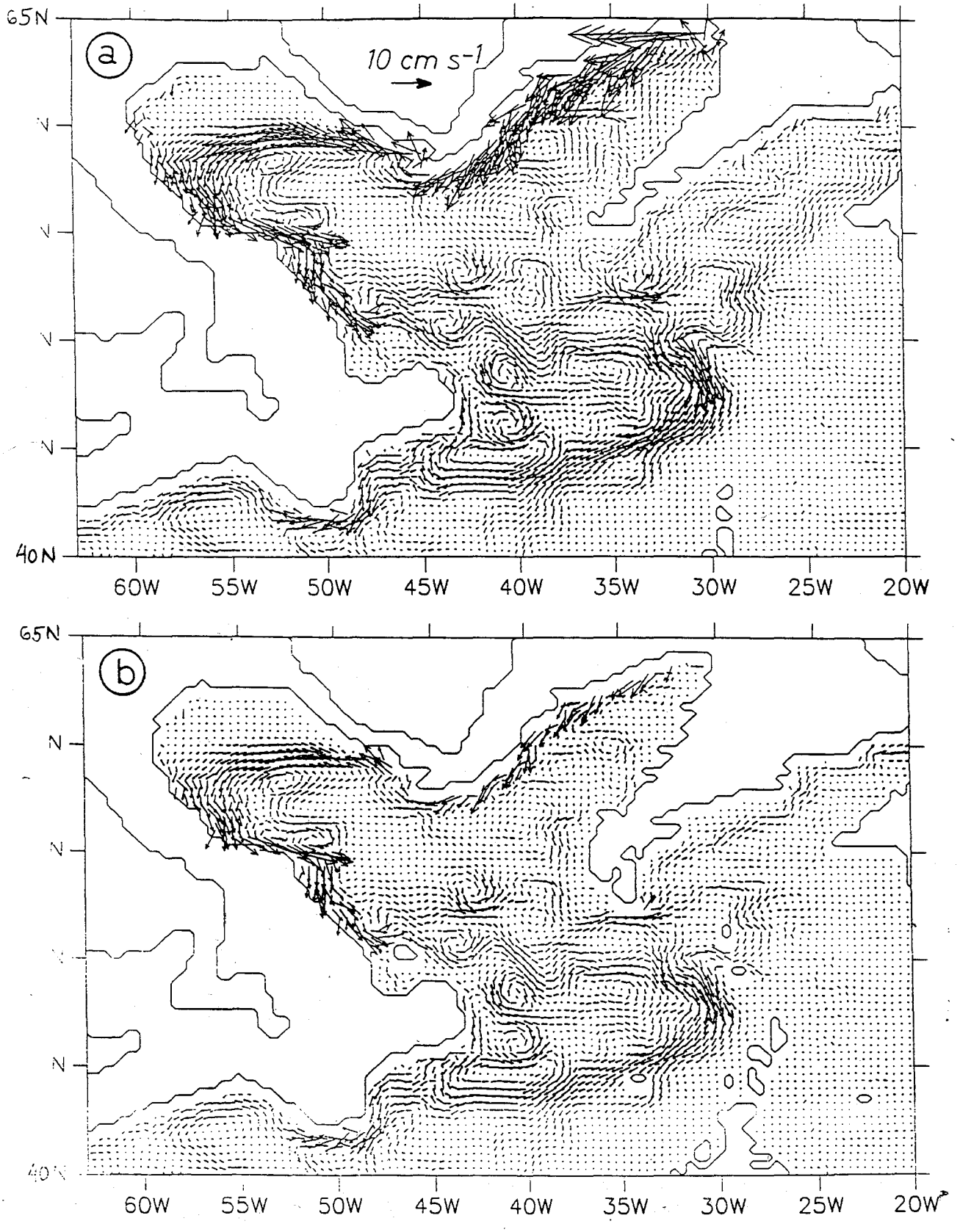

Fig. 5 Mean flow fields at 1875 m (a) and 2375 m (b) depths; high-resolution case with Levitus' buffer zone.

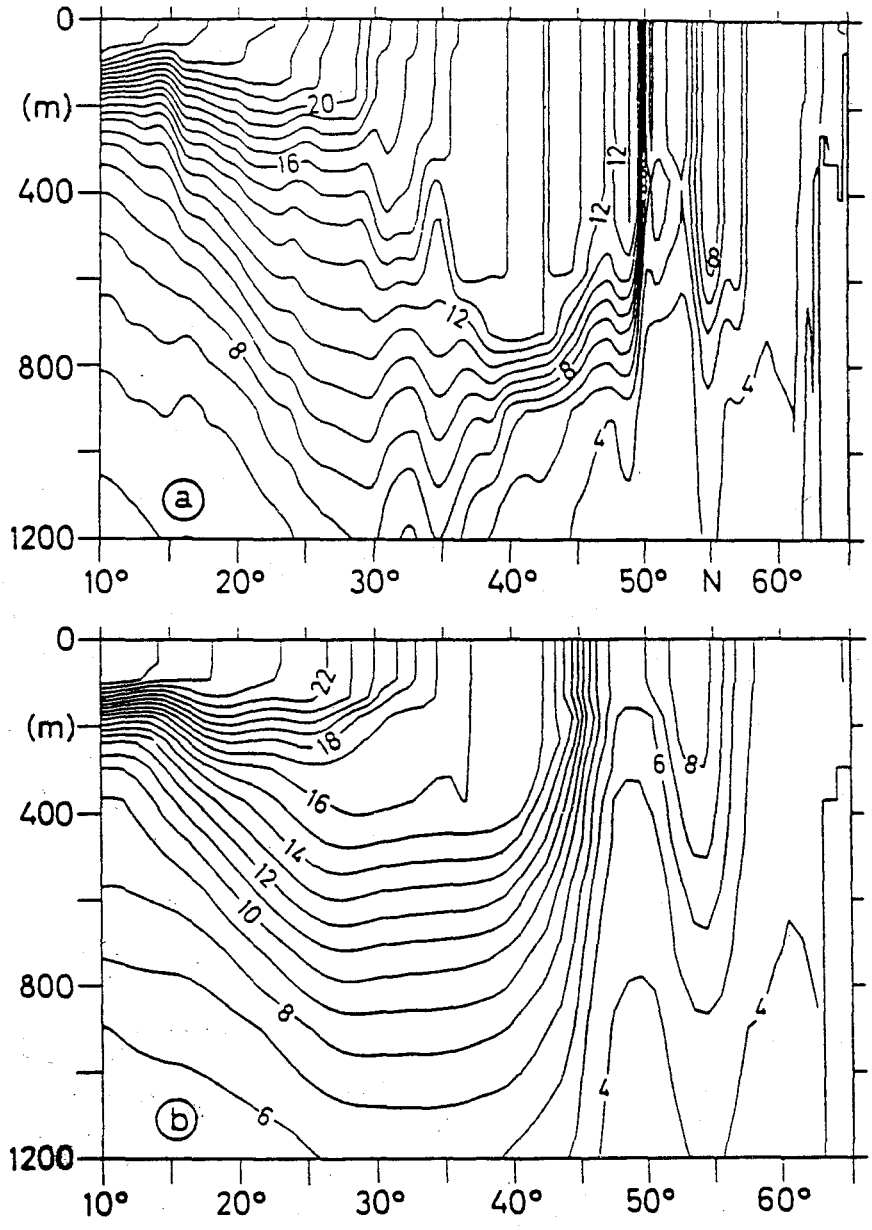

Fig. 6 Meridional sections of potential temperature in late winter (day 90) along 40° W, for a high-resolution case (a), and a medium-resolution case (b), with identical forcing.

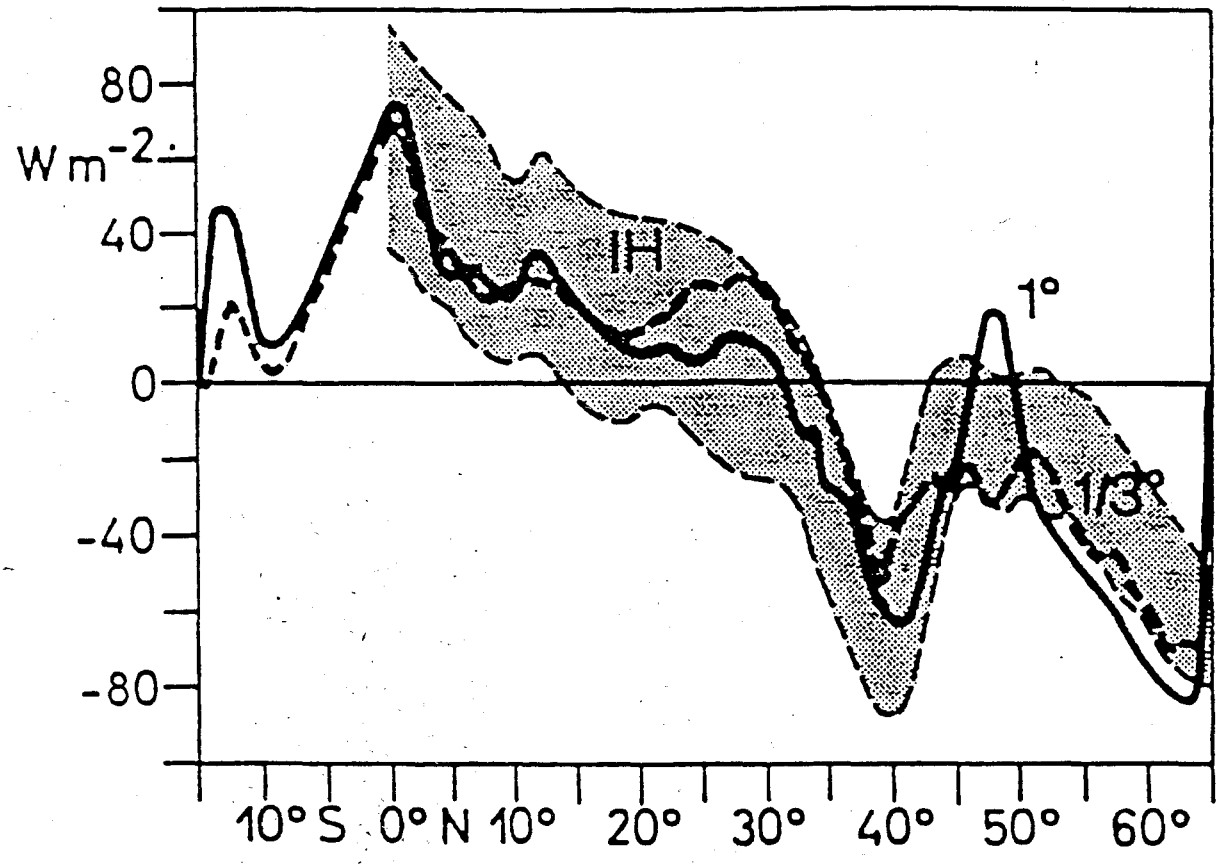

Fig. 7 Surface heat flux, zonally-averaged across the Atlantic Ocean, for the two model cases of Fig. 6; the shaded area indicates the range of uncertainty of the observed heat flux, according to Isemer and Hasse (1987).

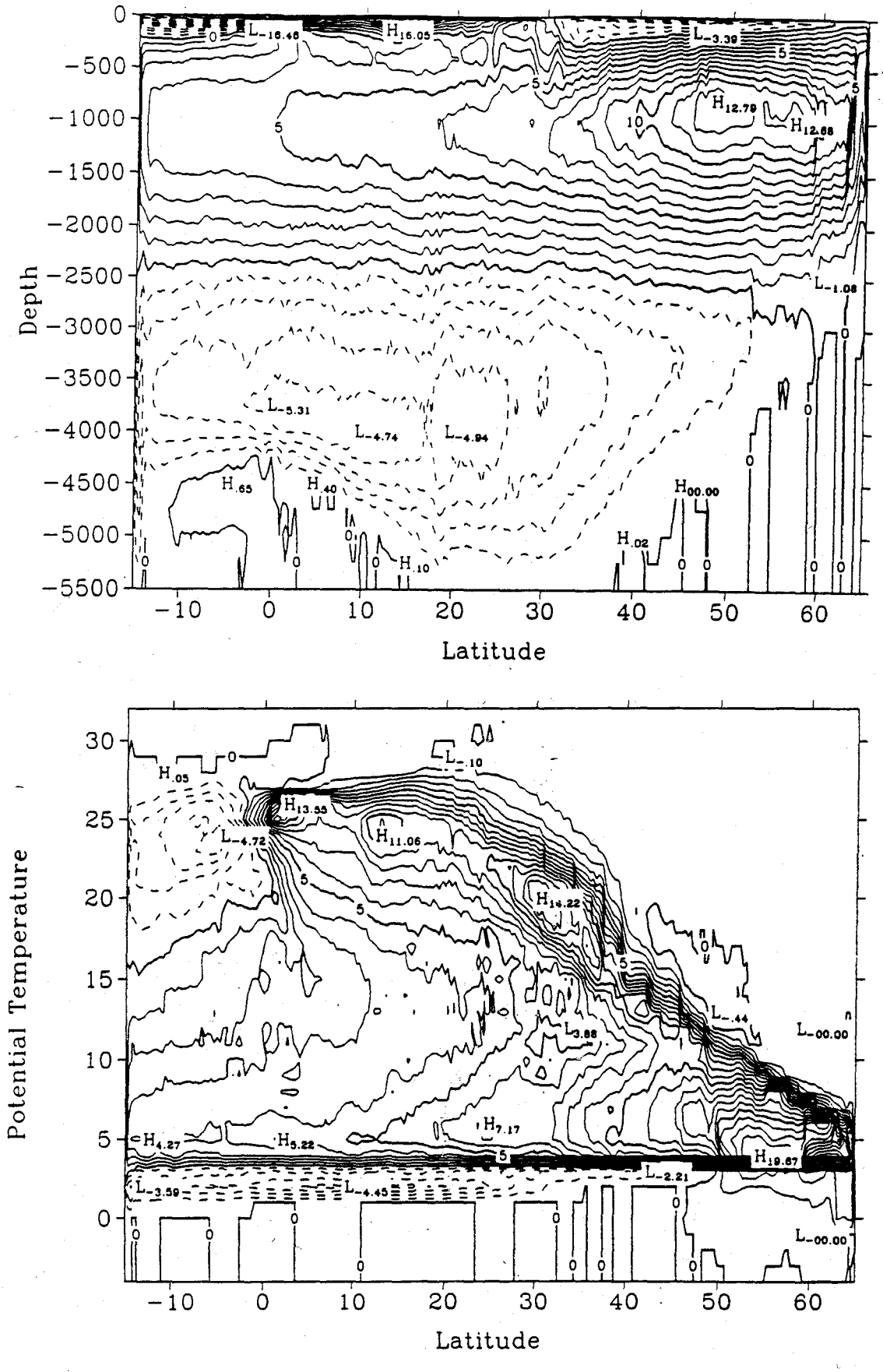

Fig. 8 Streamfunction (in Sv) of the zonally-averaged flow in (a) the latitude-depth plane, (b) latitude-potential temperature plane; for the high-resolution case in "standard" configuration (buffer zones with relaxation to Levitus' T and S).

Measuring Thermal and Velocity Structure in the Northwestern Atlantic With Acoustic Tomography

Peter Worcester
Scripps Institution of Oceanography,
University of California at San Diego
La Jolla, CA 92093

The North Atlantic Current (NAC) and its branches are key components in the transport of heat northward into the Nordic Seas and eastward toward Europe. The structure and mean properties of the NAC system, such as average pathways and mass and heat transports, and the structure, statistics, and variability of the associated mesoscale eddy field are still rather poorly known, however. A number of papers in this volume provide excellent summaries of the current state of knowledge of the NAC region, making it unnecessary to repeat a description of the NAC here. Rather, this paper focuses on two principal objectives. First, to outline a possible, but ambitious, tomographic experiment to measure both the mean and variability of a large portion of the NAC region with mesoscale resolution. This experiment would exploit the ability of a tomographic array to rapidly and repeatedly map the three-dimensional temperature and current fields of a region several hundred kilometers on a side. Second, to present early, and largely unpublished, results from recent tomographic experiments that demonstrate that tomography provides accurate measurements of ocean temperature structure, heat content, currents, and relative vorticity, and of the evolution of these quantities over time.

The tomographic experiment to be outlined is not the only one possible. A number of smaller, but still interesting, tomographic experiments with more focussed and less ambitious goals can be envisaged. Experiments with fewer instruments would either map a smaller region, such as the bifurcation region where the Gulf Stream splits into the NAC and the Azores Current, or would not be designed to map the temperature and current fields with mesoscale resolution, but rather to exploit the integrating properties of tomography. With a few instruments, for example, the seasonal cycle of heat content averaged over an area a few hundred kilometers square could be measured and its relation to surface fluxes and advection studied.

Experimental Geometry

To achieve mesoscale resolution over a significant part of the complex NAC system requires a substantial tomographic array. Figure 1 shows a strawman array design containing 16 tomographic transceivers, consisting of a mix of long-range 250 Hz units and shorter range 400 Hz units. The array as sketched is largely to the east of the main paths of the NAC and Labrador Current. It is approximately 900 km north-south and 450 km east-west and is concentrated in the northern part of the NAC system, where the mean flow is thought to be largely to the east and northeast. It is entirely in water approximately 4000 m deep.

The water properties in this region between the Azores Current, which belongs to the subtropical gyre, and the NAC, which belongs to the subpolar gyre, show a gradual transition, with tantalizing evidence of an intermediate front where the NAC curves around Flemish Cap. This simple description glosses over what appears to be an extraordinary system of fronts, currents, and eddy variability about which much is unknown, however.

The resolving properties of the array are directly evident from studying the web of ray paths between the moorings, although Fig. 1 is somewhat misleading in that for clarity it only shows a subset of the actual ray paths. If all 16 transceivers communicated, there would be n(n-1)/2 horizontal paths along which temperature and current would be measured. There would be (n-1)(n-2)/2 triangles around which the circulation, or by Stokes' theorem, the area-average relative vorticity, would be measured. The array is designed to be *coherent.* The experiment is a mapping experiment, with a sufficient density of paths to provide horizontal resolution down to roughly 50 km scales. The geometry represents a balance between the compactness needed to obtain mesoscale resolution and the large area coverage desired to measure as much of the NAC system as possible. With 16 instruments the region to be covered cannot be significantly expanded without giving up mesoscale resolution in at least some portion of the area. It is perhaps worth emphasizing that a similar number of current meter moorings distributed over the same area would form an *incoherent* array, which would provide the statistics of the flow, but would be inadequate to generate three-dimensional maps of the thermal and flow fields.

All of the tomographic transceivers would be placed at the local depth of the sound channel axis. Preliminary acoustic ray tracing using vertical sound speed profiles from the Levitus data base (Levitus, 1982) gives a number of ray arrivals for each horizontal path, with ray upper turning points at a variety of depths. The resulting vertical resolution of temperature and current for each horizontal path is very roughly equivalent to that which would be obtained by sampling at about 6 depths. The tomographic array therefore measures both the barotropic and baroclinic components of the flow. (Since the tomographic data directly provides vertical averages, heat content estimates are not aliased, however).

In a typical transmission schedule, the instruments would transmit every three hours for a day and then remain silent for two days. The travel times from the receptions would be daily averaged prior to inversion, giving three-dimensional maps of sound speed, temperature, and current at three day intervals with mesoscale resolution. The closest analogy to the type of data to be collected would be a series of Gulf Stream '60 experiments at three day intervals for a year, but with direct measurements of the barotropic and baroclinic flow fields in addition to the temperature field measurements. (Tomographic measurements are not sensitive to salinity, however.)

The strawman array shown in Figure 1 would be a large, expensive experiment. Prior to undertaking such an effort, it would be prudent to conduct a pilot study that was not mesoscale resolving, but that takes advantage of the inherent integrating properties of tomography to measure the seasonal cycle of heat content, for example, as discussed in the previous section.

Experimental Goals: Mean Properties

The region east of the Grand Banks is one of the central cross-roads of the general circulation of the North Atlantic Ocean. The northward flowing branch of the NAC feeds, through the complex system of currents in the subpolar gyre, the winter convection cells of the Greenland/Iceland/Norwegian Seas and the Labrador Sea. Thus, the NAC affects in a crucial way the thermohaline circulation of the North Atlantic Ocean. The tomographic array outlined in the previous section is designed to investigate both the mean properties of the NAC system and the eddy field associated with it. In this section we present the experimental goals for the mean properties and evidence from other experiments to show that mean quantities can be accurately measured using tomographic techniques. Eddy variability will be discussed in the next section.

The goals are:

(i) What are the mean properties of the NAC at the point of "injection" into the Northern Atlantic, roughly in the range 43-48°N, 40-45°W?

(ii) What are the mean transports of mass and heat?

(iii) Does the 10 Sv branch at about 45-46°N exist?

(iv) What are the seasonal and interannual variabilities of the mean transports of mass and heat and of heat content?

A number of recent tomographic experiments have demonstrated that the mean quantities of interest can be measured using tomographic techniques.

Temperature. While a number of experiments have shown consistency between tomographically-derived range-average sound speed (temperature) profiles and independent measurements, one of the more dramatic examples was obtained from the 1988-89 Greenland Sea Tomography Experiment (Worcester et al, 1993). Six acoustic transceivers moored in an array 200-km across transmitted to one another at four hour intervals (Figure 2). The travel times were converted to sound speed profiles using weighted least square mapping techniques ("objective mapping"). Sound speed perturbations are easily and accurately convertible to temperature perturbations, since sound speed is principally a function of temperature (see, for example, Dushaw et al, 1993a). Figure 3 shows time series of tomographically-derived, range-averaged potential temperature profiles as a function of yearday for four different propagation paths. Range-averaged profiles computed from Seasonal Ice Zone Experiment (SIZEX) data obtained on 15-16 March 1989 between moorings 1 and 6 and moorings 3 and 6 are given for comparison [SIZEX Group, 1989]. While the sparse CTD data are marginally adequate to define range averages, the comparison is generally favorable.

Figure 3 is also an example of tomography's ability to provide time series of spatial averages of the temperature field, which are difficult to obtain in any other way. Near the end of February, 1989, a sub-surface temperature maximum at several hundred meters depth disappeared over a large area of the central Greenland Sea (Figure 3). The disappearance of the subsurface temperature maximum for all of the source-receiver pairs shows that a substantial area of the gyre is modified to roughly 700-1000 m depth, although the maximum depth of mixing is not well-resolved by the tomographic data. Surprisingly, the mixing process is not associated with a simple homogeneous water column. The potential temperature at 1000 m remained warmer than the surface value throughout February and March, when averaged over paths 1-6, 3-6, and 4-5. The most nearly homogeneous temperature structure was found between moorings 4 and 6, but even there the surface generally remained cooler than the deeper water.

Heat content. Since the tomographic data are inherently integral measurements, integral quantities such as heat content are more accurately measured than are quantities defined at a point, such as temperature. Using data from a 1987 experiment in the north central Pacific Ocean, Dushaw et al. (1993a) obtained excellent agreement between heat content deduced from tomographic measurements and from concurrent CTD/XBT measurements along the acoustic paths. Comparisons were made in the upper 100 m and in the upper 2000 m for path lengths of 745, 995, and 1275 km. The measurements were also consistent with climatological trends derived from historical XBT data (Figure 4).

Current. Fewer quantitative comparisons between tomographically-derived currents and independent measurements have been made than temperature comparisons. Deployment of an array of current meters is more difficult and expensive than making a CTD and/or XBT section. Fortunately, the ocean provides an excellent test signal with which tomographically-derived currents can be compared - the barotropic tides. The tides are sufficiently large scale to be nearly constant over path lengths of about 1000 km in mid-ocean. They are sufficiently well-known to serve as a reference signal. Table 1 shows that tomographically-derived barotropic tidal currents from the 1987 Reciprocal Tomography Experiment mentioned above are in excellent agreement with barotropic tidal currents derived from a current meter mooring along one of the paths and with the predictions of tidal models due to Schwiderski (1980) and Cartwright et al. (1992) (Dushaw, 1993b).

Comparisons between low-frequency, range-averaged currents derived tomographically and low-frequency currents derived from a single current meter mooring somewhere along the acoustic path have also been done. While one does not expect agreement in detail, since the comparison is between a point measurement and a range-average, the similarities and differences between the two measurements are still instructive. For example, daily-averaged differential travel times between moorings 1 and 6 of the 1988-89 Greenland Sea Tomography Experiment were inverted and the resulting time series of current low-pass filtered to obtain the low-frequency current component along the line between the moorings. The barotropic component from the differential travel time inversion compares favorably with a simple depth-weighted average current over the upper 2000 m constructed using ADCP data from mooring 6 obtained by Schott et al. (1993) (Figure 5). The inverse procedure gives an uncertainty of ±0.7 cm/s for the barotropic component of the inversion. The degree of similarity is surprising since the tomographic result represents an average over the 106 km separation between moorings 1 and 6, while the ADCP result is a point measurement. (ADCP data from 200 m depth show a lack of coherence at separations of 50-100 km (Schott et al., 1993).) One difference that is immediately evident, however, is that the tomographic result contains substantially less high frequency energy than the ADCP depth-weighted average. Power spectra show that the spatial averaging inherent in the tomographic data has substantially suppressed energy with 10-20 day periods. Equally striking is the long time period with a southward velocity component, from October 1988 until March 1989. This result was unexpected, since mooring 6 is roughly in the center of the cyclonic Greenland Sea gyre, suggesting that the radial component of flow should be small.

Experimental Goals: Variability

Not only are the mean properties of the NAC still poorly known, but the details of how it changes in time are even more uncertain. Figure 6 shows a composite sea-surface temperature in the NAC region on 24-25 August 1984. The NAC shows up clearly, but not as a simple jet that is a continuation to the east of the Gulf Stream. Rather, the surface temperature pattern is very complex, with filaments and offshoots toward both sides of the current. Resolution of the NAC frontal structure is critical to understanding the cross-frontal exchange processes. Understanding the NAC system structure and its time variability will be possible only if processes such as path switching, ring formation, jet filamentation and shingles, and the interactions between the mean jet and the associated mesoscale eddy field, can be resolved in their detailed structure, mapped, and quantified.

The goals are:

(i) What are the characteristic space/time scales of the NAC mesoscale eddy field?

(ii) What are its statistics (kinetic and potential energies, variances)?

(iii) What are the eddy-mean flow interactions of the system?

(iv) Does the eddy field feed the mean flow or is it instead enhanced by baroclinic instability processes?

(v) What is the relationship between the Eulerian mean and eddy fields evaluated from tomography and their Lagrangian counterparts evaluated from float data?

A number of recent tomographic experiments have demonstrated that the variability of interest can be measured using tomographic techniques.

Statistical measurements. Figure 7 shows five tomographic transceivers that were deployed in a pentagon from October 1988 through August 1989 to study the eddy radiation field to the south of the Gulf Stream (Chester et al., 1993). The major scientific objective of the experiment was to proceed a step beyond estimates of the mean quantities and to determine second order quantities such as eddy kinetic energy, eddy variance, and eddy heat flux. Moreover, the experiment was purposely designed to be a *validation* experiment, with the tomographic transceivers located near five current meter moorings,.

Table 2 compares eddy second moments and average and perturbation quantities computed from the current meter and tomographic measurements. Tomographic estimates of eddy energy, Reynolds stresses, and eddy heat flux compare well with the estimates of similar quantities obtained from traditional current meter measurements. Figure 8 compares velocity and relative vorticity spectra derived tomographically and derived from current meter data. The velocity spectral estimates show a very similar structure and energy levels, exhibiting the red nature of the velocity spectrum in the region. The two relative vorticity spectra are similar at low frequency, but the tomographic estimate has less energy at high frequencies. This is as expected since the shorter period fluctuations corresponding to smaller wavelength motions are filtered out by the spatial averaging of the tomographic measurement.

The tomographic estimates of the second order statistics presented above can be used to diagnose properties of eddy-mean flow interactions. Plumb has generalized the normal Eliassen-Palm flux vector to three-dimensions. The resulting flux vector is a conservable measure of the flux of eddy activity and is parallel to the group velocity for an almost plane-wave train. Figure 9 presents a schematic of the wave vectors computed for the SYNOP tomography experiment. Three planar sections have been extracted from the fluid cube in which the tomographic array is embedded. The wave activity flux is directed southward in the plan views at 500 m and 1000 m, indicating that the source of the eddy energy is to the north of the tomographic array, in the region of the Gulf Stream.

Mapping. The most extensive comparison between sound speed (temperature) maps generated tomographically and generated from more traditional measurements was done in the 1991-92 Acoustic Mid-Ocean Dynamics Experiment/Moving Ship Tomography Experiment (AMODE-MST) (AMODE-MST Group, 1993). The AMODE-MST Experiment employed six transceiver moorings deployed in an array 700 km across between Bermuda and Puerto Rico. During June-July 1991 a receiving array was lowered from shipboard at 3-hour intervals as the ship steamed around a circle 1000 km

in diameter centered on the central source. Two complete circumnavigations of the array were completed. Extensive AXBT surveys were done in June and July to provide temperature fields with which the tomographic results can be compared. A preliminary sound speed perturbation field at 700 m computed from the moving ship tomography data is in agreement with that computed from the AXBT surveys, to within the estimated uncertainty of the difference (Figure 10). The tomographic map covers a much larger area than it was feasible to map using AXBT's, however.

Conclusions

The results presented above show that tomography is now a mature technique that can be used as another tool to study the ocean, just as one uses more traditional oceanographic instrumentation, such as current meter moorings and Lagrangian floats. Tomography provides a picture that is complementary to the ones provided by other observational tools. Utilizing a tomographic array to rapidly and repeatedly map the three-dimensional temperature and current fields of the complex NAC system in a region several hundred kilometers on a side would provide information on the mean properties and variability of the system difficult to obtain in any other way.

Acknowledgments

This paper draws freely from a number of unpublished manuscripts. The willingness of the authors to make material available prior to publication is greatly appreciated.

References

AMODE-MST Group: T.G. Birdsall, J. Boyd, B.D. Cornuelle, R. Davis, B.M.Howe, R. Knox, J.A. Mercer, K. Metzger, Jr., W.H. Munk, R.C. Spindel, and P.F. Worcester (1993). Moving ship tomography in the northwest Atlantic Ocean, EOS, in preparation.

Cartwright, D. E., R. D. Ray, and B. V. Sanchez (1992). A computer program for predicting oceanic tidal currents, NASA Tech. Memo. 104578, Goddard Space Flight Center, Greenbelt, Maryland, 21 pp.

Chester, D., P. Malanotte-Rizzoli, J. Lynch, and C. Wunsch (1993). The eddy radiation field of the Gulf Stream as measured by ocean acoustic tomography, Geophys. Res. Letters, in press.

Dushaw, B.D., P.F. Worcester, B.D. Cornuelle, and B.M. Howe (1993a). Variability of heat content in the North central Pacific in summer 1987 determined from long-range acoustic transmissions, J. Phys. Oceanogr., in press.

Dushaw, B.D., P.F. Worcester, B.D. Cornuelle, and B.M. Howe (1993b). Barotropic currents and vorticity in the North central Pacific in summer 1987 determined from long-range acoustic transmissions, J. Geophys. Res., submitted

Levitus, S. (1982).Climatological Atlas of the World Ocean, NOAA Professional Paper 13, 173 pp.

Schott, F., M. Visbeck, and J. Fischer (1993). Observations of vertical currents and convection in the central Greenland Sea during the winter of 1988/89. J. Geophys. Res., in press.

Schwiderski, E. W. (1980). Ocean tides. I. Global tide equations. II.A hydrodynamical interpolation model, Mar. Geod., 3, 161-255.

SIZEX Group (1989). SIZEX 89 Experiment Report, The Nansen Remote Sensing Center Technical Report 23, 39 pp., The Nansen Remote Sensing Center, Bergen, Norway..

Worcester, P.F., J.F. Lynch, W.M.L. Morawitz, R. Pawlowicz, P.J. Sutton, B.D. Cornuelle, O.M. Johannessen, W.H. Munk, W.B. Owens, R. Shuchman, and R.C. Spindel (1993). Evolution of the large-scale temperature field in the Greenland Sea during 1988-1989 from tomographic measurements, Geophys. Res. Letters, in press.

Wyrtki, K., and L. Uhrich (1982). On the accuracy of heat storage computations. J. Phys. Oceanogr., 12, 1411-1416.

Table 1. Amplitude and Greenwich Epoch of the eastward barotropic tidal current components for the north leg. The CRS model is the Cartwright, Ray, and Sanchez model.

Tidal Component		Acoustic Tomography	Current Meter Mooring	Schwiderski Model	CRS Model
M_2	cm/s	1.31±0.03	1.32±0.09	1.28	1.42
	°G	223±1	218±4	222	218
S_2	cm/s	0.53±0.04	0.53±0.10	0.66	0.63
	°G	272±4	280±11	270	276
N_2	cm/s	0.14±0.03	0.15±0.09	0.16	0.15
	°G	191±13	216±35	184	201
K_2	cm/s	0.12±0.04	0.10±0.07	–	0.14
	°G	268±13	280±41	–	279
O_1	cm/s	0.43±0.03	0.46±0.05	0.33	0.38
	°G	101±4	122±7	99	104
K_1	cm/s	0.75±0.04	0.74±0.06	0.45	0.53
	°G	128±2	135±5	127	100
P_1	cm/s	0.18±0.04	0.27±0.04	–	0.10
	°G	132±11	141±8	–	129
Q_1	cm/s	0.10±0.03	0.07±0.03	–	0.05
	°G	64±16	110±28	–	125

Table 2. Comparison of mesoscale fluctuations in temperature, current, and relative vorticity determined acoustically during the SYNOP tomography experiment and from concurrent current meter measurements. All comparisons are for 1000 m depth, except for the mean relative vorticity computed from the current meter measurements, which is for 550 m depth, due to the distribution of current meters.

Units	cm^2/s^2	cm^2/s^2	$(°C)^2$	°C cm/s	s^{-1}	s^{-1}
Measurement	$\frac{u'^2+v'^2}{2}$	$\overline{u'v'}$	$\overline{T'}^2$	$\overline{v'T'}$	$\bar{\zeta}$	ζ'
Current Meter	114	-23.0	0.22	-2.9	-2.1×10^{-6}†	–
Tomography	132	-18.3	0.31	-3.6	-2.1×10^{-6}	1.5×10^{-5}

† (@550 m)

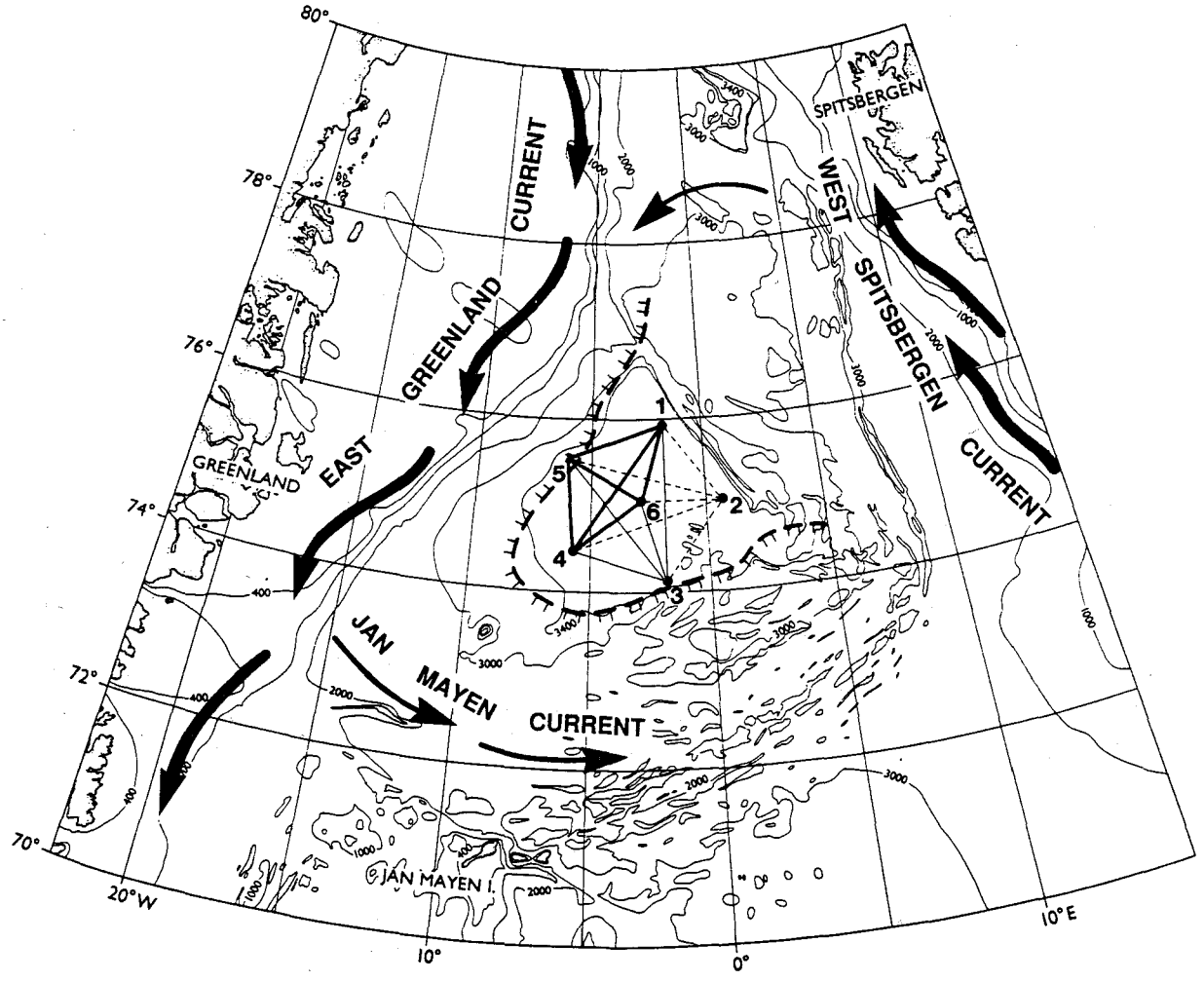

Fig. 2. Geometry of the Greenland Sea Tomography Experiment, showing the tomography transceiver locations and the principal surface currents in the experimental area. The array was within the cyclonic Greenland Sea gyre. Heavy solid lines connect acoustic transceivers. Light solid lines indicate ray paths for which one way travel time data were obtained. The dashed lines are ray paths emanating from mooring 2, which failed 20 days after deployment, but gave reciprocal data until that time. The 20% ice edge on 15 March 1989, derived from SSM/I data, is also shown. (Reproduced from Worcester *et al.*, 1993.)

Fig. 3. Time series of range-averaged potential temperature profiles along 4 paths of the tomographic array. Total ice concentrations in % (from SSM/I data) at the path endpoints are plotted below the images. Range-averaged profiles computed from Seasonal Ice Zone EXperiment (SIZEX) data obtained on 15–16 March 1989 between moorings 1 and 6 and moorings 3 and 6 are given for comparison [SIZEX Group, 1989]. Comparisons with point measurements from temperature sensors on the moorings are also favorable except during the early winter when acoustic conditions are severely degraded by the ice. (Reproduced from Worcester *et al.*, 1993.)

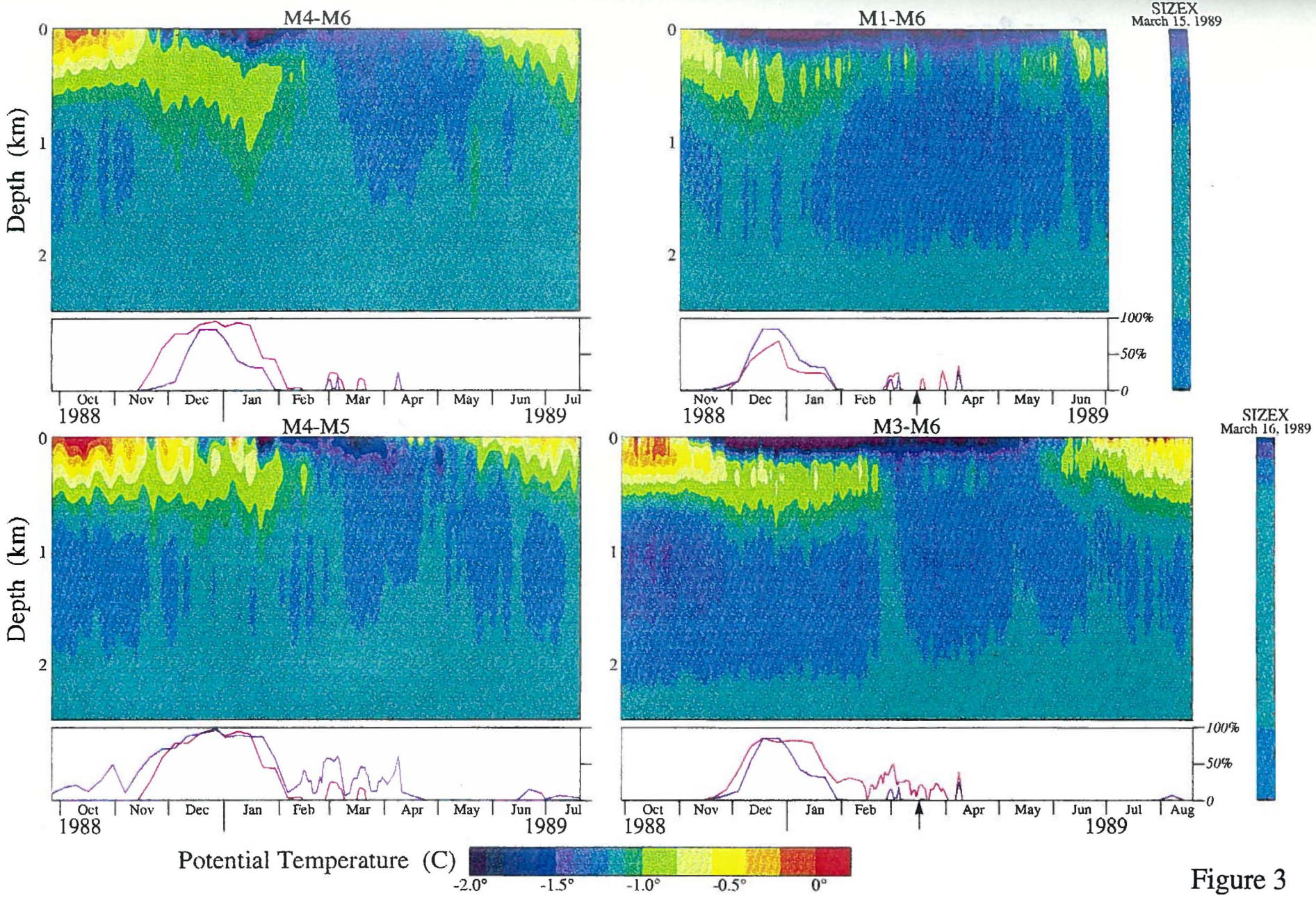
M4-M6
M1-M6
SIZEX
March 15, 1989
Depth (km)
0
1
2
100%
50%
0
Oct
Nov
Dec
Jan
Feb
Mar
Apr
May
Jun
Jul
Aug
1988
1989
M4-M5
M3-M6
SIZEX
March 16, 1989
Potential Temperature (C)
-2.0°
-1.5°
-1.0°
-0.5°
0°

Figure 3

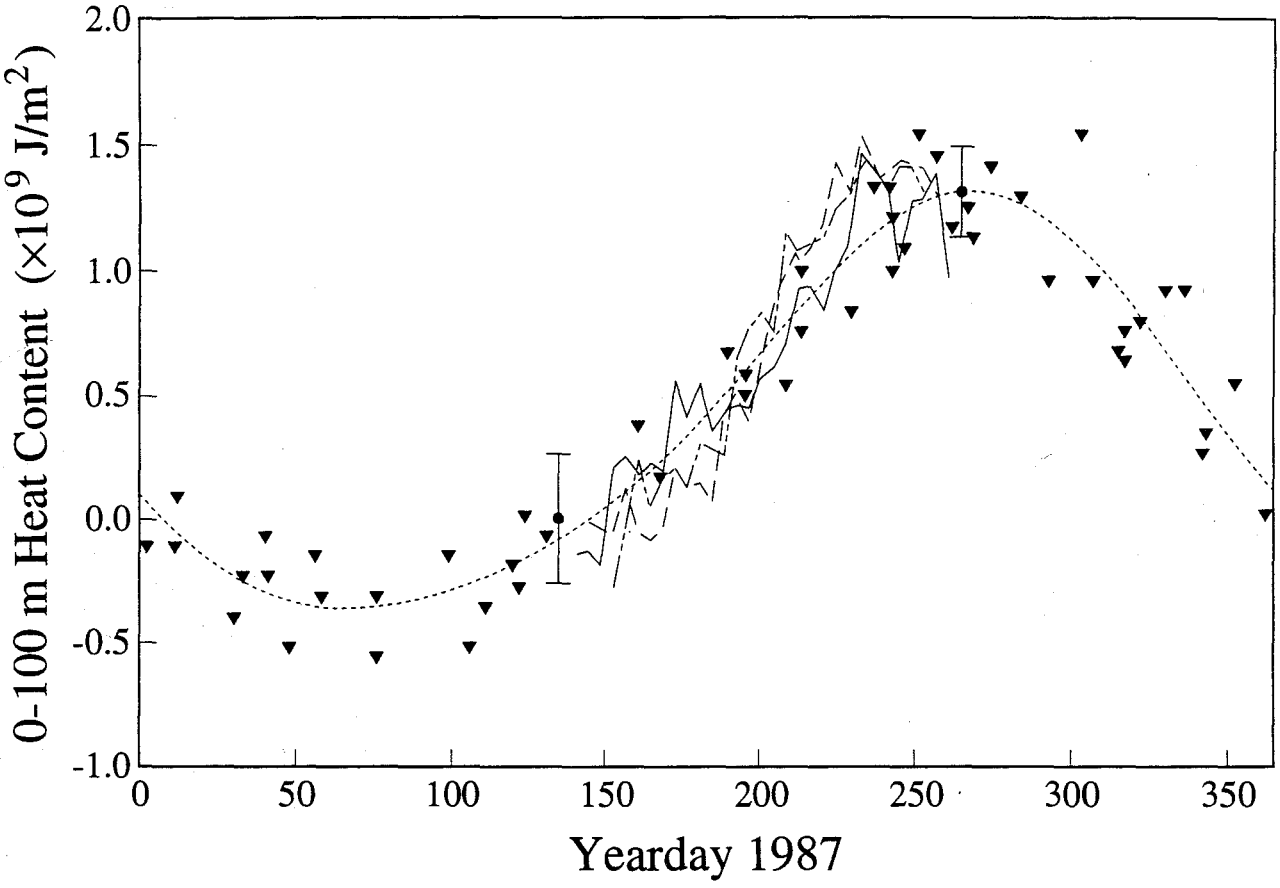

Fig. 4. Comparison of the heat content change in the top 100 m determined acoustically during the 1987 Reciprocal Tomography Experiment in the north central Pacific Ocean with the XBT results compiled by Wyrtki and Uhrich (1982). Heat content is shown for the three legs of the tomographic triangle (solid is the north leg, 745 km range; dash is the east leg, 995 km range; and dash-dot is the west leg, 1275 km range). Beginning and ending error bars of the acoustically derived heat content are shown. The triangles are heat content derived from individual XBT sections; the dotted curve is the annual cycle determined from the XBT data. The XBT and acoustic results have been aligned to zero at the start of the acoustic time series. The change in heat content determined acoustically is consistent with the annual cycle determined by Wyrtki and Uhrich. (Modified from Dushaw *et al.*, 1993a.)

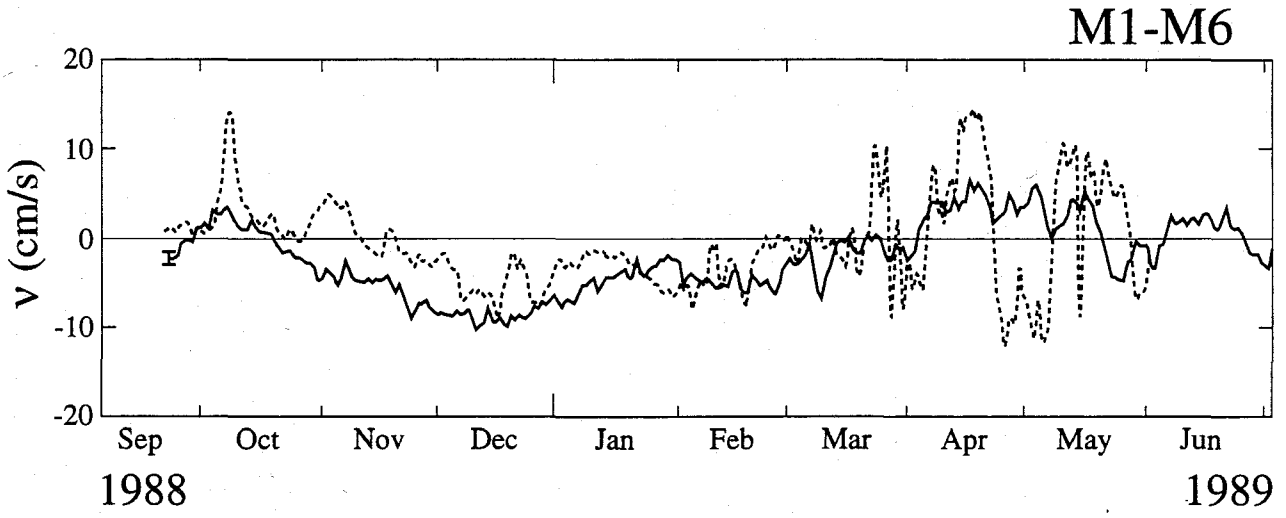

Fig. 5. Depth average current between moorings 1 and 6 in the 1988–89 Greenland Sea Tomography Experiment. The solid curve was constructed from differential travel times between moorings 1 and 6, while the dashed curve is the component of flow parallel to the line between moorings 1 and 6 constructed from ADCP measurements on mooring 6 (Schott *et al.*, 1993). Differential travel times are only sensitive to the component of flow parallel to the ray paths. Positive velocity is to the north. Both series were low pass filtered to remove tidal energy. (Courtesy of the Greenland Sea Tomography Group.)

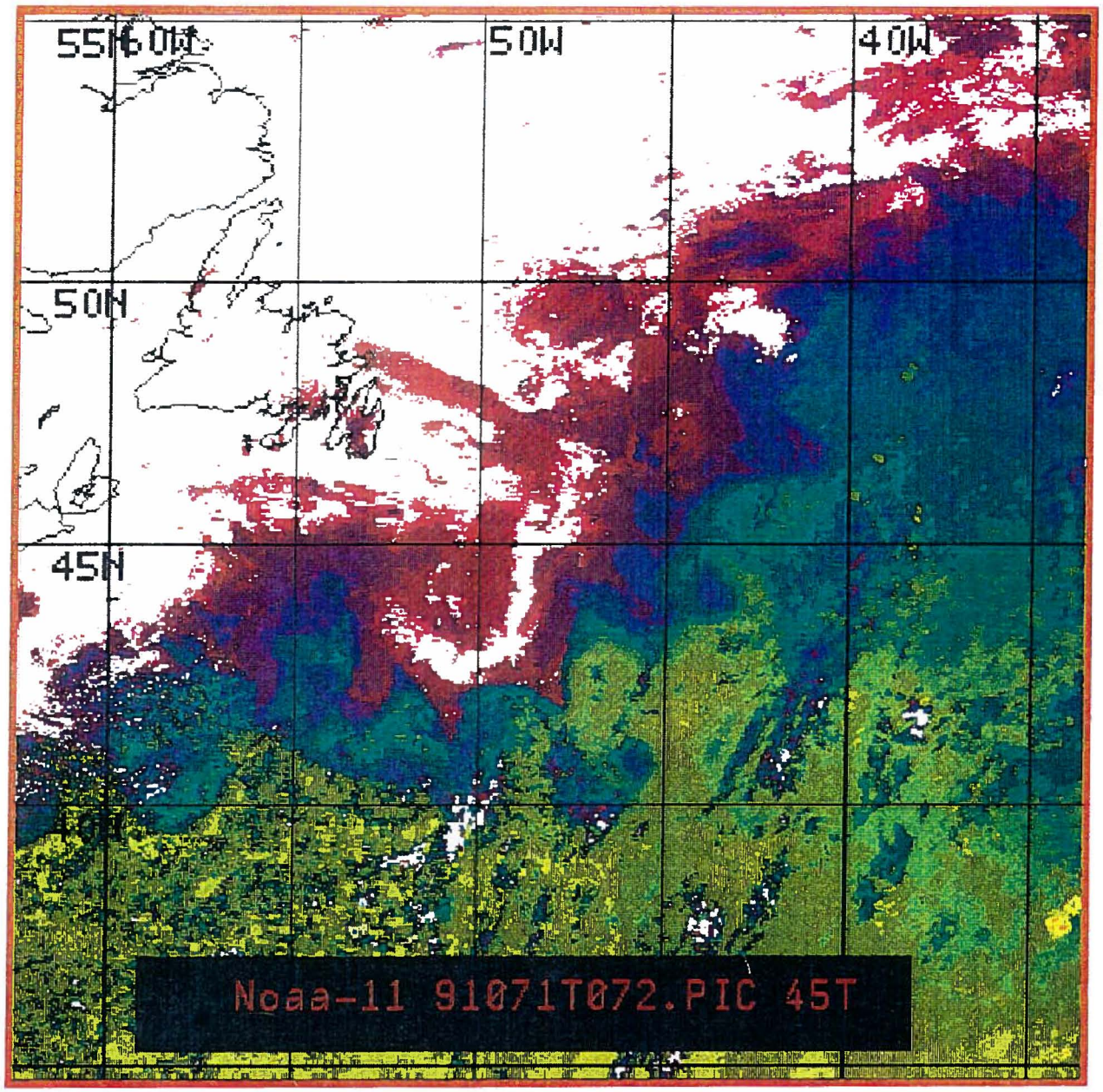

Fig. 6. Composite sea-surface temperature in the NAC region on 24–25 August 1983, showing the complex surface pattern. (Courtesy of R. Watts and P. Cornillon.)

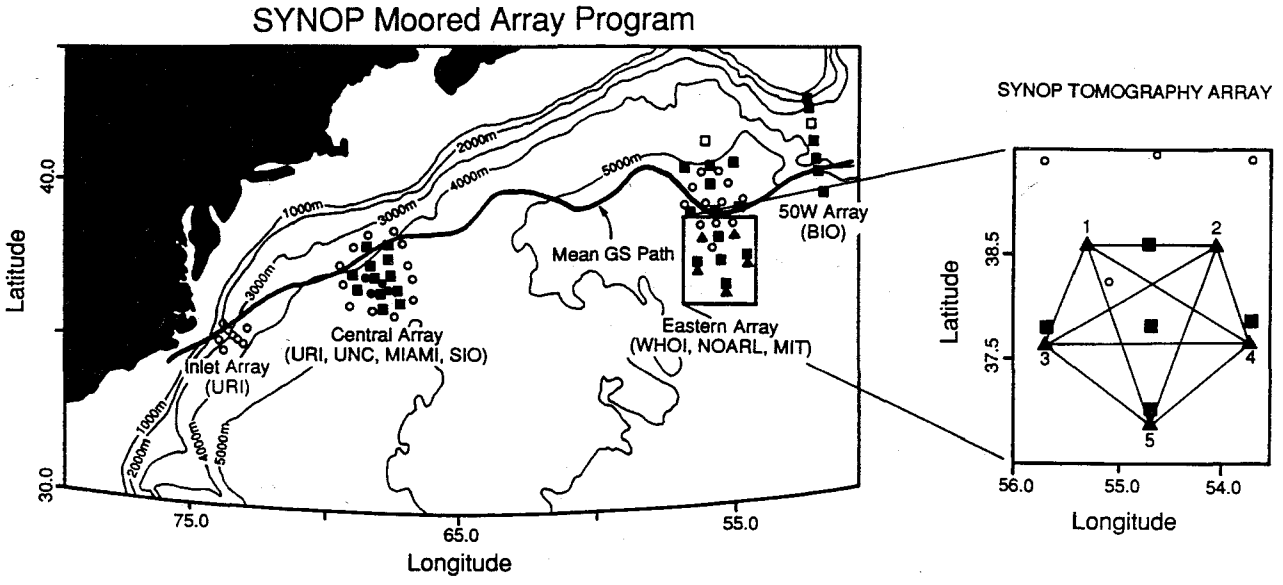

URI.....University of Rhode Island
BIO.....Bedford Institute of Oceanography
MIT.....Massachusetts Institute of Oceanography
NOARL...Naval Oceanographic and Atmospheric Research Laboratory
UNC.....University of North Carolina
SIO.....Scripps Institute of Oceanography
WHOI...Woods Hole Oceanographic Institute

Fig. 7. Observational plan of the Synoptic Ocean Prediction (SYNOP) Experiment. The field work consisted primarily of three arrays — the inlet, central, and eastern arrays. Solid blocks: locations of current meter moorings. The solid triangles in the square comprising the southern portion of the eastern array indicate the location of the tomographic transceivers. A blow-up of this square, of which the tomographic array was part, is to the right of the full plan. (Reproduced from Chester *et al.*, 1993.)

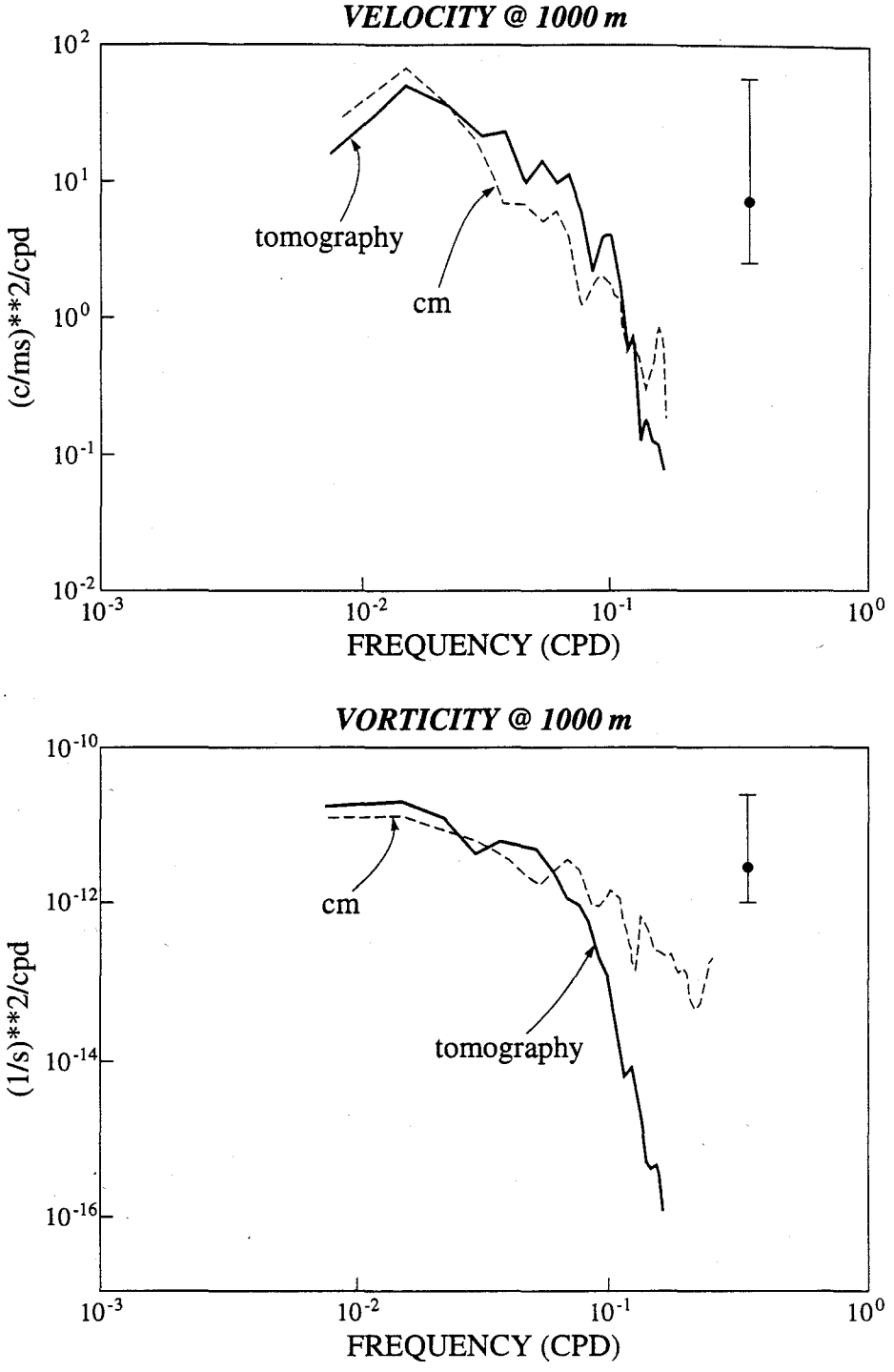

Fig. 8. Spectra of current (top) and relative vorticity (bottom) at 1000 m depth. The velocity spectrum derived from the tomographic measurement between moorings 2 and 5 (solid line) is compared with the velocity spectrum derived from daily averaged velocities measured at a current meter in the center of the tomographic array (dashed line) in the top panel. The relative vorticity spectrum derived from the tomographic measurement over the quadrilateral 2-3-4-5 of Fig. 7 (solid line) is compared with the relative vorticity spectrum derived from nearby current meters in the bottom panel. (Reproduced from Chester *et al.*, 1993.)

ELIASSEN – PALM FLUX VECTOR

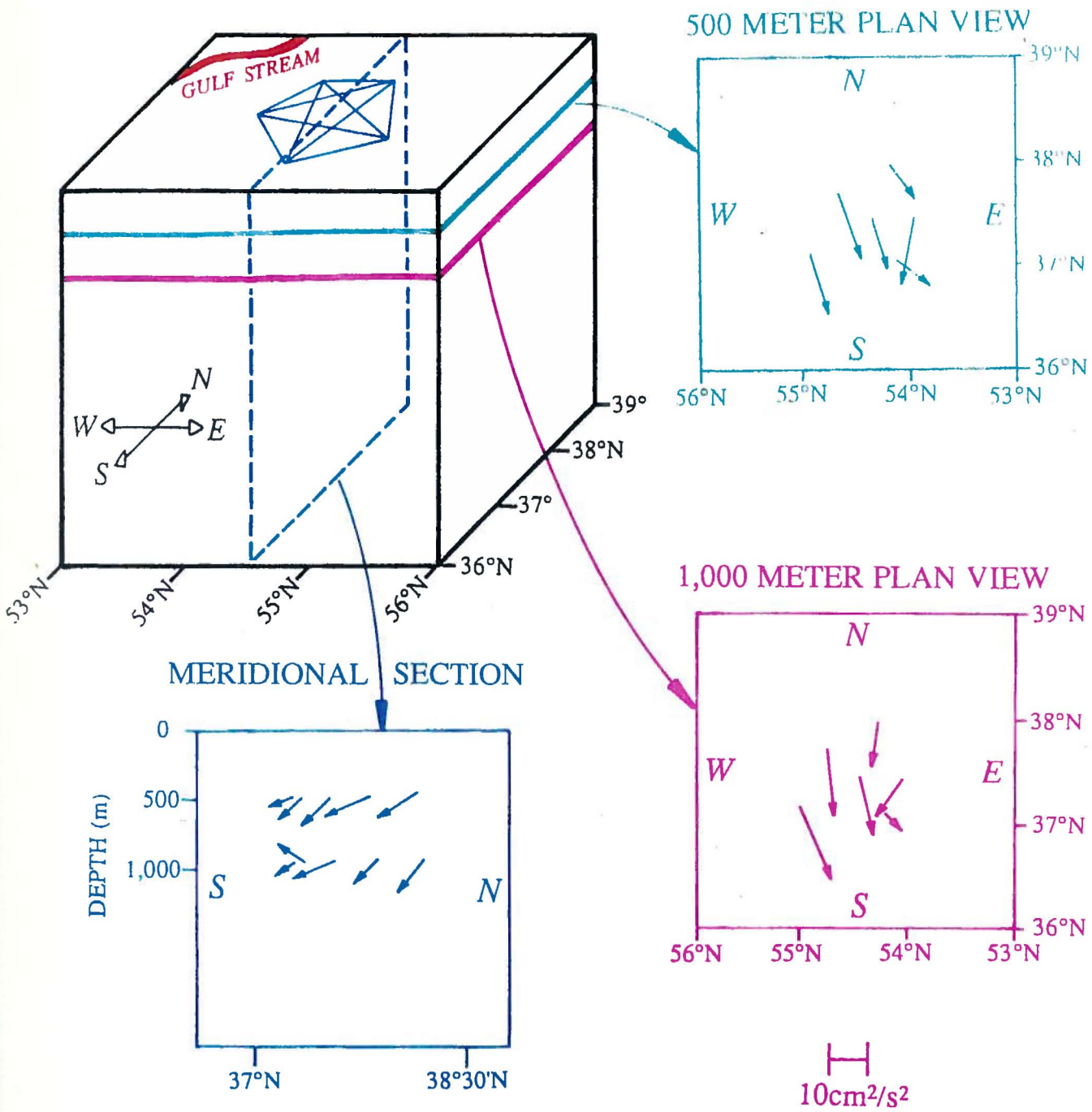

Fig. 9. A schematic of the generalized Eliassen-Palm flux vectors for the SYNOP tomography array. The flux vectors have been projected onto horizontal planes at 500 m and 1000 m depths and onto a north-south vertical slice that cuts the array in the middle. (Reproduced from Chester *et al.*, 1993.)

ELIASSEN – PALM FLUX VECTOR

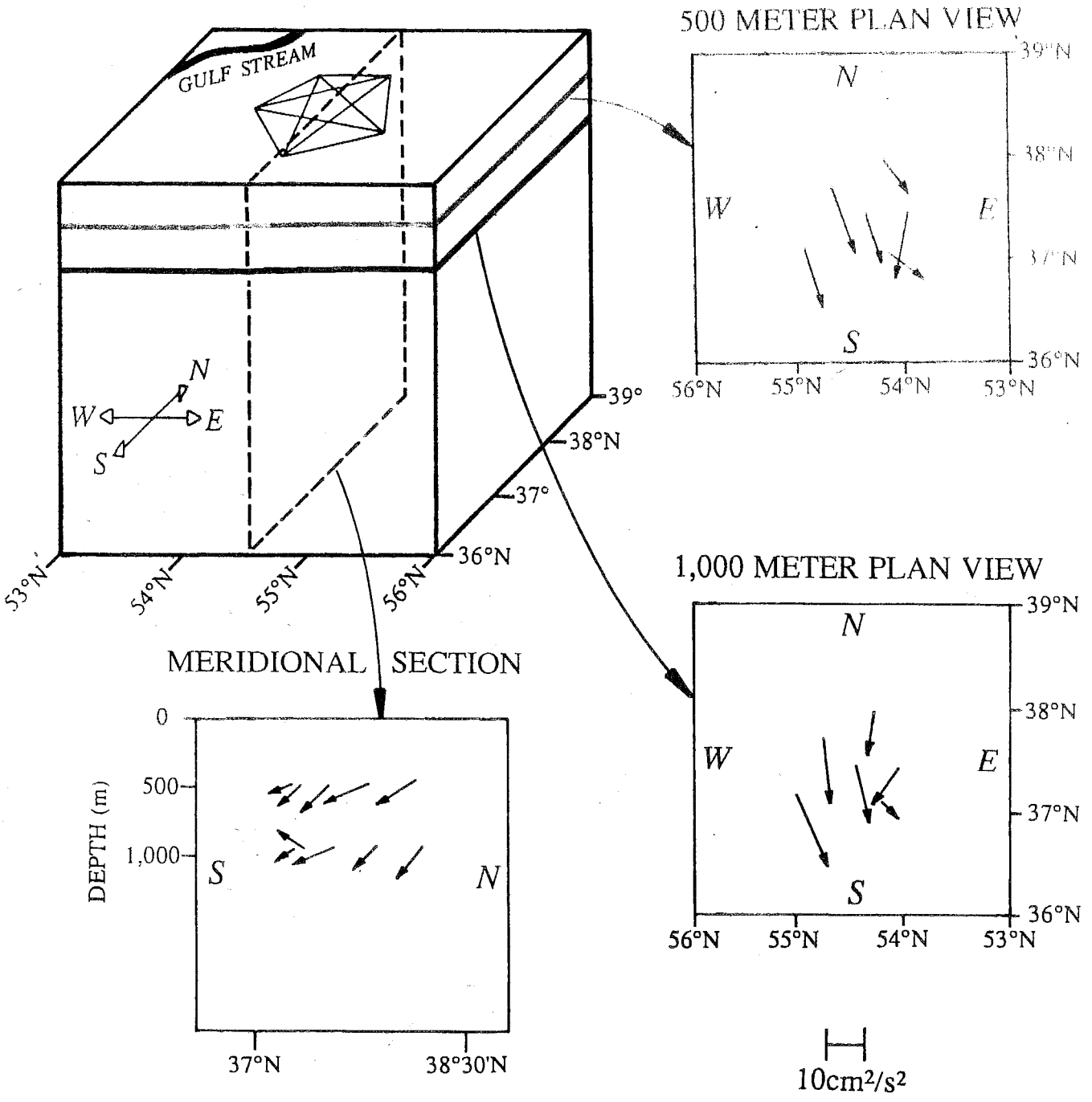

Fig. 9. A schematic of the generalized Eliassen-Palm flux vectors for the SYNOP tomography array. The flux vectors have been projected onto horizontal planes at 500 m and 1000 m depths and onto a north-south vertical slice that cuts the array in the middle. (Reproduced from Chester *et al.*, 1993.)

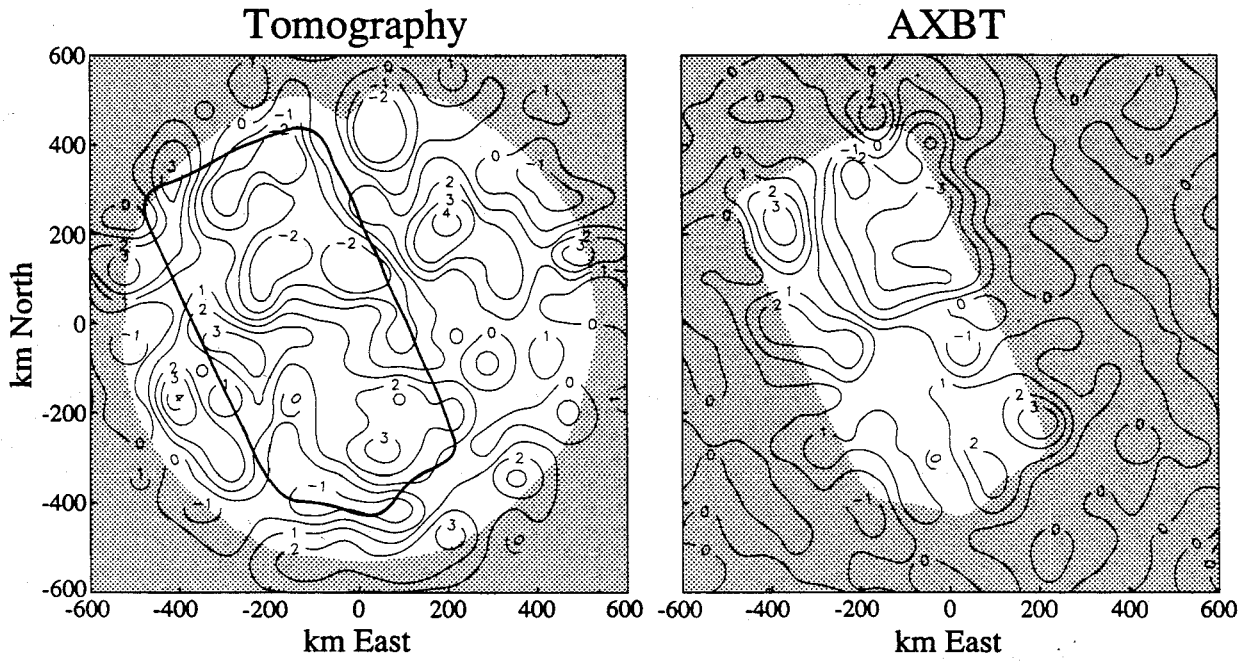

Fig. 10. Sound speed perturbation field at 700 m during the 1991–92 AMODE/MST tomography experiment determined tomographically and from an AXBT survey. The tomographic map combines data from 93 ship stops performed between 8–26 July 1991, while the AXBT survey was performed between 14–22 July 1991. The contour interval is 1 m/s (roughly 0.2°C). In the stippled regions the estimated uncertainty exceeds 1 m/s. The 1 m/s estimated uncertainty contour for the AXBT data is plotted on the tomographic map to make comparison easier. (Courtesy of the AMODE–MST Group.)

VIII. EXTENDED ABSTRACTS

The North Atlantic Current and its Associated Eddy Field: Observations and Model Results

W. Krauss, Kiel University
Germany

The NAC is a continuation of the Gulf Stream south of the Grand Banks of Newfoundland. Is is associated with a strong thermohaline front which separates western North Atlantic central water from Labrador Current water and slope water. Temperature and salinity differences across the current in the upper 500 m reach 15°C and 3‰, respectively and very intensive mixing takes place between these water masses. The current turns around Flemish Cap and follows mainly the 4000 m contour towards north. Between 51°N and 52°N it suddenly turns towards east, loses its frontal character after crossing the Mid-Atlantic ridge and becomes a broad gentle flow towards the Faroe-Shetland Channel and Island. Across the MAR it transports about 25 Sv (Fig. 1). This picture is supported by the mean climatology (Levitus data set) by inverse models, altimeter data, surface drifters and SST.

Contrary to that, Schmitz and McCartney (Rev. of Geophys. 31, 1993) try to reestablish the concept of the Worthington gyre, which shows the NAC as an anticyclonic gyre separated from the Gulf Stream. We have no evidence for the existence of such a gyre. Fig. 2 displays the stream function of the mean currents for the central North Atlantic as derived from drifter data drogued at 100 m depth (more than 36000 buoy days). Also shown is the Worthington gyre. This gyre is a misinterpretation of the very intensive eddy field on the warm side of the NAC. This eddy field is known to be very vigorous. It is seen in hydrographic surveys in the Newfoundland Basin, in altimeter data and surface drifters.

Numerical models perform badly in the area of the NAC. One obvious reason for that is the highly smoothed Levitus climatology which is used in these models. In models with coarse resolution the NAC does not turn around Flemish Cap but flows south of the Grand Banks straight towards east or northeast.

Eddy resolving models show the peculiarity that the main water masses of the NAC flow through Flemish Pass instead of surrounding Flemish Cap along the continental slope. Furthermore, eddy intensity is not properly modeled even in models with a resolution of 1/6°.

Problems which have to be solved are among others:

- Why do numerical models badly perform in the northern North Atlantic compared to the Subtropics?

- Why does the NAC flow into the northwest corner and suddenly turn eastward at 51°-52°N?

- By which mechanism are the anticyclones produced at the offshore side of the NAC?

- What mechanism separates the Azores Current from the NAC?

- Is the continental slope of Newfoundland an area where major amounts of North Atlantic Deep Water are produced by mixing?

- Does the NAC gain kinetic energy from the contrast between Labrador Current and Gulf Stream water?

In order to solve these problems and to improve our knowledge on the thermohaline circulation in the North Atlantic, major field studies and numerical modeling are required.

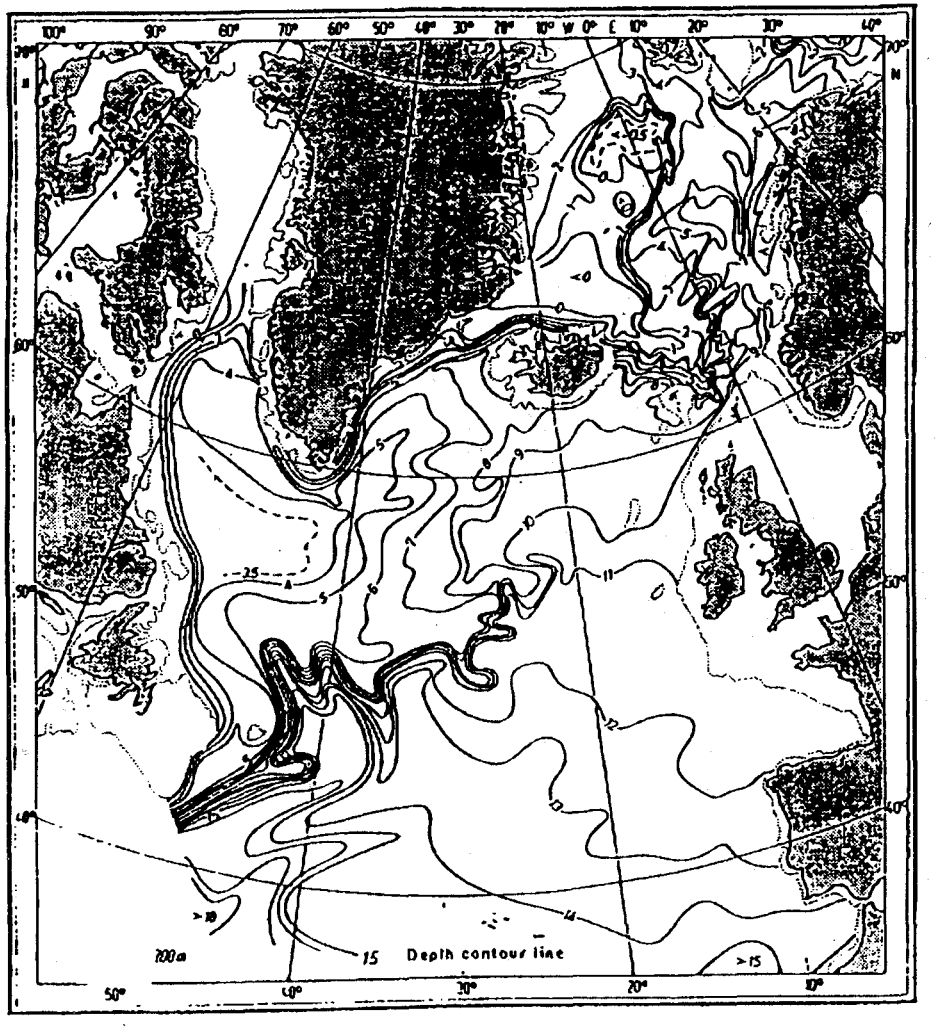

Fig. 1a: T°C at 200 m depth (IGY 1957/58)

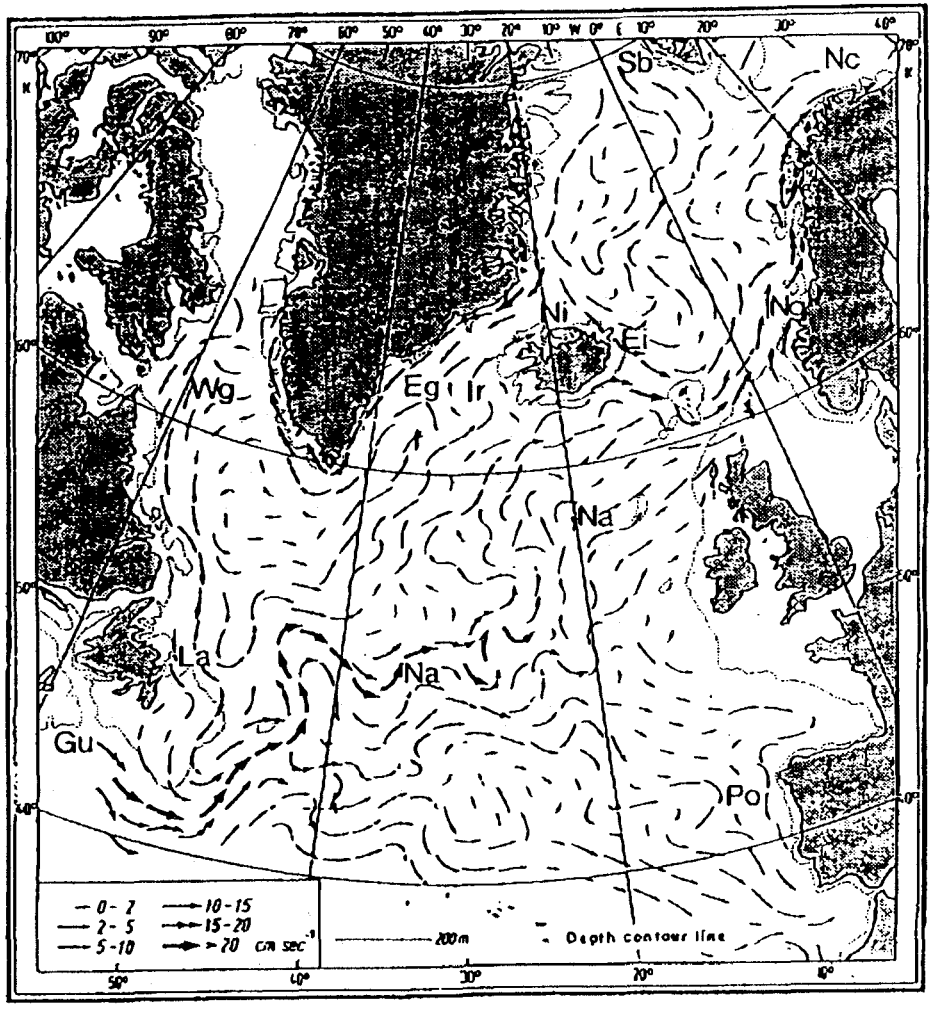

Fig. 1b: Geostrophic currents (IGY 1957/58)

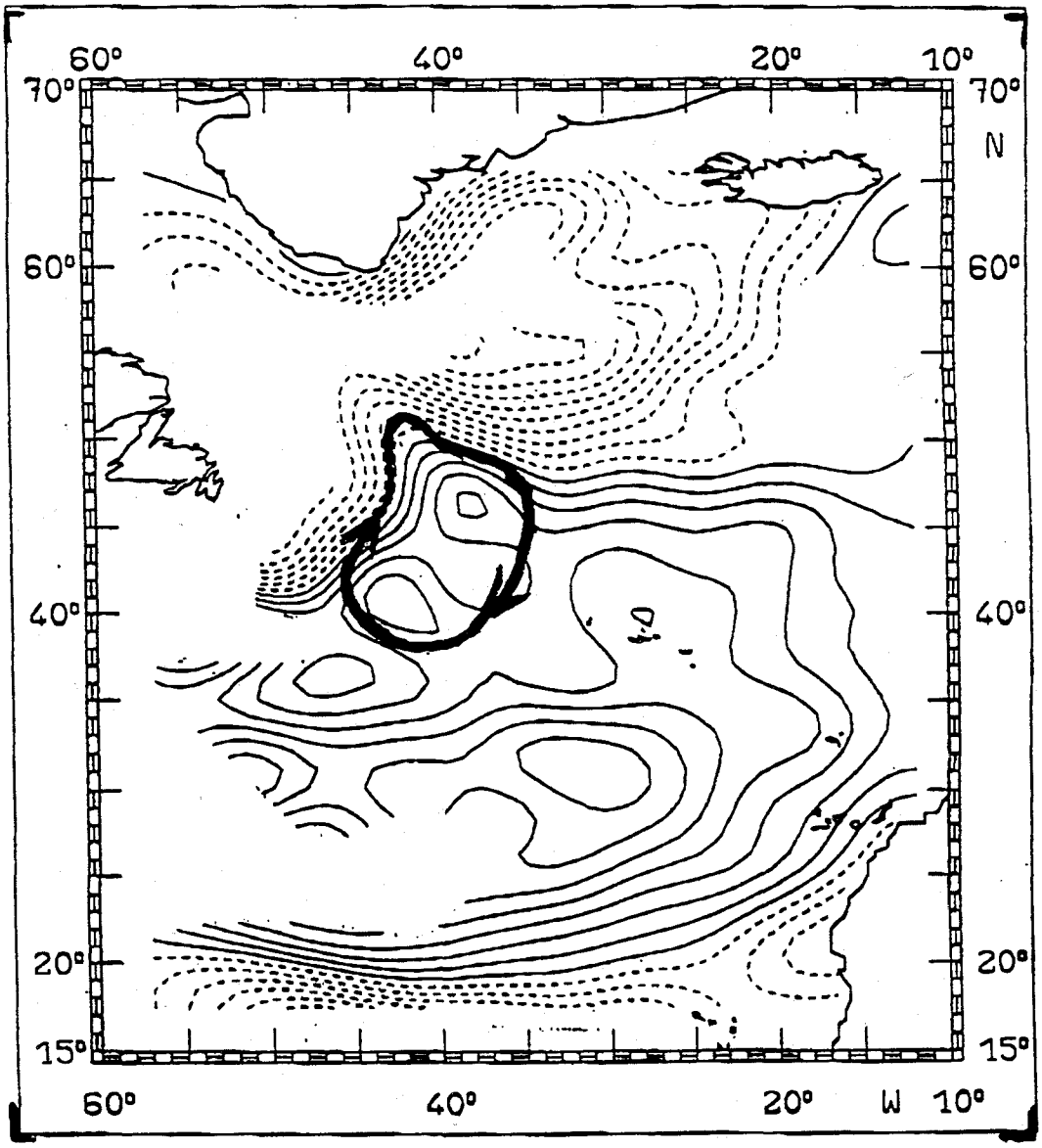

Fig. 2: Streamfunction of the mean current field of the northern North Atlantic as derived from drifter data drogued at 100 m. Heavy curve: Worthington gyre

The North Atlantic Current in the Northwest Atlantic

R. Allyn Clarke
Ocean Circulation Division
Physical and Chemical Sciences
Bedford Institute of Oceanography
Dartmouth, NS, B2Y 4A2
Canada

Maps of the net air-sea heat flux such as those by Isemer and Hasse (1985), show that the region of maximum heat transfer associated with the Gulf Stream, turns northward near 45°W so that the 100 W m^{-2} isoline crosses 50°N. This feature results from the North Atlantic Current carrying warm salty waters from the Gulf Stream extension region that lies along 40°N, northward along the 4000 meter isobath of the continental rise east of the Grand Banks of Newfoundland.

These charts also show that the waters inshore of the Gulf Stream and the North Atlantic Current are gaining heat from the atmosphere. These shelf and slope regions are the pathway of the cold low salinity Arctic outflows dominated in the western North Atlantic by the Labrador Current. Dickson et al (1988) interpretation of the North Atlantic transport scheme first proposed by Dietrich shows the convergence of the Arctic outflow and the North Atlantic Current east of the Grand Banks.

There have been a number of recent analyses of the spatial and temporal variability of the SST fields of the Atlantic Ocean. An early example of these analysis is that by Weare (1977). The maximum amplitude (12°C) of the seasonal variation of SST in the Atlantic Ocean is found in the Gulf Stream, North Atlantic Current and inshore regions of the Northwest Atlantic between 35°-50°N and 45°-80°W. Similarly, the interdecadal and interannual variability patterns have their maximum amplitudes in the same region with the maximums being shifted slightly to the north and east to be more pronounced in the North Atlantic Current east of Newfoundland than was the seasonal pattern.

It is important in this region to look at the circulation on the shelf as well as in the offshore. The Labrador Current flows southward along the edge of the Labrador shelf as a well defined current jet and density, temperature and salinity front. Its core is found near the 1000 meter isobath. The current jet becomes somewhat less well defined when it encounters the deeper waters of the northeastern Newfoundland shelves but is sharpened up again when it encounters the northern edge of the Grand Banks. Most of the Labrador Current follows the bathymetry to flow southward along the western flank of Flemish Pass. (Some Labrador Current Water is found north of Flemish Cap.)

Circulation models for the Labrador and Newfoundland shelves driven by a pressure head across the Labrador shelf at some northern latitude reproduce the frontal and jet like structure of the Labrador Current until it reaches the Tail of the Grand Banks. In the model simulations, the Labrador Current turns westward to follow the bathymetry on the southern edge of the Grand Banks. Hydrographic data, ocean drifters, and ice berg trajectories indicate that most of the Labrador Current transport in fact turns offshore at this point to form a cyclonic circulation bounded on the north by Flemish Cap and on the east by the North Atlantic Current. Within this circulation is found a water that is known as mixed water that is a mixture of Labrador Current and North Atlantic water masses.

I know of no models that reproduce either the offshore turning or the splitting of the Labrador Current. This may not be surprising since the ocean models don't include the shelf currents and the shelf models don't include the ocean currents. It may well be that the behaviour of the Labrador Current at the Tail of the Banks is determined by offshore pressure gradients that are established by the Gulf Stream and the North Atlantic Current.

Because of the range of water masses in this region, it is important to use density horizons rather than level surfaces when examining hydrographic and tracer fields. Clarke et al (1980) used $\sigma_\theta = 27.2$ to describe the circulation in the upper layers. The depth of this surface ranges from less than 100 meters in the mixed water region just east of the Grand Banks to deeper than 700 meters in the Newfoundland Basin offshore of the North Atlantic Current and deeper than 800 meters in the Sargasso Sea to the south of the Gulf Stream. A strong ridge is formed a little to the northeast of the axis of the Southeast Newfoundland Ridge reaching to 39°N 44°W where some of the isolines turn westward into the Sargasso Sea, some eastward toward the Azores and the rest northwestward to form the North Atlantic Current. The surface also exhibits anticyclonic circulation within the Newfoundland Basin. Inshore of the North Atlantic current suggests a weak cyclonic circulation within the mixed water region with the possibility that this is split into two cyclonic cells near the axis of the Newfoundland Seamounts.

Salinity on this surface ranges from less than 34 psu along the upper continental slope to greater than 35.3 psu in both the Sargasso Sea and the Newfoundland Basin and greater than 34.4 psu in the southeast corner. Salinity also decreases as one moves to the northeast toward Milne Seamount. The salinity contours mimic the surface topography near the Southeast Newfoundland Ridge. There is considerable variability on short spatial scales in the mixed water region suggesting the presence of small eddies or lenses of different waters in this region.

This surface follows the oxygen minimum within the Gulf Stream/Sargasso Sea system. Oxygen concentrations range from greater than 7 ml l^{-1} in Flemish Pass and along the edge of the Grand Banks to less than 3.5 ml l^{-1} in the Sargasso Sea just south of the Gulf Stream as it crosses 50°W. Oxygen values gradually increase as one moves northward through the Newfoundland Basin. Because the Ice Patrol did not measure oxygen content, we have not the coverage of the mixed layer region that we had for salinity.

These large scale maps do not represent the remarkable strength of the frontal structures in this region. We have mapped the North Atlantic Current from Flemish Cap to the Newfoundland Seamounts using a towed profiling CTD system (BATFISH). In the upper 200 meters, temperature and salinity change by more than 5°C and 1 psu in less than 2 nautical miles and by more than 10°C and 2.6 psu in 10 nautical miles on level surfaces. The slope of the density surfaces across the front is somewhat less than that of the temperature and salinity surfaces; however, a surface like $\sigma_\theta = 27.0$ deepens by more than 100 meters over 5 nautical miles while its temperature and salinity change by more than 5°C and 1 psu. These data were collected in the fall of 1987 and the deep frontal structure is capped by a low density surface layer some 50 meters thick. This surface layer contains warm salty cores a few miles offshore of the front and cold fresher cores a similar distance inshore. These cores are 10-20 meters thick and a few miles across and appear on all seven BATFISH sections across the North Atlantic Current along 400 km of its length with no systematic change in their core salinities. This suggests that mixing on small spatial scales across the North Atlantic Current is not particularly intense.

Salinity distributions on density surfaces in the Newfoundland Basin, show that for $\sigma_\theta \leq 27.4$, the North Atlantic Current represents a front separating the low salinity inshore waters from the high salinity offshore waters. Offshore of the North Atlantic Current, the salinity still increases toward the southeast corner (Mediterranean Water influence); however, the gradient is weaker and more variable suggesting weak eddies and lenses. For $\sigma_\theta \geq 27.6$, the overall salinity gradient with increasing salinity to the southeast remains but there is virtually no evidence of a salinity front associated with the North Atlantic Current. On some of the surfaces, there is a lot of small scale variability suggesting that lenses and eddies are part of the mixing process. As one moves in the deep waters, the isohalines rotate to lie more east-west than their southwest to northeast orientation on higher density surfaces.

The transient tracer data taken in the North Atlantic in the last two decades, leave us with the impression that the intermediate and deep waters of the sub-polar gyre of the North Atlantic are all rather well ventilated with the western boundary regions being only somewhat better ventilated than the interior. In the sub tropical gyre, tracers such as tritium and CFC's are still only found in significant concentrations in the deep western boundary currents. This observation must mean that there has been significant exchange between the deep western boundary currents and the interior within the sub-polar gyre. The simple conceptual model of North Atlantic Deep Water being formed in the Nordic Seas, overflowing the Greenland-Iceland-Faroe-Shetland ridges, forming a deep boundary current that then flows as a continuous current down the western side of the North Atlantic to the equator and beyond is too simple. There must be significant recirculation of deep water north of the Tail of the Grand Banks. The Southeast Newfoundland Ridge may be a point that controls the exchange of deep waters into the rest of the North Atlantic basin.

Bedford Institute of Oceanography, in collaboration with University of Rhode Island, is about to initiate a new field program to examine this complex part of the North Atlantic Circulation. An array of 8 current meter moorings will be set across the North Atlantic Current between the Southeast Newfoundland Ridge and the Newfoundland Seamounts in August 1993 for a period of up to 22 months. URI will add inverted echo sounders to this array. During the period that the mooring array is in place, we will conduct three full depth hydrographic/tracer surveys of the region from 50°W to 47°N. These surveys will divide the region into five closed boxes that will permit us to make transport estimates of the Labrador Current, Gulf Stream and North Atlantic Current and all their branches.

URI's RAFOS float releases in the upper 500 metres, surface drifter releases by University of Kiel and the Ice Patrol, satellite altimetry, ship board ADCP measurements, repeated occupations of WOCE section A2 by BSH Hamburg and possible upper ocean hydrography by the State Oceanographic Institute, Moscow will provide good coverage of this complex area during 1993-1995.

Clarke, R.A., H.W. Hill, R.F. Reiniger and B.A. Warren, 1980. Current system south and east of the Grand Banks of Newfoundland. J. Phys. Oceangr. 10, 25-65.

Dickson, R.R., J. Meinke, S-A. Malmberg and A.J. Lee, 1988. The "Great Salinity Anomaly" in the Northern North Atlantic, 1968-82. Progress in Oceanography 20(3), 103-151.

Isemer, H-J. and L. Hasse, 1985. The Bunker Climate Atlas of the North Atlantic Ocean. Volume 2: Air-Sea Interactions. Springer-Verlag, Berlin, Heidelberg, New York, Tokyo. 218 pp.

Weare, B.C., 1977. Empirical orthogonal analysis of Atlantic Ocean surface temperatures. Quart. J. R. Met. Soc., 103, 467-478.

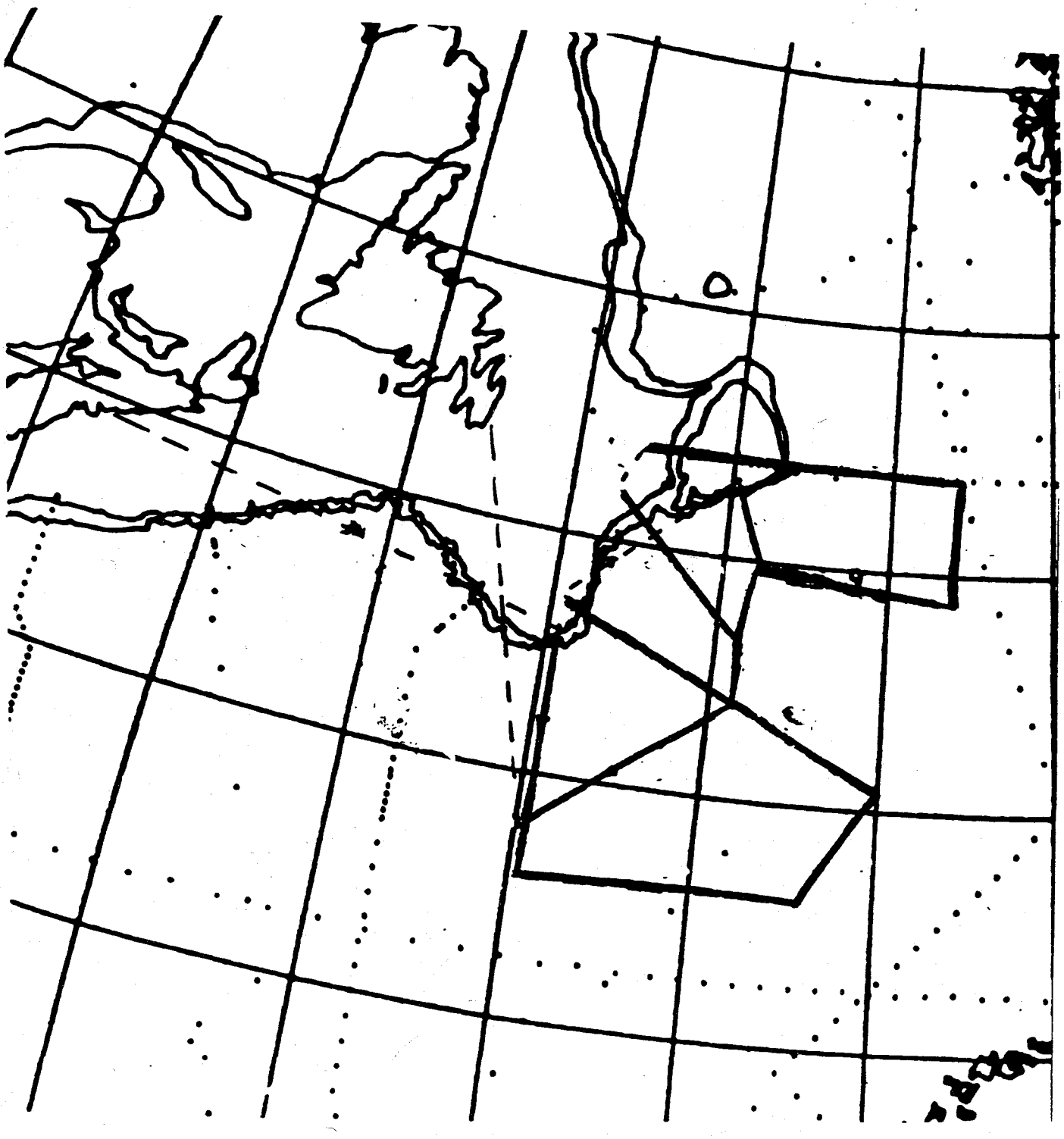

Figure 1

The Grand Banks and North Atlantic Climate Variability: A Modeler's Viewpoint

Kirk Bryan
GFDL/NOAA
P.O. Box 308
Princeton University
Princeton, NJ 08542

1. Bjerknes's Hypothesis

The Grand Banks can be thought of as the railroad switching yard of the Atlantic. It appears to be a bewilderingly complex region of converging ocean currents with a great deal of mesoscale variability. The Grand Banks presents formidable problems for measurement and interpretation and, except for its great importance for understanding Atlantic Ocean circulation, would not appear to be a rewarding region for study. Without an ability to monitor changes in circulation in the Grand Banks region, however, we may never be able to anticipate the changes in North Atlantic climate which are felt in the average surface temperature for the entire Northern Hemisphere.

On time scales of 3 to 4 years, the El Niño phenomenon dominates Northern Hemisphere climate variability. At the surface, this type of variability has its greatest amplitude in the Equatorial Pacific, but also has a great influence on the downstream circulation over North America. The climate record indicates another type of variability in surface temperatures with a period of many decades, and a maximum amplitude in high latitudes. In fact, the greatest amplitude seems to be located in the northwestern North Atlantic. Bjerknes (1964) studied the historic record of SST's and concluded that decadal North Atlantic climate variability might be explained by changes in the intensity of the thermohaline circulation. At the time of its publication, Bjerknes's (1964) paper received little attention.

Fortunately, nature provided new opportunities to study Bjerknes's ideas in the decades following World War II. As documented by Lazier (1980), normal winter convection in the Labrador Sea apparently ceased for a period of years in the late 1960's and early 1970's. This episode was followed by a decade of very strong cooling in the surface waters of the northern North Atlantic.

Fig. 1 and Fig. 2 from Levitus (1990) show how the sea level gradient across the North Atlantic Current between Halifax, Nova Scotia and Bermuda intensified in the 1950's and then relaxed in the early 1970's. The peak to trough amplitude is nearly 20 cm! The pattern of dynamic height change between these two periods is shown in Fig. 2 and demonstrates that the difference results in Fig. 1 for a single pair of stations are representation of a broad geographical area. Clearly the North Atlantic Current (NAC) appears to have weakened and the exchange between the surface waters of the subtropical and subarctic cells as well.

2. The Model of Delworth et al. (1993)

Delworth et al. (1993) have analyzed a multi-century integration of the GFDL coupled ocean-atmosphere model. They have found very low frequency variations in North Atlantic climate, which appear to be consistent with Bjerknes's (1964) hypothesis for North Atlantic climate variability. Variations of the intensity of the thermohaline circulation of the Atlantic in their simulation are only about 10% of the average amplitude, and a pronounced shoulder in the variability spectrum appears at a period of about 50 years. Typical sea surface temperature anomalies generated by the GFDL

model are shown in Fig. 3, which is taken from the WCRP/CLIVAR report. In the same figure, SST anomalies calculated by Kushnir (1993) are shown for comparison. Kushnir's data indicate the difference in SST before and after the cold event in the late 1960's.

The pattern of SST anomaly indicated by the model and observations both show a dipole signature in which the boundary separating the two poles runs along the outer boundary of the Grand Banks (as far as it can be resolved by a low resolution model). This appears to be associated with northward and southward moving branches of the thermohaline circulation, as manifested by the North Atlantic Current and the Labrador Current, respectively. As the thermohaline circulation intensifies, the SST contrast between the Grand Banks and the open ocean to the east intensifies and vice-versa.

3. Where Do We Go From Here?

In spite of its limitations, the results of Delworth et al. (1993) provide for the first time a quantitative demonstration of the viability of Bjerknes's hypothesis. An obvious first step is to check the robustness of this result using models of greater resolving power, which can be checked in more detail with observations.

The model results suggest that significant climate variability may arise from changes in the thermohaline circulation of only 10%. At present, it seems unlikely that measurements of poleward heat transport can be made to within ±30% (Bryden and Hall, 1980). Thus we have a very stringent requirement for monitoring heat transport.

Almost all proposed methods of estimating the total thermohaline overturning have many difficulties associated with them, particularly if an accuracy of 10% is required. Some of the problems are discussed in the famous CAGE report (Dobson et al., 1982). In view of these problems in obtaining the poleward flux of heat accurately, it would seem better to measure water mass anomalies in the northern North Atlantic. Measurements of water mass changes coupled by estimates of the surface flux of heat and water would provide an indirect measure of the change of poleward transport into the area. The changes in water mass properties represent a time-integral of the heat transport anomalies, and are thus less subject to sampling errors than measurements of transport.

Recommendations

We require time-series measurements of water mass properties in the northwestern Atlantic. At one time, systematic measurements were made from Weather Ships BRAVO and CHARLEY. We need to establish a new monitoring system that will provide the equivalent information. To my knowledge, two systems have recently emerged which might provide this type of monitoring. They are the ALACE (Autonomous Lagrangian Circulation Explorer) floats developed in the WOCE program and the TAO mooring developed by TOGA for use in the equatorial Pacific. Both appear capable of taking temperature and salinity measurements, which remain stable for extended periods of time.

The ALACE floats have the advantage of ease of deployment and the capability of making temperature and salinity measurements throughout the water column. Their disadvantage is that they are apt to drift out of the area of interest - the Labrador Sea and the axis of the North Atlantic Current and its poleward extension.

The TAO array moorings have the advantage of remaining in a fixed position with a proven record of reliability. Their disadvantage is a relatively higher cost in

deployment than the ALACE floats, and an ability to only measure water mass properties in the upper part of the water column.

Field tests are needed to determine the relative merits of these two systems for the northwest North Atlantic.

References

Bryden, H.L., and M.M. Hall, 1980: Heat transport in ocean currents across 25°N latitude in the Atlantic, Science, 207, 884-886.

CLIVER, 1992: CLIVAR: A study of variability and predictability. World Climate Research Program, World Meteorological Organization, Geneva.

Delworth, T., S. Manabe, and R. Stouffer, 1993: Interdecadal variability of the thermohaline circulation in a coupled ocean-atmosphere model, accepted by J. Climate.

Dobson, F.W., F.P. Bretherton, D.M. Burridge, J. Crease, E.B. Kraus, and T.H. Vonder Haar,1982: The "Cage" Experiment: A Feasibility Study. World Climate Program Report 22, World Climate Research Program, World Meteorological Organization, Geneva.

Kushnir, Y., 1993: Interdecadal variations in North Atlantic sea surface temperature and associated atmospheric conditions, accepted by J. Climate.

Lazier, J., 1980: Oceanic conditions at Ocean Weather Ship BRAVO, 1964-1974, Atmos. Ocean., 18, 227-238.

Levitus, S., 1990: Interpentadal variability of steric sea level and geopotential thickness of the North Atlantic Ocean, 1970-74 versus 1955-59, J. Geophys. Res., 95(C4), 5233-5238.

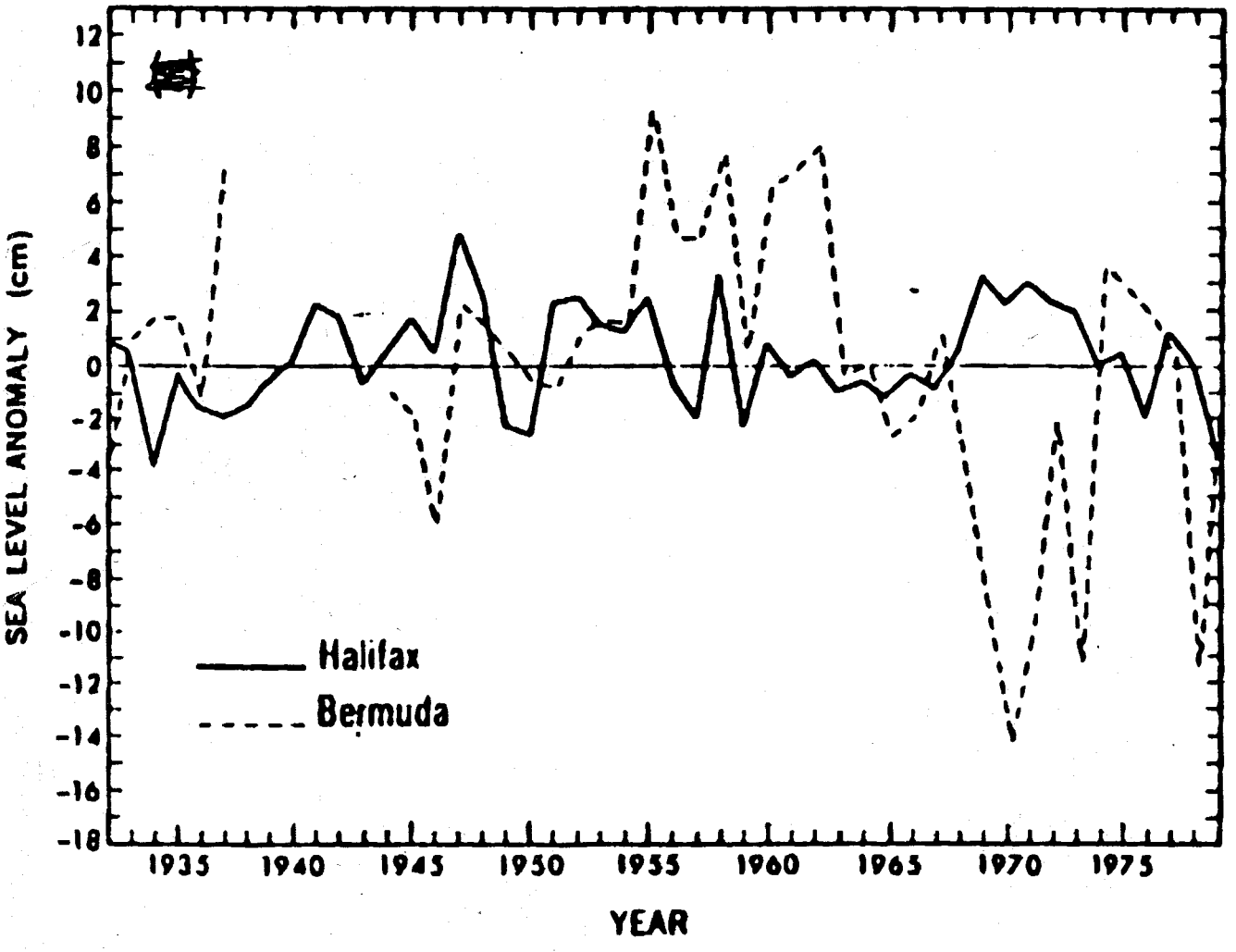

Fig. 1. Sea level curves for Halifax and Bermuda (from Levitus, 1990).

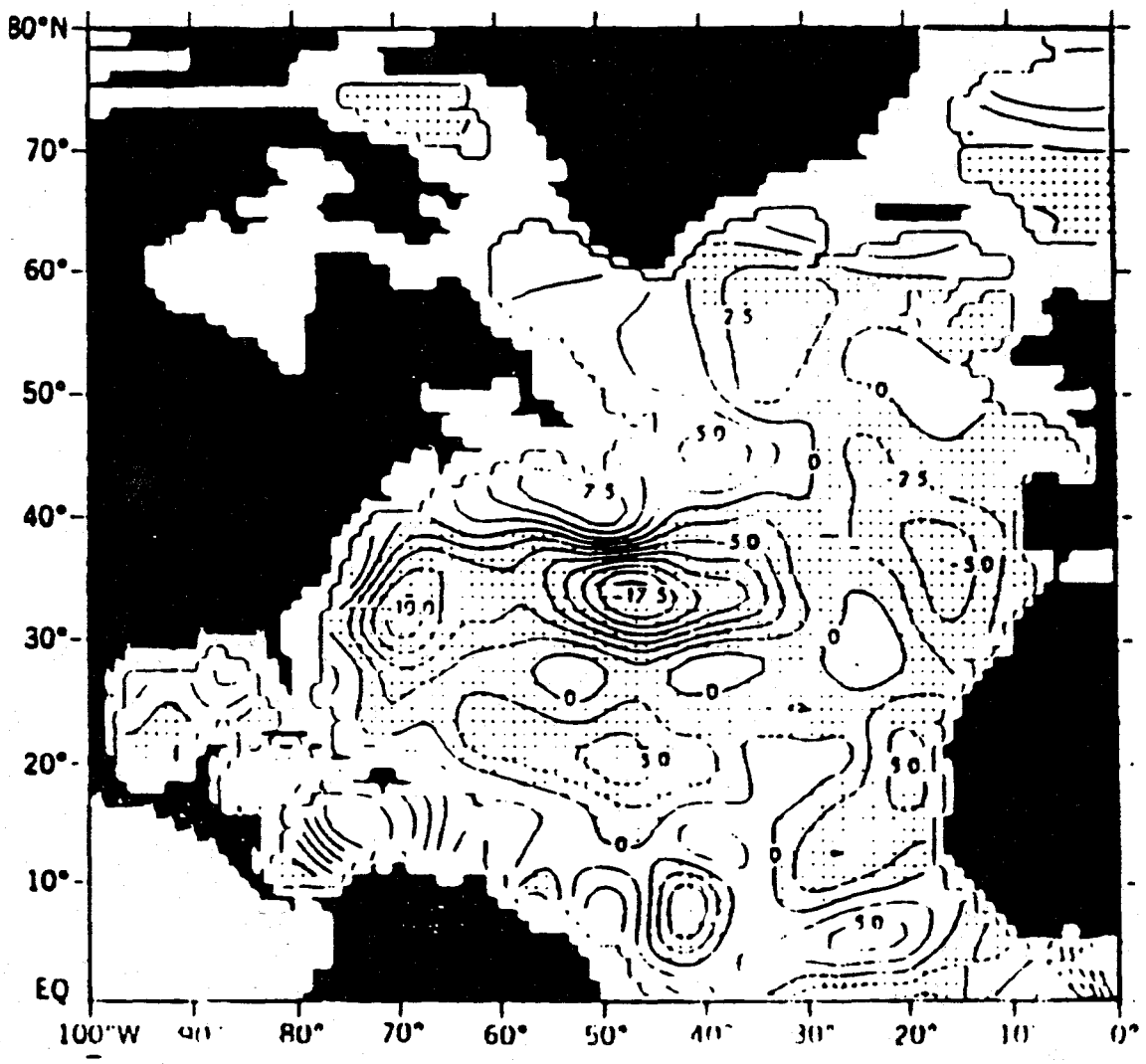

Fig. 2. Difference in steric height, 0-1500 decibars, for the period 1970-1974 minus 1956-1960 (from Levitus, 1990).

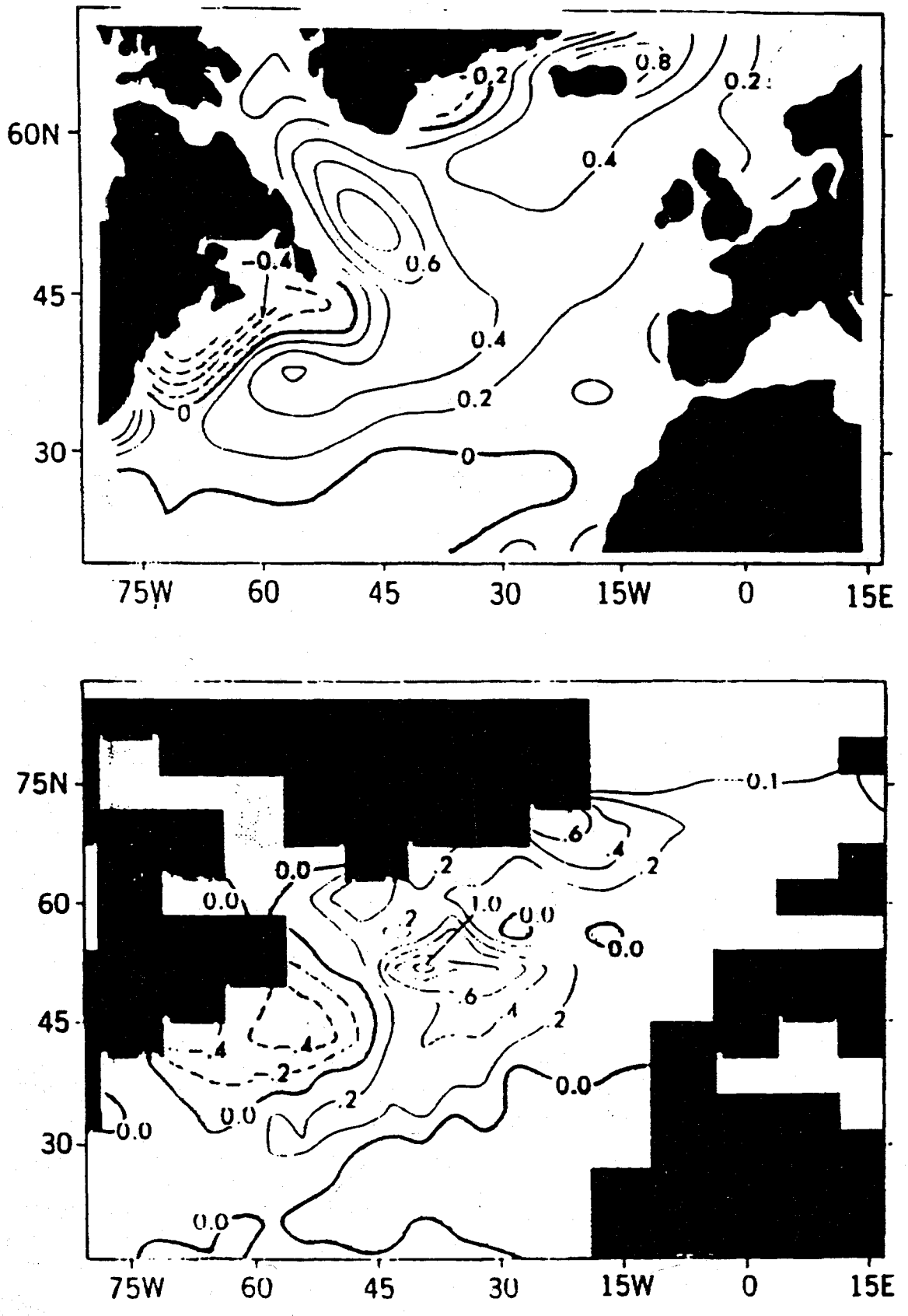

Fig. 3. (upper panel) SST differences between 1950-1960 minus 1965-1980 (from Kushnir, 1993). (lower panel) SST difference obtained in the GFDL coupled model. Four decades of stronger thermohaline circulation are subtracted from four decades of weaker thermohaline circulation (Delworth et al., 1993). (Figure from CLIVAR, 1992.)

Surface Climate Variations Over the North Atlantic During Winter 1900-1989

Clara Deser and Maurice Blackmon
CIRES
Campus Box 449
University of Colorado
Boulder, CO 80309

Two dominant modes of wintertime sea surface temperature (SST) variability in the North Atlantic during 1900-89 have been identified by Deser and Blackmon (1993), on the basis of empirical orthogonal function analysis of data from the Comprehensive Ocean-Atmosphere Data Set (COADS). The first mode is associated with the global surface warming trend during the 1920's and 30's, and indicates that the warming was concentrated along the Gulf Stream east of Cape Hatteras (not shown). The second mode involves SST variations southeast of Newfoundland, at the boundary between the subtropical and subpolar ocean gyres (Fig. 1). Weaker SST anomalies of opposite polarity off the southeastern coast of the United States are also associated with this mode. The time series of SSTs east of Newfoundland, shown in Fig. 2, exhibit quasi-decadal (and biennial) fluctuations, with amplitudes ~1.5°C. The 'decadal' fluctuations are irregular in length, and have been more pronounced since the mid-1940's.

Figure 3a shows the time series of winter sea ice concentration anomalies in the Davis Strait/Labrador Sea region, based on data from Walsh and Johnson (1979). Decadal variability is evident in the sea ice record, with peaks occurring in the winters of 1957/58, 1971/72, and 1983/84. Figure 3b shows the sea ice record superimposed upon the (inverted) time series of the 2nd EOF of winter SST. The decadal fluctuations in SSTs east of Newfoundland are closely linked to decadal variations in sea ice in the Labrador Sea, with periods of greater than normal sea ice extent preceding periods of colder than normal SSTs east of Newfoundland by ~2 years. The 2-yr lag correlation between the sea ice and SST records is -0.76, significant at the 99% level. Deser and Blackmon (1993) suggested that cold, fresh waters resulting from the melting of sea ice could be advected into the Newfoundland region by the Labrador Current, 1-2 years later. Fig. 4 shows the lag regression maps between SSTs and the sea ice index in the concurrent and following 4 winters. It may be seen that the cold SST anomaly associated with extensive sea ice in the Labrador Sea propagates around the southeastern tip of Newfoundland in ~2 years. The SST anomalies spread eastward across the basin in years 2 and 3, and decay by year 4.

Deser and Blackmon (1993) also showed that the decadal SST variations near Newfoundland are closely associated with atmospheric circulation changes over the North Atlantic and western Europe (Fig. 5). They noted that the wind-SST relationships were local in both space and time, with stronger (weaker) than normal westerly winds coincident with cooler (warmer) than normal SSTs east of Newfoundland. Deser and Blackmon (1993) interpreted these relationships as indicative of the atmosphere forcing the ocean, consistent with upper ocean mixed layer theory. For example, stronger than normal winds will cool the ocean mixed layer by enhancing the fluxes of latent and sensible heat from the ocean surface and by accelerating the entrainment of cooler water from below. However, they also noted that in the atmospheric general circulation model experiment of Palmer and Sun (1985), the atmospheric response to SST variations near Newfoundland is similar to the wind pattern shown in Fig. 5.

The observational results outlined above, together with Palmer and Sun's (1985) study, suggest the following working hypothesis. A cold fresh water anomaly formed

after a period of extensive sea ice in the Labrador Sea is advected southward along the coast of Newfoundland by the Labrador Current. This initial SST perturbation in the vicinity of Newfoundland excites a large-scale atmospheric response, which not only reinforces the initial SST anomaly, but also induces SST anomalies of basin-extent through mixed layer processes. While this rudimentary scenario attempts to physically link the decadal sea ice variations with the large-scale decadal SST and atmospheric circulation anomalies over the North Atlantic, much work remains to document and understand the nature of the quasi-decadal cycles of North Atlantic climate.

References

Deser, C., and M.L. Blackmon, 1993: Surface climate variations over the North Atlantic during winter: 1900-89, J. Climat., to appear in October.

Palmer, T.N. and Z. Sun, 1985: A modelling and observational study of the relationship between sea surface temperature in the north-west Atlantic and the atmospheric general circulation, Quart. J. Roy. Meteor. Soc., 111, 947-975.

Walsh, J.E. and C.M. Johnson, 1979: An analysis of Arctic sea ice fluctuations, 1953-77, J. Phys. Oceanog., 9, 580-591.

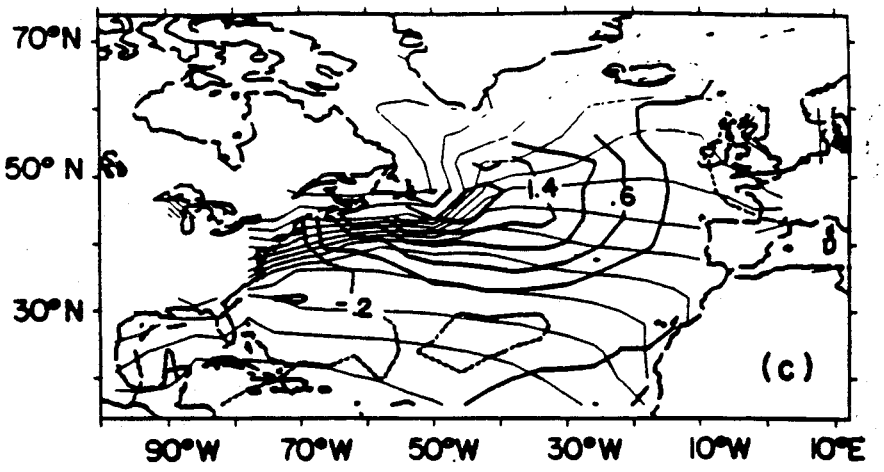

Fig. 1. EOF 2 of North Atlantic SST anomalies based on un-normalized winter (November-March) means, 1900 - 1989 (bold solid and dashed contours). This mode accounts for 12% of the variance. Also shown is the climatological SST distribution (thin contours).

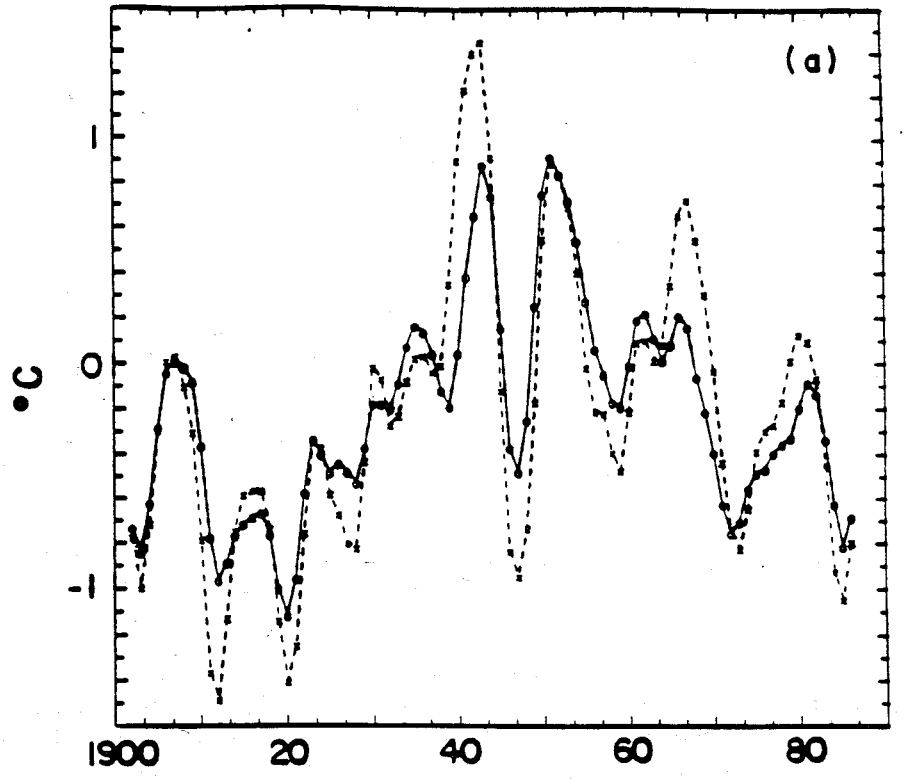

Fig. 2. Time series of winter SST (solid) and surface air temperature (dashed) anomalies east of Newfoundland [52-40°N, 50-30°W]. The time series have been smoothed with a 5-point binomial filter.

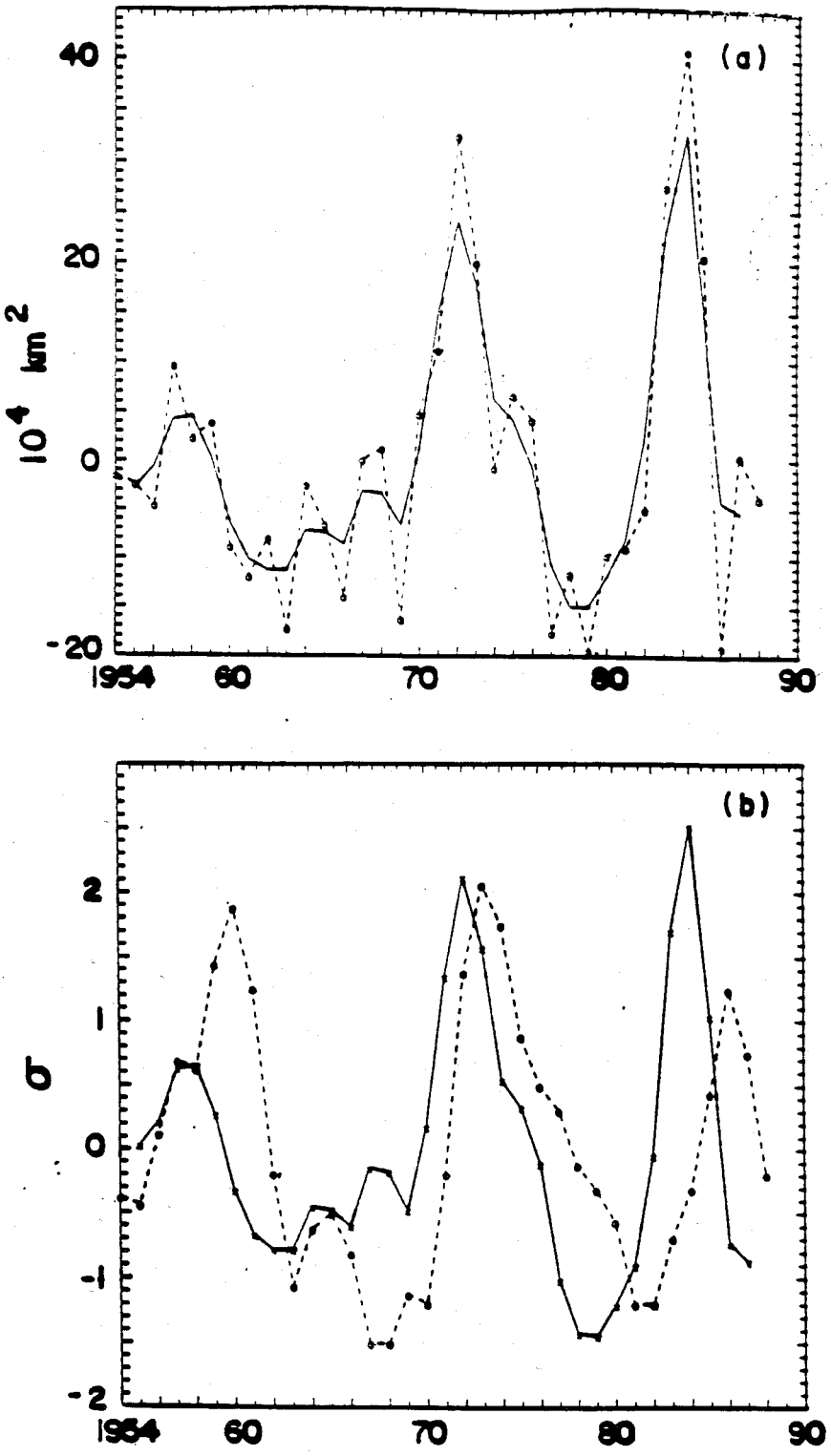

Fig. 3. (a) Time series of winter sea ice area anomalies (10^4 km^2) in the Davis Strait/Labrador Sea region from Agnew (1991), based on data from Walsh and Johnson (1979). The circles denote the winter (December-February) anomaly, plotted in the year in which January occurs. The solid curve shows the data smoothed with a 3-point binomial filter. (b) Standardized sea ice anomalies from (a) (solid curve) superimposed upon the standardized time series of EOF 2 of North Atlantic winter (November-March) SST (dashed curve). Note that the SST time series has been inverted. Both the sea ice and SST time series have been smoothed with a 3-point binomial filter and detrended by subtracting a least-squares parabola based on the period 1950-88.

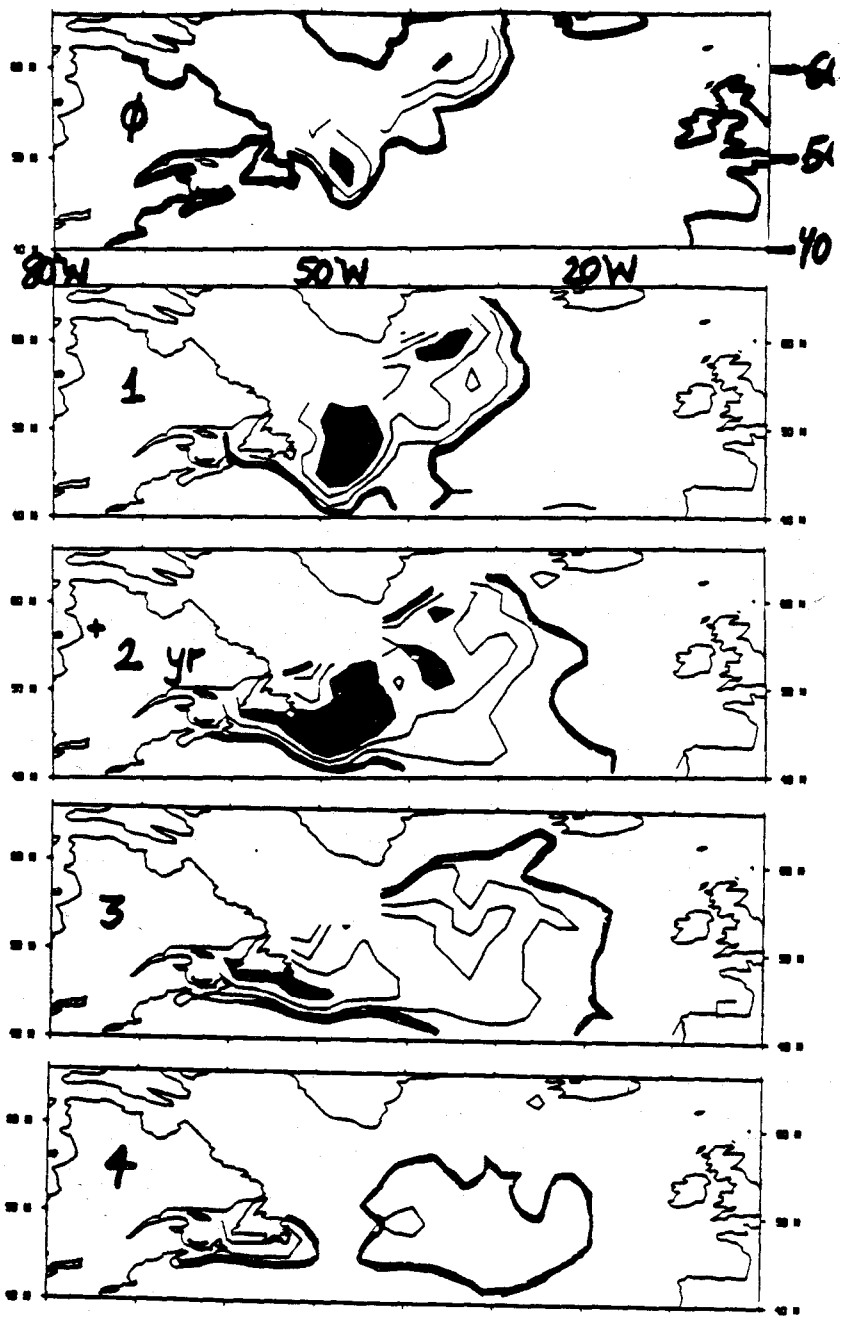

Fig. 4. Lag regression maps of winter SST upon the Labrador Sea Ice index. Upper panel indicates the SST anomalies during a winter of extensive sea ice (lag 0); subsequent panels indicate the SST anomalies in the following, 2nd, 3rd, and 4th winters. Only negative SST contours are shown. Contour interval is the same for all panels.

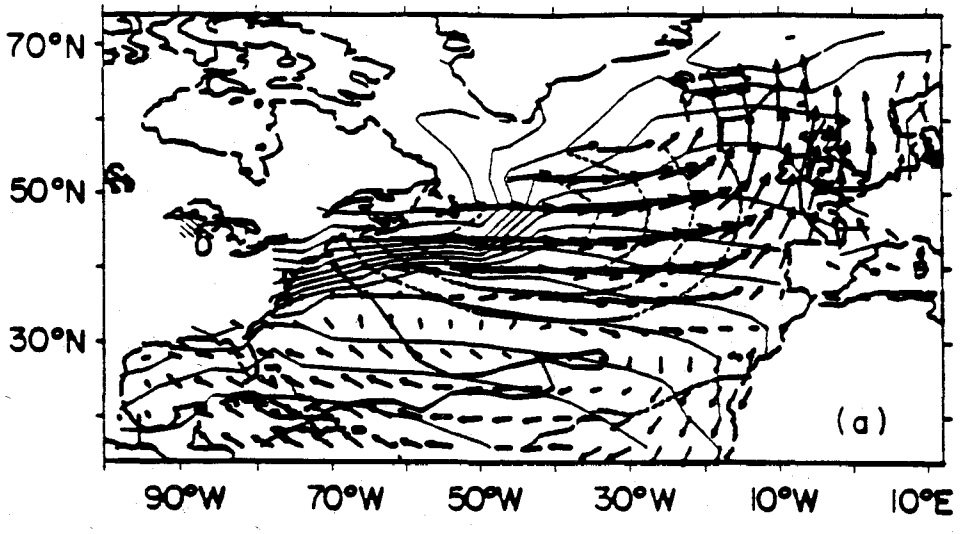

Fig. 5. SST (bold solid and dashed contours) and wind anomalies (arrows) regressed upon the time series of EOF 2 of SST. Also shown is the climatological SST distribution (thin solid contours). Note that EOF 2 of SST has opposite polarity to that shown in Fig. 1, and has been smoothed in space with a 3-point binomial filter.

Historical and Recent Upper Ocean Temperature Data in the Atlantic Ocean

Robert L. Molinari
National Oceanic and Atmospheric Administration
Atlantic Oceanographic and Meteorological Laboratory
Miami, Florida 33149

Upper ocean temperature (UOT) data have been collected using expendable bathythermographs (XBT) in the North Atlantic since 1966. These data can serve as a resource for future North Atlantic Current (NAC) studies in two areas. Firstly, the historical data can be used to assist in experiment design. Secondly, data collected in real-time can provide upper ocean temperature information during the NAC field phase. Specific details on the utility of the XBT data, including future analysis plans at AOML, follow.

The XBT data have been collected by both research and merchant vessels, the latter typically serving as Volunteer Observing Ships (VOS). The VOS provide a economical means of obtaining UOT data along the major shipping lanes. Historically, much of the early XBT sampling was in the vicinity of the Grand Banks as will be demonstrated shortly.

In terms of providing a framework for experimental design, the historical data can be used to generate a mean monthly climatology of temperature distributions at various depths. Figure 1 shows the number of calendar months with data on a 2° of latitude by 4° of longitude grid during the period 1967-1992. South of about 50°N, in the Grand Banks region, adequate data exist to generate annual signals. Sample box averages can be used to generate mean annual fields at various depths (Fig. 2) and mean monthly climatologies and anomalies at the same levels. Recognizing that simple averages tend to smooth intense gradients unrealistically, we are considering other methods for generating climatologies in regions such as the Gulf Stream. The climatologies can then be used to provide the context for placing instrumentation in three-dimensional space, designing research vessel tracklines, etc.

Other averages can be formed to study interannual variability. In particular, at AOML we are beginning to investigate the effects of oceanic variability (e.g., shifts in Gulf Stream position; position/intensity changes in the subtropical/subpolar gyres, etc.) on SST anomalies. Data available for such studies become more numerous in the mid and late 1970's (Fig. 3). Biannual averages and anomalies relative to the long-term means of SST and temperature distributions at various depths (Fig. 4) can then be analyzed to search for correlations between surface and subsurface features.

Figure 5 shows the proposed WOCE VOS tracklines in the North Atlantic. Data from these ships are available in real-time through satellite links. Greater vertical resolution is available after the vessel's return to port and transmittal of the data to national data centers. Ideally, the lines are to be occupied monthly with 4 probes launched per day. Assuming a typical ship speed of 15 knots, station spacing is about 170 km. In the Grand Banks area lines AX3 and AX4 have been occupied for several years. Line AX2 is to be implemented by the summer of 1993. The VOS lines will be occupied through the WOCE timeframe (1997) and will probably be continued after 1997 as part of a Global Ocean Observing System (GOOS). If adequate scientific justification can be provided, new lines can be implemented.

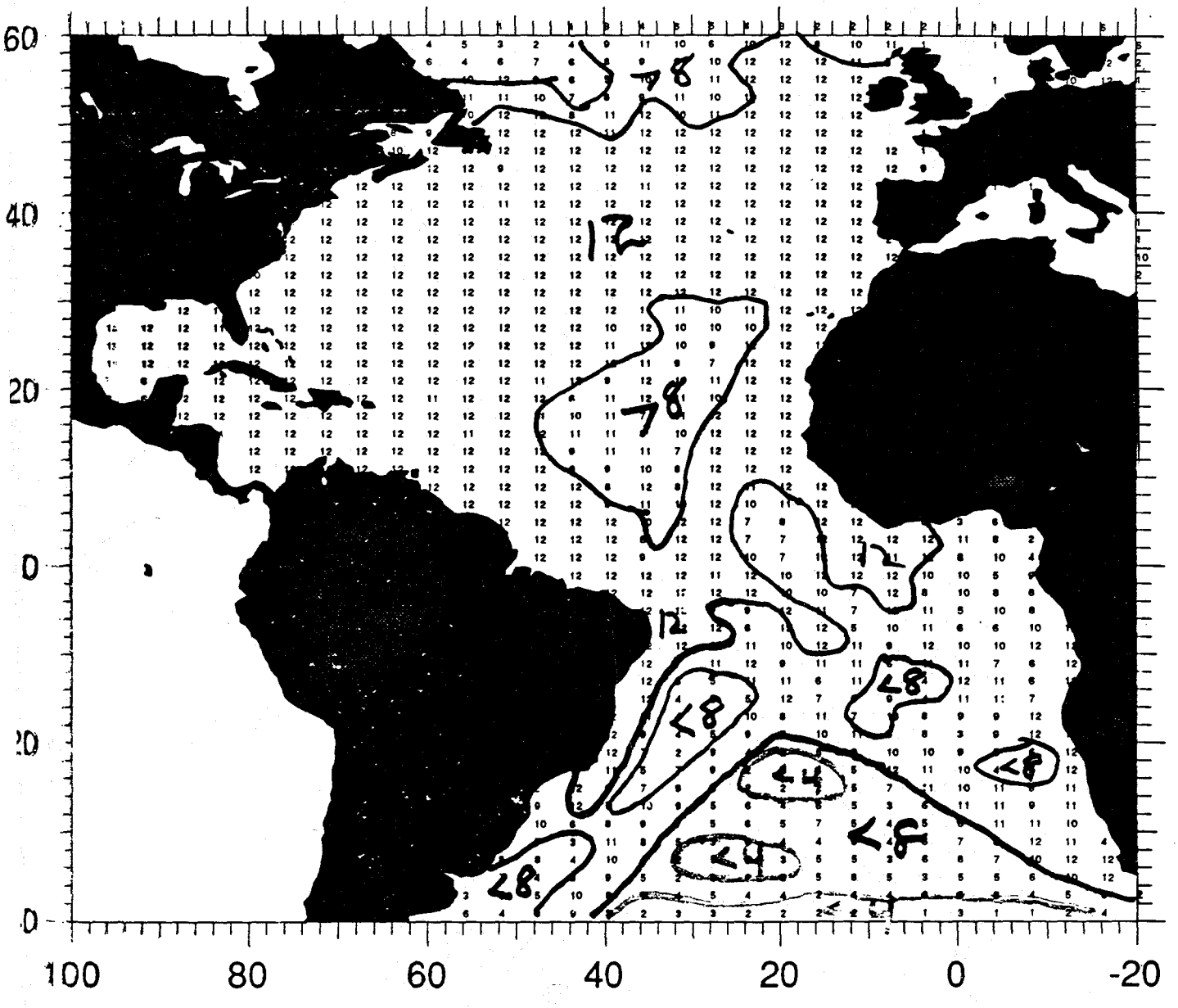

Figure 1: Number of calendar months with data during the period 1967-1992. The data are averaged onto a 2° of latitude by 4° of longitude grid.

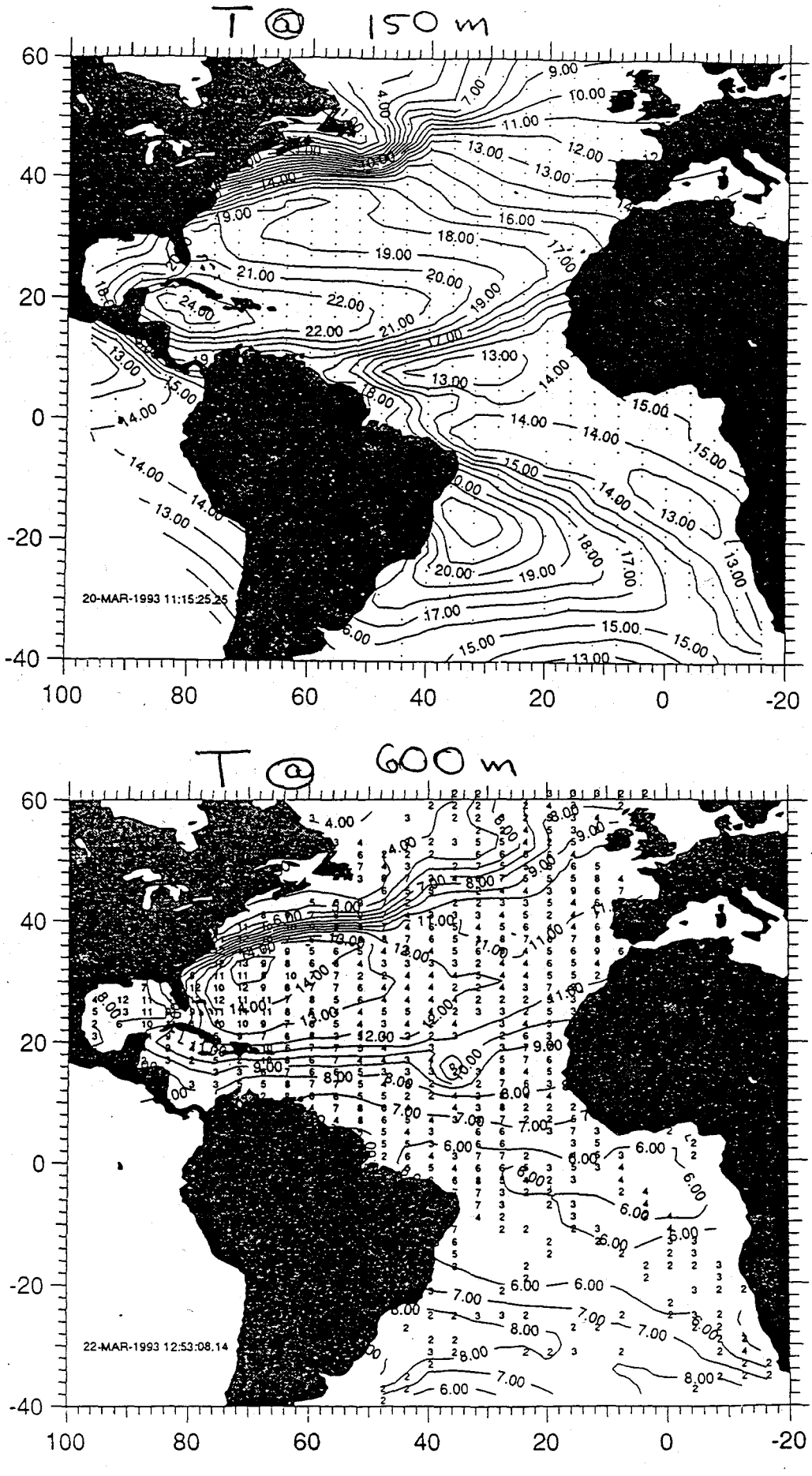

Figure 2: Mean annual temperature distribution at 150m and 600m.

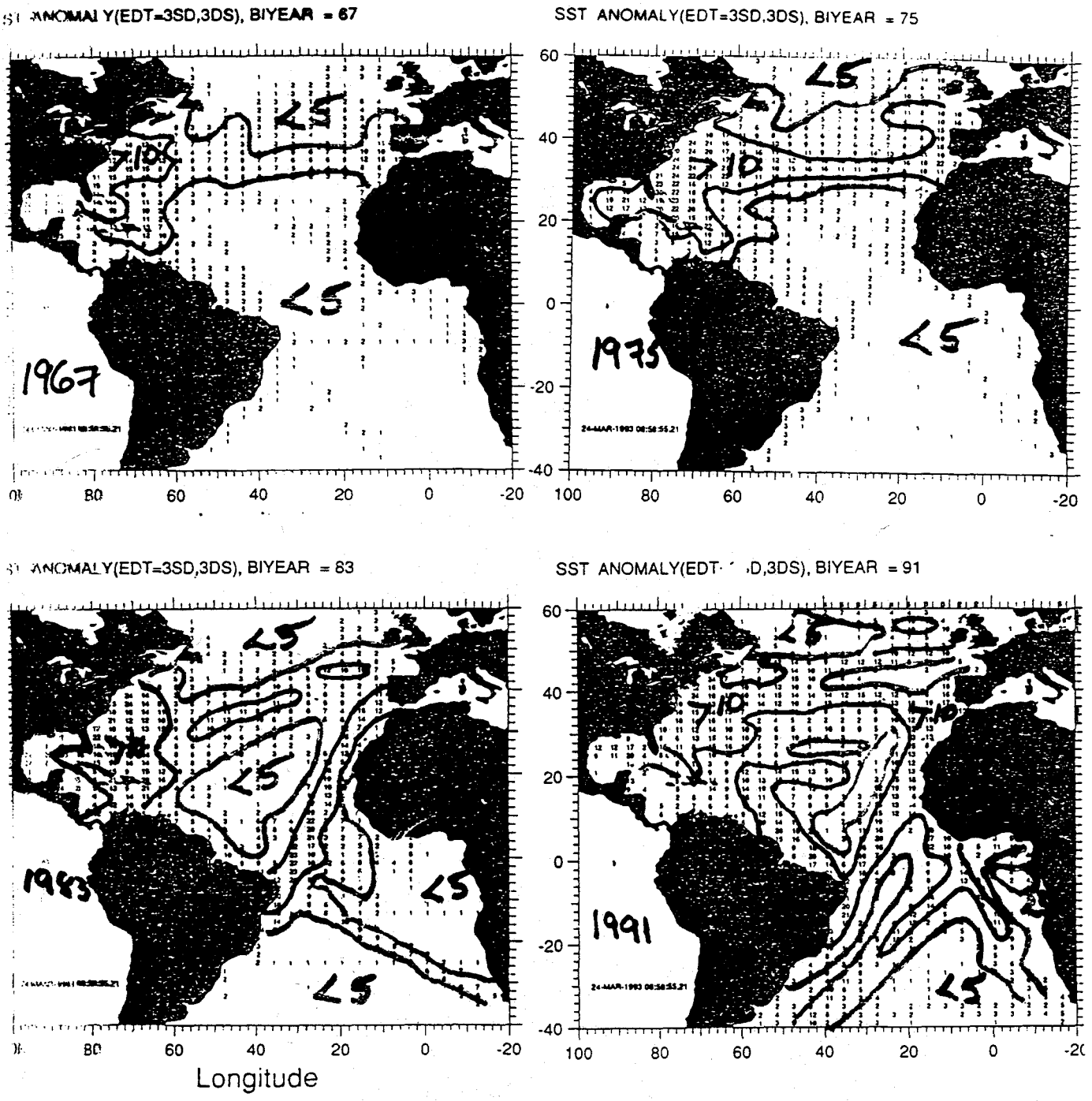

Figure 3: Number of months with data during the biannual period starting on the year indicated (a 2° x 4° grid as in Figure 1).

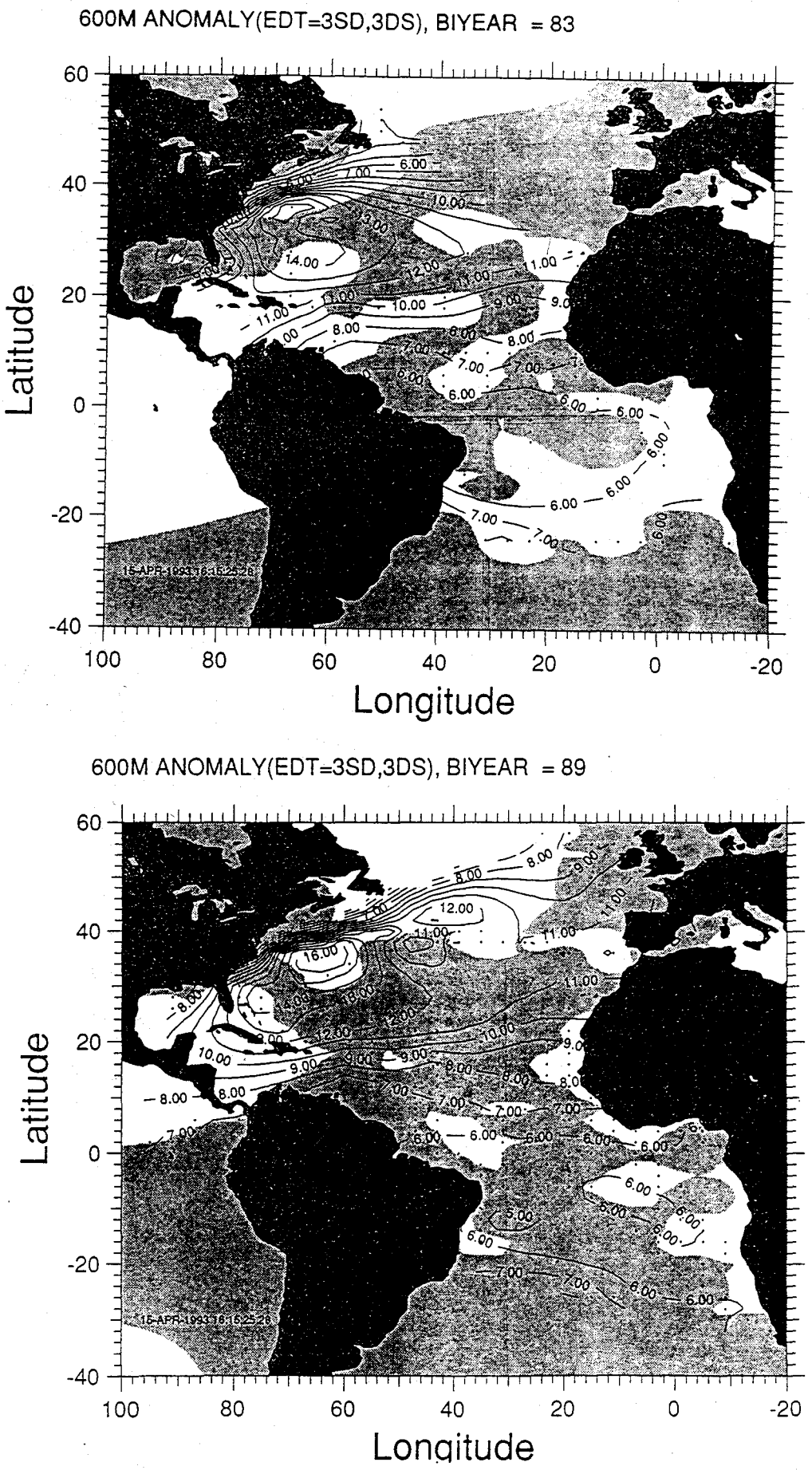

Figure 4: Mean biannual temperature distribution at 150m during the two periods indicated.

Proposed WOCE VOS XBT network.

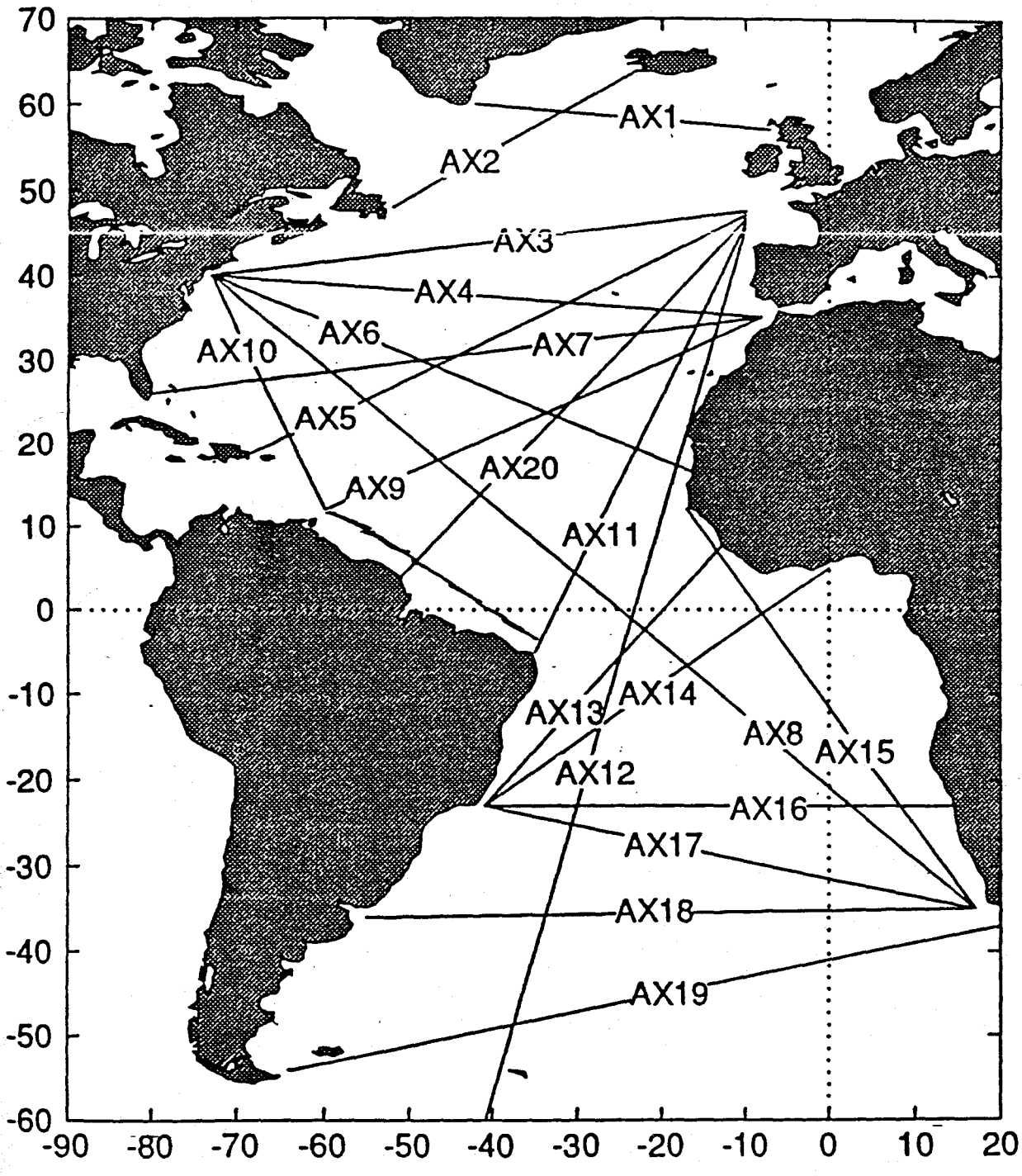

Figure 5: The proposed WOCE VOS tracklines in the Atlantic Ocean.

Currents South of the Grand Banks at 50°W: Estimates of Mass Transport

Ross Hendry
Ocean Circulation Division
Physical & Chemical Sciences Branch, Scotia-Fundy Region
Fisheries and Oceans, CANADA

Bedford Institute of Oceanography
P.O. Box 1006
Dartmouth, Nova Scotia, CANADA B2Y 4A2

A moored array study called the Intergyre Exchange Experiment took place from April 1988 to January 1990 in the region south of the Grand Banks where the Gulf Stream encounters the Southeast Newfoundland Ridge. The goals of the study were to provide estimates of the transports of the Gulf Stream and the Deep Western Boundary Current (DWBC) based on direct measurements, to investigate the possibility of other westward inflows at intermediate levels north of the Gulf Stream, and generally to explore the spatial structure and temporal variability of the regional circulation.

Measurements were obtained from up to four levels between 400 m and 4000 m on seven moorings in a north-south line along 50.15°W between 42.38°N at 2000 m depth and 39.25°N at 5350 m depth. These data provided the first long-term moored measurements from this area.

As foreseen in the experimental design, the Gulf Stream jet intermittently occupied the range of latitudes covered by the moored array. The moored temperature measurements suggest 40.2°N for the median latitude of the shoreward edge of the Gulf Stream, using the intersection of the 10°C isotherm with the 600 dbar pressure horizon as a proxy indicator. The thermocline Gulf Stream jet was entirely within the study area less than 25 per cent of the time, based on finding temperatures warmer than 14°C at 600 dbar at the southernmost mooring.

Gridded zonal flow fields based on the moored data yielded instantaneous eastward volume transports of approximately 100 million cubic meters per second (100 Sv) for the Gulf Stream itself, increasing in some instances to nearly 160 Sv if local recirculations associated with rings and meanders were included. The eastward volume transport from the fraction of the mean Gulf Stream sampled by the moored array was approximately 30 Sv. Formal errors on the mean eastward volume transport taking into account both sampling errors associated with low-frequency variability and the uncertainty of the spatial interpolation were larger than the estimated mean eastward transport.

Over the abyssal plain, currents associated with the Gulf Stream were highly coherent in the vertical between 400 and 4000 m and generally showed nearly unidirectional flow. The shoreward edge of the synoptic Gulf Stream, based on the 600 m temperature criterion, occasionally meandered as far north as 41°N to depths of just over 4000 m. Deep flows in approximately the same direction as the upper level jet were also present in many of these cases. These observations suggest that Gulf Stream dynamics can adjust to retain a full-depth jet structure over the Ridge in spite of the 1400 m reduction in depth moving from the abyssal plain. It seems that the Stream is not necessarily constrained to flow passively around the Ridge along constant f/H contours.

Potential temperatures were estimated from measured pressure and temperature and an assumed temperature-salinity relationship and interpolated to the same grid as the

zonal flow components to calculate volume transports in potential temperature classes. The DWBC, defined as all westward flow north of 41°N with potential temperature less than 3°C, gave a volume transport of 8 Sv with an uncertainty of 4 Sv. The formal errors on estimated transport from the northern part of the array were relatively lower than for the mean eastward transport because in the northern sector the mean flows were relatively large compared to sampling errors associated with time-variable flows, and because denser spatial sampling was achieved.

An energetic warm-core eddy that penetrated shoreward to the 2000 m isobath dominated the moored measurements over the Southeast Newfoundland Ridge during July-September 1989. Near-bottom flow at the northernmost mooring in 2000 m depth exceptionally reversed direction to eastward during this period, and at times during the three-month interval the inferred DWBC transport nearly vanished. This provides an example of short-term variations in DWBC transport associated with mesoscale variability.

Speed and temperature data from 4000 m and velocity and temperature data from 800 m at Mooring 883 at 40.16°N in 4800 m depth suggest the occurrence of intermittent bottom-intensified bursts of westward flow associated with cooler temperatures when the Gulf Stream jet moves seaward. This suggests a potential pathway for colder fractions of North Atlantic Deep Water to enter the Sohm Abyssal Plain that is worthy of further study.

The measurements yielded an estimated mean westward mass transport for latitudes north of 41°N of 6 Sv in the 3 to 4°C potential temperature range associated with Labrador Sea Water with a formal standard error of 4 Sv. The ultimate source of this water is an interesting point for future observational studies. The nearly two years of direct measurements give a suggestion of an annual-period variation of zonal flow in this temperature range, giving a fall or wintertime maximum westward transport.

There was an estimated 3 Sv of mean westward flow north of 41°N at potential temperatures greater than 4°C, with a standard error of 2 Sv. This brings the total westward transport north of 41°N over all temperature ranges to an estimated 17 Sv.

Surface Drifter Measurements in the North Atlantic Near Newfoundland

D.L. Murphy
International Ice Patrol
1082 Shennecossett Road
Avery Point
Groton, CT 06340-6095

1. Introduction

In 1976 the International Ice Patrol began a program of releasing satellite-tracked buoys in the western North Atlantic Ocean east of Newfoundland, Canada. In the first few years, the goal was simply to evaluate the drifter technology and to determine if the buoy tracks were in substantial agreement with the mean current field that was calculated from many years of hydrographic data collected by Ice Patrol (Soule, 1964). These mean current data form the basis of Ice Patrol's efforts at predicting iceberg movement.

After the technology proved itself, satellite-tracked buoys became an integral part of Ice Patrol's operations, routinely providing near real-time current data to the iceberg drift model. The buoy-derived currents are used to modify the mean currents temporarily in the region through which the buoy is moving. Shortly after a buoy departs a region, the currents revert to the mean values from the data base. The Ice Patrol budget does not permit the maintenance of a large array of drifting buoys over the entire operations area (40-52°N; 39-57°W), and for the entire iceberg season (nominally, March-September). Thus, we focus our attention on the offshore branch of the Labrador Curent, which flows southward through Flemish Pass, then along the eastern slope of the Grand Banks of Newfoundland. This current is a major factor in the movement of icebergs into the North Atlantic shipping lanes. The number of buoys deployed each year depends on the extent, both in space and time, of the iceberg threat. Typically, Ice Patrol launches and tracks 6-15 buoys each year.

2. Data Acquisition

There have been several changes in the type of buoy used by Ice Patrol. Most of the data have been collected using FGGE buoys, named after the First Global GARP (Global Atmospheric Research Program) Experiment. They are 3 m long spar buoys with a 1-m diameter flotation collar at the waterline. A 2 m by 10 m window shade drogue was tethered to the hull. The length of the tether varied somewhat, starting at 10 m in the late 1970s and early 1980s, but most of the data are from buoys with 30-50 m tethers. In 1991, Ice Patrol began using a modified version of the WOCE/TOGA buoys (World Ocean Circulation Experiment/Tropical Ocean Global Atmosphere). These buoys consist of a 35 cm diameter surface sphere with a subsurface holey sock drogue. The WOCE/TOGA LaGrangian Drifters (Sybrandy and Niiler, 1991) are designed as mixed-layer drifters, thus have drogues centered at 15 m. The Ice Patrol WOCE-type buoys have drogues centered at 50 m. Ice Patrol deploys its drifting buoys from HC-130 aircraft, during routine iceberg reconnaissance patrols.

The number of fixes per day from each buoy has varied somewhat over the years. In the first few years of the program, when the NIMBUS-6 satellite was used for buoy positioning, 1-2 fixes were received each day. Since 1982 Ice Patrol has used the ARGOS system. The FGGE buoys usually provided about 6-7 positions per day, while our limited experience with the WOCE-type buoys suggests that we can now expect about 4 per day. The nominal accuracy for the position data is 350 m (for ARGOS Class-

2 fixes). By far, the most recent period (1982-present) has the highest quality and most densely sampled data.

3. Data Set

The Ice Patrol drifting buoy program, which is now in its 18th year of existence, has accumulated over 125 buoy trajectories in the western North Atlantic Ocean. By far, the most densely sampled areas are the offshore branch of the Labrador Current and the North Atlantic Current in the vicinity of Flemish Cap. In 1989, Ice Patrol used the data set to modify the mean current data base in its area of operations (Murphy et al., 1990).

Ice Patrol plans to continue deploying drifting buoys at approximately the same rate as in the past. We are currently reviewing the drifting-buoy data base to ensure its completeness and accuracy. We plan to provide the reviewed data to the National Oceanographic Data Center (NODC) and the Marine Environmental Data Service (MEDS). Although a substantial portion of the drifting-buoy data are now in the MEDS archives, those data were mostly provided via the Global Telecommunications System (GTS).

4. References

Murphy, D.L., W.E. Hanson, and R.L. Tuxhorn, 1990, Modifications to Ice Patrol's Mean Current Data Base. Appendix C to Report of the International Ice Patrol in the North Atlantic, Bulletin No. 76, CG-188-45, 86 pp.

Soule, F.M., 1964. The normal topography of the Labrador Current and its environs in the vicinity of the Grand Banks of Newfoundland during the Iceberg Season. Woods Hole Oceanographic Institution, Ref. No. 64-36, 9 pp.

Sybrandy, A. and Niiler, P.P., 1991. WOCE/TOGA SVP LaGrangian drifter constructio manual, SIO Reference 91/6. Scripps Institution of Oceanography, La Jolla, CA 92093, 58 pp.

Interaction of the Deep Western Boundary Current With the North Atlantic Current

Robert S. Pickart
Woods Hole Oceanographic Institution
Woods Hole, MA 02543

North Atlantic Current Meeting, WHOI, April 19-20, 1993

1. Introduction

Over the past several years there has been a renewed effort, both through modelling and observation, to understand the manner in which the Deep Western Boundary Current (DWBC) and Gulf Stream interact at Cape Hatteras were they cross. It has been revealed that the two currents dynamically influence each other in a complex fashion, and that the consequences of this interaction may in fact be basin-wide. Since the Gulf Stream again comes in contact with the DWBC off the Grand Banks of Newfoundland (where the Southeast Newfoundland Rise diverts the DWBC southward), we might expect a similar type of interaction between the two currents. Below, some of the latest ideas regarding the Cape Hatteras crossover are discussed. Based on these results, two hypotheses are put forward regarding the role of the second interaction near the Grand Banks on the bifurcation of the Gulf Stream and recirculation of the DWBC.

2. Cape Hatteras Crossover

As part of the recent Synoptic Ocean Prediction Experiment (SYNOP), an array of bottom current meters and inverted echo sounders were maintained at the Gulf Stream-DWBC crossover point. During this time a detailed hydrographic/tracer survey of the crossover was also undertaken. Recent models have also addressed the crossover, including primitive equation numerical models and analytical studies. One of the more striking numerical results was that of Thompson and Schmitz (1989) who showed that the separation latitude and downstream meander characteristics of the Gulf Stream were highly sensitive to the strength of the DWBC. In their model the Gulf Stream was confined to the upper layer while the DWBC was contained in the lower layer; the dynamical mechanism influencing the separation was a thinning of the Gulf Stream layer due to the DWBC crossing. This relationship still remains to be tested observationally, but the SYNOP array has revealed that there is indeed a dynamical link between the two currents at the crossover.

Figure 1 shows how the lower layer f/H contours are influenced by the Gulf Stream flowing over the continental slope at Cape Hatteras. It is seen that the DWBC flows downslope (across bathymetric contours) along lines of constant f/H in response to the sloping thermocline of the Gulf Stream. This is precisely as predicted by the model of Hogg and Stommel (1985). It should be noted that the SYNOP current meters are all 100 m above the bottom, and hence they measure the deepest portion of the DWBC which is able to pass directly underneath the Gulf Stream (since the Gulf Stream does not extend to the bottom here). The recent hydrographic survey has revealed, however, that the upper portion of the DWBC collides with the subsurface Gulf Stream, and a large portion of the DWBC recirculates into the interior with the Gulf Stream (Figure 2). Pickart and Smethie (1993) have further shown that this entrainment of DWBC water apparently lowers the potential vorticity of the separated Gulf Stream and thus might influence its downstream character.

This type of collision process has been studied analytically by Agra and Nof (1993), who have investigated the separation which occurs when two opposing boundary currents collide (Figure 3). Interestingly, they found that the angle of separation is large even if the opposing current (the DWBC in this case) is much weaker than the main current. Perhaps the upper part of the DWBC plays a role in the Gulf Stream separation through this mechanism. Also of interest is the discovery that a portion of the DWBC, denser than the Gulf Stream water coming off the shelf, recirculates as well to form the deeper Gulf Stream (Figure 4). Apparently there is a dynamical coupling between this layer and the Gulf Stream layer above. Curiously, the onshore-most portion of the DWBC in this layer does seem to make it through the crossover (Figure 4).

To summarize, a substantial portion of the DWBC recirculates with the Gulf Stream, even in layers denser than the Gulf Stream water coming off the shelf. This allows for the possibility that both the mechanism of Thompson and Schmitz (1989) as well as that studied by Agra and Nof (1993) may be at work at Cape Hatteras contributing to the Gulf Stream separation. From the DWBC viewpoint, while a substantial portion of the transport recirculates at the crossover, Pickart and Smethie (1993) have shown that just to the south there is a compensating entrainment of offshore water into the DWBC. Thus, while the DWBC experiences no net transport loss due to the crossover, there is a complete exchange of water, which has strong consequences regarding the thermohaline through-put of northern source waters.

3. Interaction at the Grand Banks

As Gulf Stream nears the Southeast Newfoundland Rise (SNR) it again comes in contact with the DWBC (Figure 5), allowing for a similar interaction to that which occurs at Cape Hatteras. There are two significant differences, however, in that this is not a complete crossover since the DWBC turns northward after negotiating the SNR, and at this location the Gulf Stream extends quite deep (all the way to the bottom on occasion). Figure 5 shows that, in the mean, the Gulf Stream flows over the outer part of SNR and thus should always encounter the offshore part of the DWBC. For a deep-reaching Gulf Stream the resulting collision should cause recirculation of the offshore-most (deepest) part of the DWBC. The oxygen sections of Figure 6 show that such a deep recirculation does indeed occur. The section north of the SNR shows high-oxygen DWBC water as deep as 4800 m, whereas the section west of the SNR is devoid of any DWBC water deeper than 3800 m. That some recirculation of the DWBC occurs at the SNR is not a new concept, but the collision mechanism is perhaps one of the causes.

The Gulf Stream is of course not stationary at the SNR (in contrast to Cape Hatteras where the Gulf Stream meanders very little). In the region of the SNR the meander envelope of the Gulf Stream is quite large (Figure 7); it is seen that only one standard deviation to the north, the Gulf Stream is shallower than 3500 m which puts it right over the core of the DWBC (Figure 6). Recent evidence indicates that the position of the DWBC can also fluctuate as much as 1000 m across the continental slope (Pickart, 1992). Thus, the interaction of these two currents is time-varying: both currents can shift laterally (on varying time scales) causing different degrees of a Gulf Stream-DWBC crossover.

4. Two Hypotheses

Based on the recent discoveries regarding the Gulf Stream-DWBC crossover at Cape Hatteras and the above discussion of the circulation near the Grand Banks, here are two hypotheses regarding the dynamical interaction of the DWBC and Gulf Stream (North Atlantic Current) at the SNR.

HYPOTHESIS #1: The DWBC plays a dynamical role in the Gulf Stream bifurcation

The idea is as follows. When circumstances are such that the Gulf Stream encounters the core of the DWBC (i.e. a strong degree of crossing), the subsequent path and dynamics of the Gulf Stream/North Atlantic Current are altered. This occurs either by 1) the direct collision mechanism or 2) lower layer coupling/recirculation (which occurs at Cape Hatteras, Figure 4). In the latter case, the Gulf Stream will extend further to the bottom and thus "feel" the topography more as it reaches the SNR. In both of these cases the Gulf Stream will take a more southerly excursion: in case 1 because of the separation after the collision, and in case 2 because the resulting deep reaching current will tend to flow around the ridge (to avoid vertical compression). Thus, in both cases one might expect a stronger bifurcation of the Gulf Stream, i.e. more recirculation and less continuation to the North Atlantic Current. The reverse of this is when the two currents "miss" each other, in which case the Gulf Stream takes a more direct path eastward and makes a smoother transition to the North Atlantic Current.

Figure 8 shows two realizations of the Gulf Stream transitioning into the North Atlantic Current which support this idea. In Figure 8a the Gulf Stream (temperature $\geq 10°C$) enters the domain to the north presumably encountering the core of the DWBC, and subsequently flows around the SNR. In Figure 8b the Gulf Stream approaches the region from farther south and flows right over the SNR. Note that these different routes also affect where the North Atlantic current ultimately leaves the domain (further north in Figure 8b).

HYPOTHESIS #2: The Gulf Stream causes substantial recirculation/exchange of the DWBC at the Southeast Newfoundland Rise

At Cape Hatteras it was found that a significant portion of the DWBC water was replaced as a result of the crossover–by recirculation and subsequent entrainment of offshore water. A similar process might be occurring here whereby part of the DWBC recirculates (via the two mechanisms discussed in hypothesis #1) and is then replaced further to the west by cyclonic recirculation of the deep Gulf Stream. This implies that the Gulf Stream-DWBC interaction at the SNR might be an important mechanism by which the interior basin is ventilated by newly formed deep water.

5. References

Agra, C. and D. Nof, 1993: Collision and separation of boundary currents, J. Phys. Oceanog., in press.

Hogg, N.G. and H. Stommel, 1985: On the relationship between the deep circulation and the Gulf Stream, Deep Sea Res., 32, 1181-1193.

Pickart, R.S. and D.R. Watts, 1990: Deep Western Boundary Current variability at Cape Hatteras, J. Mar. Res., 48, 765-791.

Pickart, R.S., 1992: Space-time variability of the Deep Western Boundary Current oxygen core, J. Phys. Oceanog., 22, 1047-1061.

Pickart, R.S. and W.M.Smethie, Jr., 1993: How does the Deep Western Boundary Current cross the Gulf Stream? J. Phys. Oceanog., in press.

Thompson, J.D. and W.J. Schmitz, 1989: A limited-area model of the Gulf Stream: Design, initial experiments, and model-data intercomparison, J. Phys. Oceanog., 19, 791-814.

Qui, B., 1993: Determining the mean Gulf Stream and its recirculations through combining hydrographic and altimetric data, J. Geophys. Res., submitted.

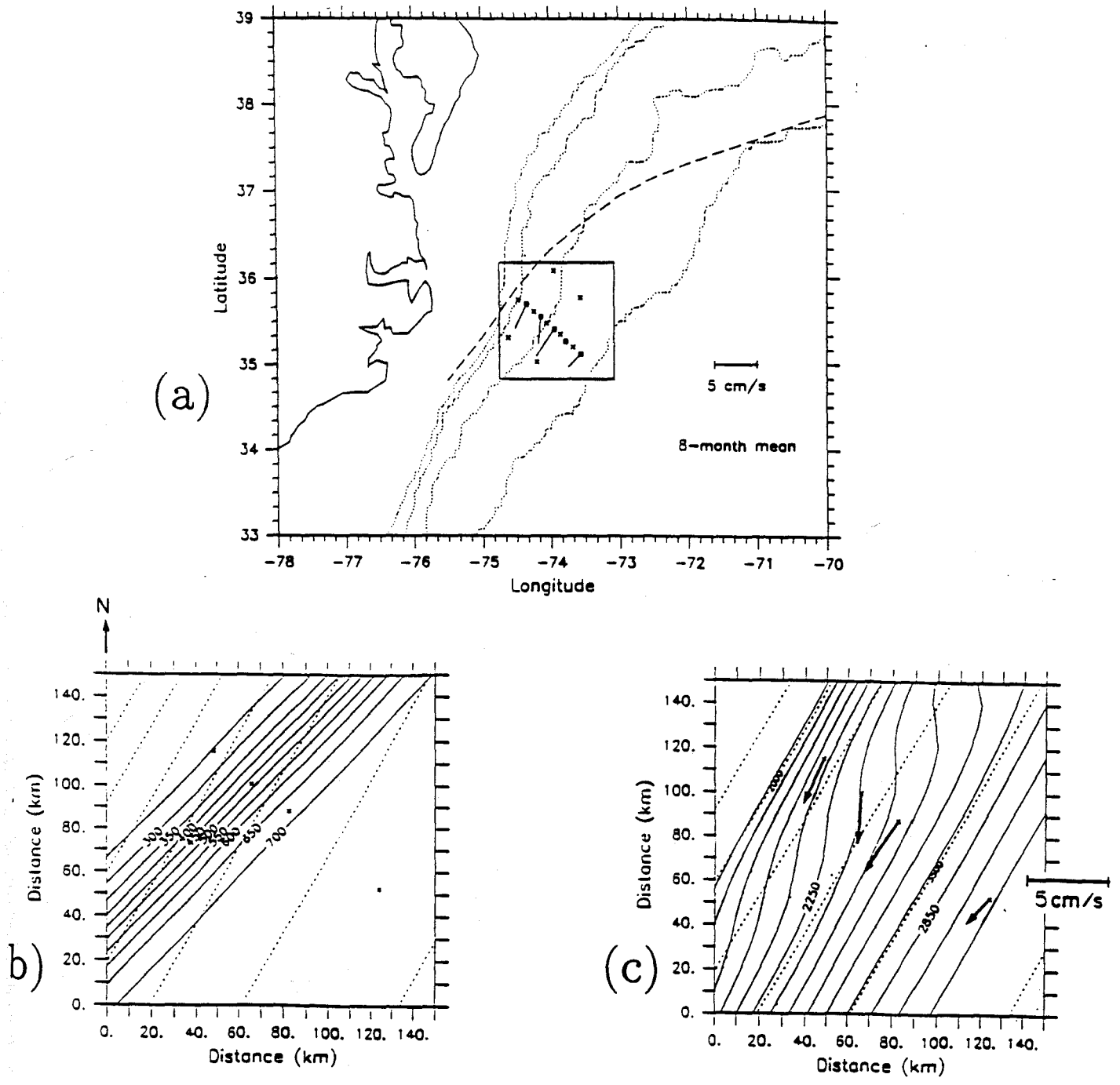

Figure 1: (a) Mean currents of the DWBC from the SYNOP Inlet Array (adapted from Pickart and Watts (1990)). (b) Simplified representation of the mean 12C isotherm topography of the Gulf Stream (solid lines), and bathymetry (dashed lines). (c) Lines of constant deep layer thickness (difference of 12C topography and bottom depth in (b)), with the mean current vectors from (a) overlayed.

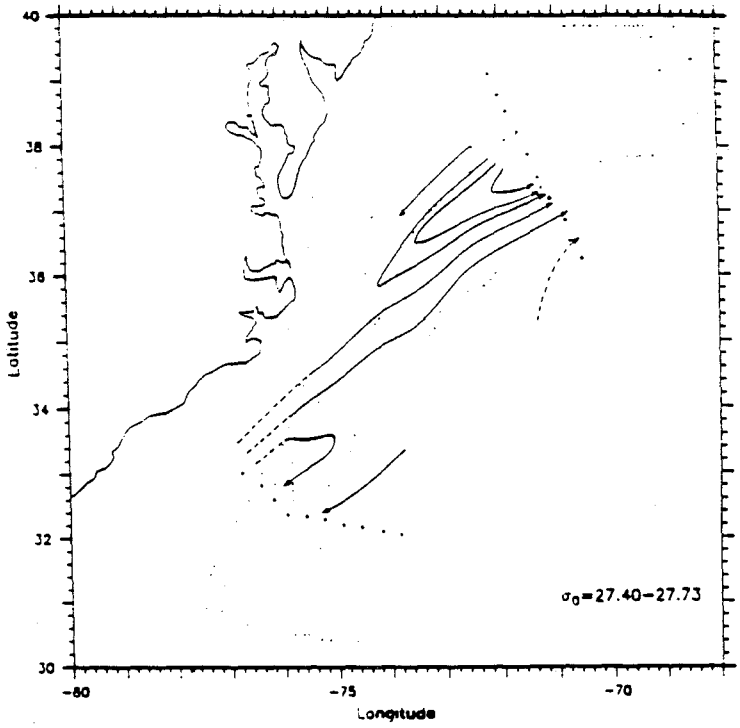

Figure 2: Absolute geostrophic flow trajectories in the density layer corresponding to the upper part of the DWBC (from Pickart and Smethie (1993)).

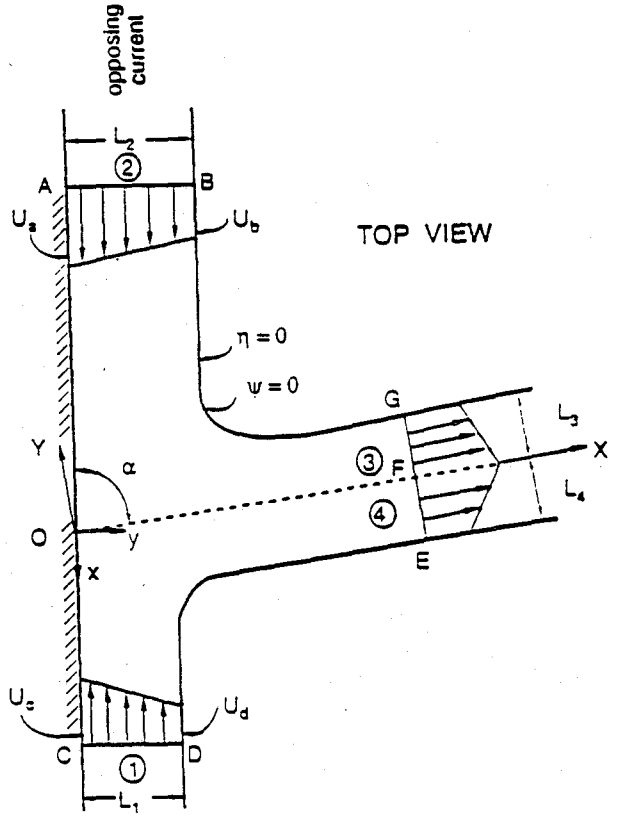

Figure 3: Schematic showing the collision and resulting separation of two opposing boundary currents (from Agra and Nof (1993)).

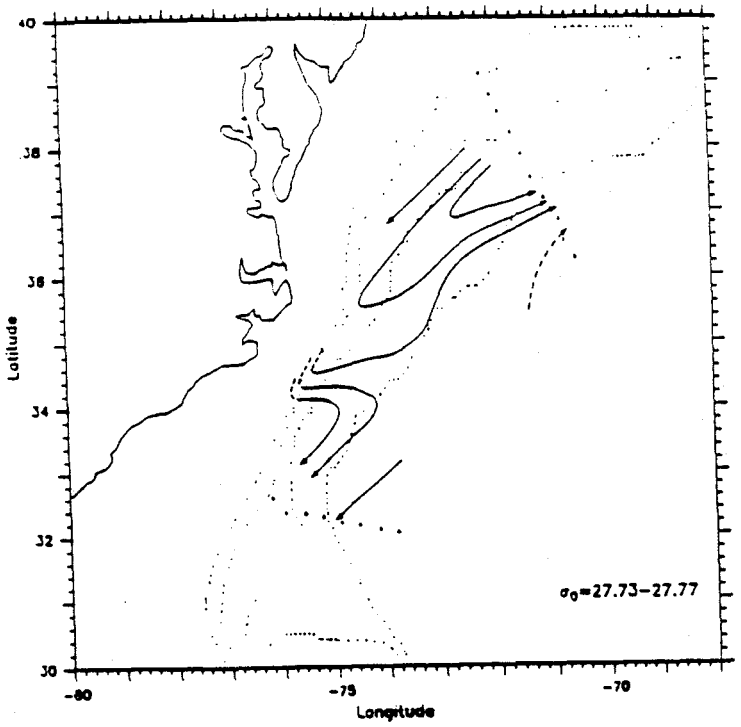

Figure 4: Absolute geostrophic flow trajectories in the density layer directly below that of Figure 2 (from Pickart and Smethie (1993)). This layer is denser than the Gulf Stream water coming off the shelf.

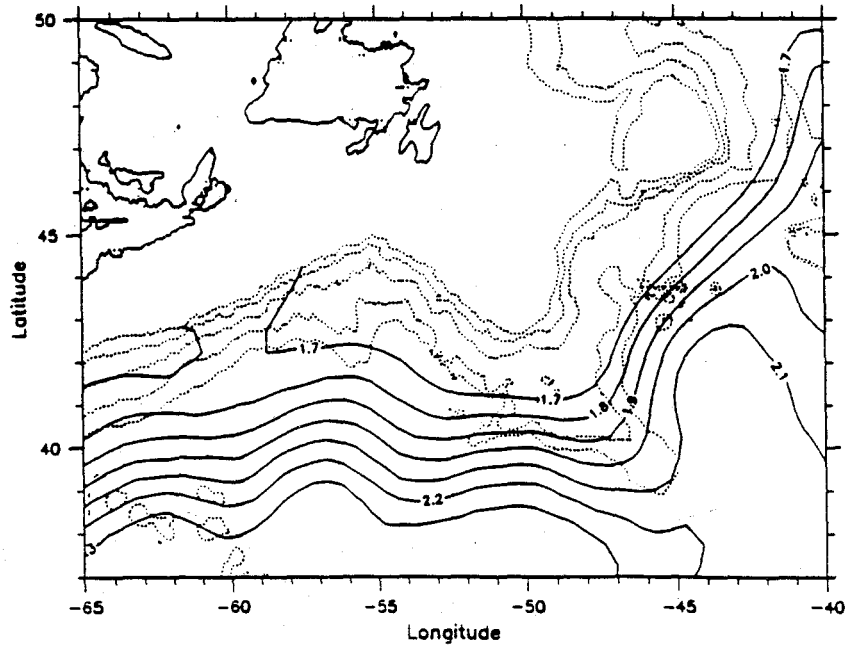

Figure 5: Mean dynamic topography of the sea surface relative to 3000 db using the NODC North Atlantic hydrographic data set (from Qui, 1993).

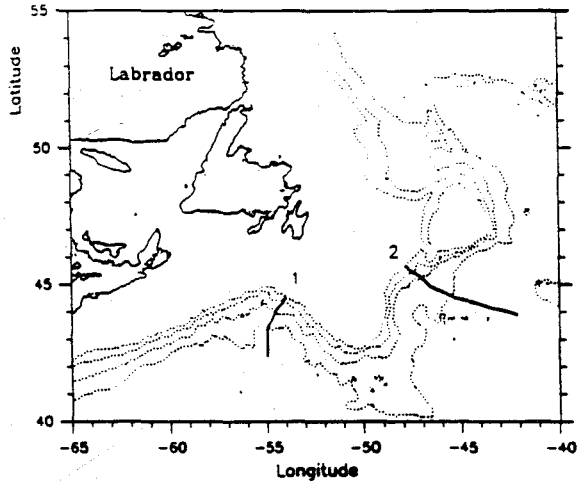

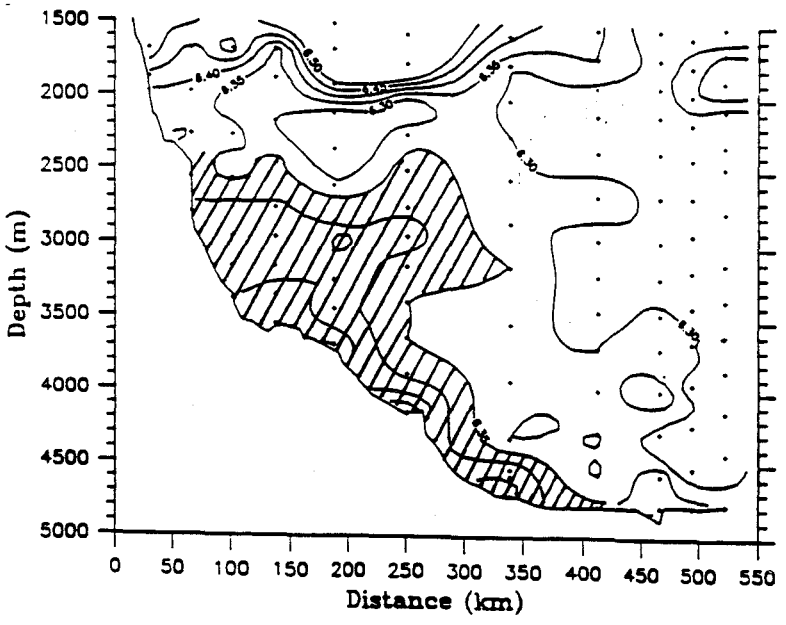

Section 2 Oxygen (ml/l)

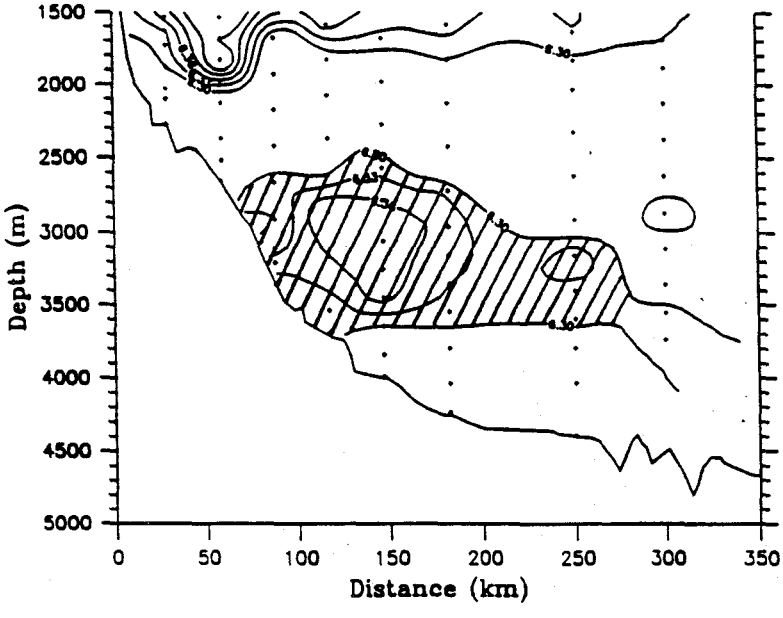

Section 1 Oxygen (ml/l)

Figure 6: (a) Deep oxygen section north of the SNR occupied in 1991. The high-oxygen DWBC water is shaded. (b) Oxygen section west of the SNR occupied in 1991.

Preliminary Results From the TOPEX/Poseidon Altimeter Mission

Detlef Stammer and Carl Wunsch
Department of Earth, Atmospheric & Planetary Sciences
Massachusetts Institute of Technology
Cambridge, MA 02138

Satellite altimetry is a powerful tool for studying the dynamics of the ocean circulation. Because it provides almost synoptic observations of the surface geostrophic current fields with global coverage, it is uniquely suited for studying a large part of the wavenumber-frequency spectrum of ocean variability.

During the last decade the technique of satellite altimetry has reached a stage at which quantitative estimates of various aspects of the ocean general circulation have become feasible, such as the ocean eddy field, the variations of ocean boundary current transports, and the computation of eddy kinetic energy or wavenumber and frequency spectra. Earlier altimeter missions gave a false impression of the accuracy which can be reached. Due to their poor data quality, many previous studies based on SEASAT and GEOSAT data were therefore confined to high-energy western boundary current regions such as the Gulf Stream and its extension. Furthermore, because of the poorly known marine geoid, and the large orbit error the majority of studies were confined to the ocean mesoscale variability.

Recently, a joint U.S./French TOPEX/Poseidon satellite was launched into an orbit at 1336 km altitude with an inclination of 66°. The TOPEX/Poseidon mission was specifically designed to make measurements of the sea surface height field with the precision necessary to study the dynamics of the global large-scale ocean circulation and of its variability. There is a particular emphasis on interannual and decadal time scales. It is hoped from this and any future altimeter mission to get estimates of the ocean response to climate changes in the flow fields and heat transport, or sea level rise. The satellite has been measuring the global sea surface height using a radar altimeter system along the same tracks on earth every 10 days since late September 1992. The radar instrument likewise provides information on the surface wave field and the near surface wind speed from its return pulse shape and amplitude.

To illustrate the remarkable precision of the TOPEX/Poseidon mission, the attached figure shows a preliminary estimate of the absolute sea surface height field measured by the satellite during a single 10-day period from November 22 to December 1, 1992. The figure was composed from the observed sea surface height relative to an estimate of the marine geoid by averaging the alongtrack data in 2° x 2° areas. The figure is based on the preliminary TOPEX IGDR data set which contains only rough estimates of the satellite ephemeris and environmental corrections with uncertainties exceeding by far the currently distributed precise GDR data set. Therefore it is very important to note that during the construction of the figure none of the corrections necessary for SEASAT and GEOSAT were made. Although it can and will be greatly improved, the figure readily gives a spatially coherent picture of the global large-scale ocean current field which is consistent with a priori knowledge of the large-scale circulation from climatological hydrographic data and global high-resolution numerical circulation models. Future ocean field experiment designs must account for this remarkable new capability.

Figure Caption

Global mean dynamic sea surface height field measured by the U.S./French TOPEX/Poseidon satellite during the 10-day period November 22 to December 1992. The figure was composed by averaging the observed alongtrack sea surface height data relative to an estimate of the marine geoid in 2° x 2° areas. Spatial scales less than about 500 km were eliminated by applying a Shapiro low-pass filter. The contour interval is 10 cm.

TOPEX/Poiseidon Sea Surface Topography Repeat 7
mean removed

2x2 deg

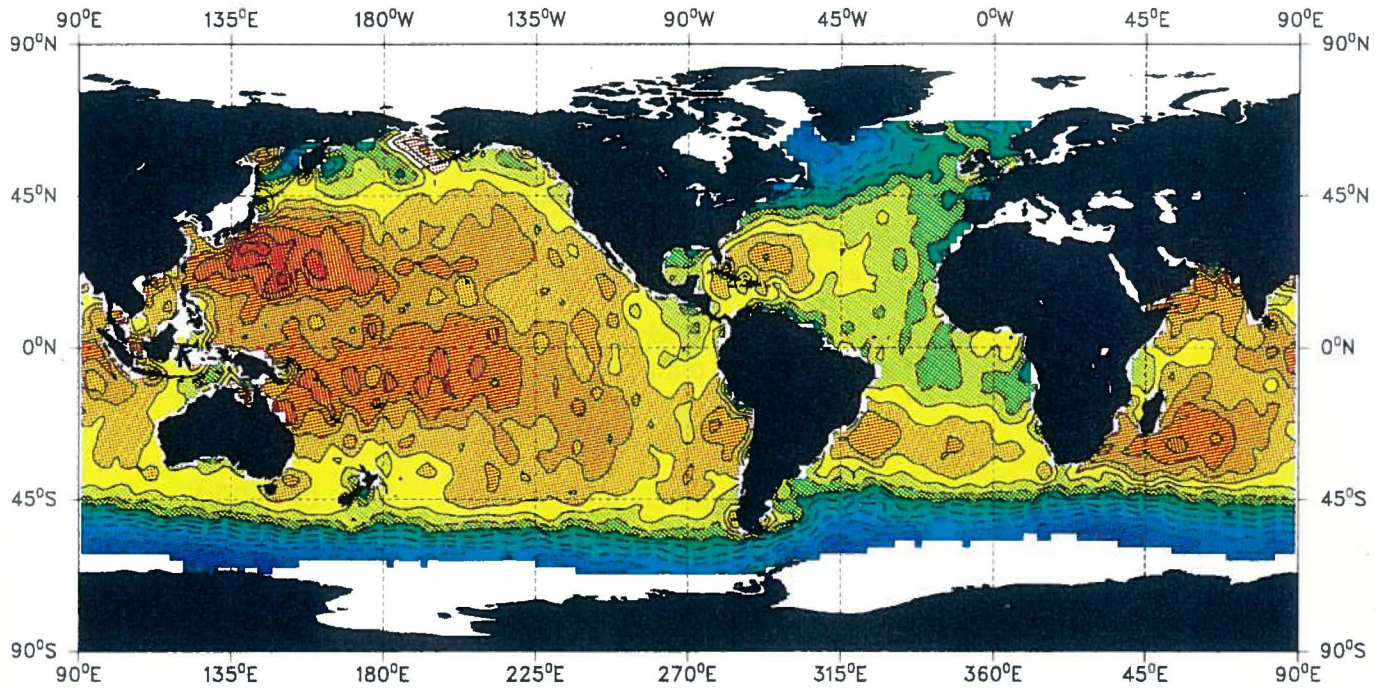

VIII. WORKSHOP AGENDA

The North Atlantic Current (NAC) System, A Workshop Sponsored by NSF/NOAA/ONR

Woods Hole Oceanographic Institution
Carriage House
April 19-20, 1993

Monday, April 19, 1993

8:30-8:40 AM	*Dr. Paola Malanotte-Rizzoli*, MIT Opening remarks and motivation for the workshop
8:40-9:30	*Prof. Wolfgang Krauss*, Kiel University The North Atlantic current and its associated eddy field. Observation and model results.
9:30-10:20	*Dr. Claus Böning*, Kiel University and *Dr. William Holland*, NCAR Problems and achievements in modeling the NAC system
10:20-10:40	Coffee break
10:40-11:30	*Prof. Thomas Rossby*, URI The NAC: at the crossroads of the wind-driven and thermohaline circulations
11:30-12:15 PM	*Dr. Allyn Clarke*, BIO The North Atlantic Current in the Northwest Atlantic
12:15-1:00	Lunch break
1:00-1:50	*Prof. Arnold Gordon*, Lamont Observatory TheACCP Program and the NAC
1:50-2:20	*Dr. Kirk Bryan*, GFDL The role of the Grand Banks in the North Atlantic climate variability
2:20-2:40	*Dr.Maurice Blackmon*, CIRES Surface climate variations over the North Atlantic during winter 1900-1989
2:40-3:00	*Dr. Robert Molinari*, NOAA/AOML Historical and recent XBT coverage in the Newfoundland Grand Banks region
3:00-3:20	Coffee break
3:20-3:40	*Dr. Detlef Stammer*, MIT Preliminary results from the TOPEX/POSEIDON altimeter mission

3:40-4:20	*Dr. Randolph Watts*, URI Key transects in the Newfoundland Basin for determining the Western Boundary Current structure: Volume and heat transports, and *Dr. Douglas Luther*, SIO Measuring NAC volume and heat transport from the sea floor
4:20-5:00	*Dr. Peter Worcester*, SIO Measuring thermal and velocity structure in the northwestern Atlantic with acoustic tomography
5:00-5:30	Discussion session

Tuesday, April 20, 1993

8:30-9:00 AM	*Dr. Eli Katz*, Lamont Observatory Tracking the downstream location of the NAC with an IES array
9:00-9:20	*Dr. Ross Hendry*, BIO Currents south of the Grand Banks at 50 West: estimates of mass transport
9:20-9:40	*Dr. Donald Murphy*, U.S. Coast Guard Surface drifter measurements in the North Atlantic near Newfoundland
9:40-10:00	*Dr. Robert Pickart*, WHOI The interaction of the Deep Western Boundary Current with the NAC
10:00-10:20	*Dr. Michael McCartney*, WHOI "Reactions"
10:20-10:40	Coffee break
10:40-12:30 PM	Discussion session *Dr. Thomas Rossby*, discussion leader • What are the key scientific issues and objectives of a possible national program on the NAC system? • What are the key field components of such a program?
12:30-1:30	Lunch break and seminar
1:30-3:00	Discussion session *Dr. Paola Malanotte-Rizzoli*, discussion leader • What are the key modeling issues of such a program? • What could be a reasonable timeline for such a program?
3:00-3:30	Coffee break
3:30-4:30	Discussion session *Dr. Paola Malanotte-Rizzoli*, discussion leader • Final issues-Timeline for the production of the workshop scientific report and possible future meetings for the specific design of the NAC program components.
4:30	Adjournment

IX. LIST OF PARTICIPANTS

Dr. Maurice Blackmon
NOAA/ERL
325 Broadway
Boulder, CO 80303-3328

Dr. Claus Boning
Institut fur Meerskunde an der
Universitat Kiel
Dusternbrooker Weg 20
2300 Kiel
GERMANY
(*presently at* National Center for
Atmospheric Research, Boulder, CO 80303)

Dr. Amy Bower
Woods Hole Oceanographic Institution
Woods Hole, MA 02543

Dr. Kirk Bryan
Geophysical Fluid Dynamics Lab/NOAA
Princeton University
P.O. Box 308
Princeton, NJ 08542

Dr. Allan D. Chave
Clark South 281
Woods Hole Oceanographic Institution
Woods Hole, MA 02543

Dr. Allyn Clarke
Bedford Institute of Oceanography
P.O. Box 1006
Dartmouth, NS B2Y 4A2
CANADA

Dr. Bruce Cornuelle
IGPP, A-025
Scripps Institution of Oceanography
La Jolla, CA 92093

Stephanie Dutkiewicz
Graduate School of Oceanography
University of Rhode Island
Narragansett Bay Campus
Narragansett, RI 02882

Dr. Jean H. Filloux
Physical Oceanography Research Division
Scripps Institution of Oceanography
La Jolla, CA 92093

Prof. Glenn Flierl
Room 54-1426
Massachusetts Institute of Technology
Cambridge, MA 02139

Sandra Fontana
Graduate School of Oceanography
University of Rhode Island
Narragansett Bay Campus
Narragansett, RI 02882

Sarah Gille
Woods Hole Oceanographic Institution
Woods Hole, MA 02543

Dr. Isaac Ginis
Graduate School of Oceanography
University of Rhode Island
Narragansett Bay Campus
Narragansett, RI 02882

Dr. David Goodrich
Office of Global Programs
National Oceanic
& Atmospheric Administration
1100 Wayne Avenue
Suite 1225
Silver Spring, MD 20910

Dr. Arnold Gordon
Lamont-Doherty Geological Observatory
of Columbia University
Palisades, NY 10964

Jim Hamilton
Bedford Institute of Oceanography
P.O. Box 1006
Dartmouth, NS B2Y 4A2
CANADA

Dr. Ross Hendry
Bedford Institute of Oceanography
P.O. Box 1006
Dartmouth, NS B2Y 4A2
CANADA
(*presently at* Groupe de Recherche de
Geodesie Spatiale (GRGS)
18 avenue Edouard Belin
31055 Toulouse Cedex
FRANCE)

Dr. Nelson Hogg
Woods Hole Oceanographic Institution
Woods Hole, MA 02543

Stephan Howder
Graduate School of Oceanography
University of Rhode Island
Narragansett Bay Campus
Narragansett, RI 02882

Dr. Bruce Howe
Applied Physics Laboratory
University of Washington
1013 NE 40th St.
Seattle, WA 98105

Dr. Eric Itsweire
National Science Foundation
Division of Ocean Sciences
Room 609
1800 G Street, NW
Washington, D.C. 20550

Dr. Eli Katz
Lamont-Doherty Geological Observatory
of Columbia University
Palisades, NY 10964

Edward Kearns
Graduate School of Oceanography
University of Rhode Island
Narragansett Bay Campus
Narragansett, RI 02882

Dr. Kathryn Kelly
Clark 321A
Woods Hole Oceanographic Institution
Woods Hole, MA 02543

Birgit Klein
Woods Hole Oceanographic Institution
Woods Hole, MA 02543

Dr. Barry Klinger
Massachusetts Institute of Technology
Cambridge, MA 02139

Prof. Wolfgang Krauss
Institut fur Meereskunde an der
Universitat Kiel
Dusternbrooker Weg 20
2300 Kiel
GERMANY

Dr. John Lazier
Bedford Institute of Oceanography
P.O. Box 1006
Dartmouth, NS B2Y 4A2
CANADA
(*presently at*
School of Oceanography, WB-20
University of Washington
Seattle, WA 98195)

Pascal LeGrand
Massachusetts Institute of Technology
Cambridge, MA 02139

Dr. Scott Lindstrom
Graduate School of Oceanography
University of Rhode Island
Narragansett Bay Campus
Narragansett, RI 02882

Dr. Douglas Luther
University of Honolulu, HI 96822
(*presently at*
Mail Code A-030
Scripps Institution of Oceanography
La Jolla, CA 92093)

Prof. Jochem Marotzke
Room 54-1514
Massachusetts Institute of Technology
Cambridge, MA 02139

Prof. John Marshall
Room 54-1526
Massachusetts Institute of Technology
Cambridge, MA 02139

Dr. Michael McCartney
Clark 344C
Woods Hole Oceanographic Institution
Woods Hole, MA 02543

Chris Meinen
Graduate School of Oceanography
University of Rhode Island
Narragansett Bay Campus
Narragansett, RI 02882

Dr. Robert Molinari
NOAA/AOML
4301 Rickenbacker Causeway
Miami, FL 33149

Dr. Donald Murphy
International Ice Patrol
U.S. Coast Guard
1082 Shennecossett Road
Groton, CT 06340-6095

Prof. Joseph Pedlosky
Woods Hole Oceanographic Institution
Woods Hole, MA 02543

Dr. Robert S. Pickart
Clark 340A
Woods Hole Oceanographic Institution
Woods Hole, MA 02543

Dr. Kurt Polzin
Woods Hole Oceanographic Institution
Woods Hole, MA 02543

Dr. Mark Prater
Graduate School of Oceanography
University of Rhode Island
Narragansett Bay Campus
Narragansett Bay, RI 02882

Bo Qiu
Woods Hole Oceanographic Institution
Woods Hole, MA 02543

Dr. Phil Richardson
Woods Hole Oceanographic Institution
Woods Hole, MA 02543

Prof. Paola M. Rizzoli
Massachusetts Institute of Technology
Room 54-1416
Cambridge, MA 02139

Prof. Thomas Rossby
Graduate School of Oceanography
University of Rhode Island
Narragansett Bay Campus
Narragansett, RI 02882

Clark Rowley
Graduate School of Oceanography
University of Rhode Island
Narragansett Bay Campus
Narragansett, RI 02882

Dr. Thomas Sanford
Applied Physics Laboratory
and School of Oceanography
University of Washington
1013 NE 40th St.
Seattle, WA 98105

Dr. Ray Schmitt
Woods Hole Oceanographic Institution
Woods Hole, MA 02543

Prof. Friedrich Schott
Institut fur Meereskunde an der
Universitat Kiel
Dusternbrooker Weg 20
2300 Kiel
GERMANY

Dr. Uwe Send
Institut fur Meereskunde an der
Universitat Kiel
Dusternbrooker Weg 20
2300 Kiel
GERMANY

Dr. William Smethie
Lamont-Doherty Geological Observatory
of Columbia University
Palisades, NY 10964

Dr. Detlef Stammer
Massachusetts Institute of Technology
Cambridge, MA 02139

Karen Tracey
Graduate School of Oceanography
University of Rhode Island
Narragansett Bay Campus
Narragansett, RI 02882

Dr. Martin Visbeck
Institut fur Meereskunde an der
Universitat Kiel
Dusternbrooke Weg 20
2300 Kiel
GERMANY

Dr. Randolph Watts
Graduate School of Oceanography
University of Rhode Island
Narragansett Bay Campus
Narragansett, RI 02882

Dr. Ric Williams
Massachusetts Institute of Technology
Cambridge, MA 02139

Dr. Peter Worcester
IGPP, A-025
Scripps Institution of Oceanography
La Jolla, CA 92093

Prof. Carl Wunsch
Room 54-1520
Massachusetts Institute of Technology
Cambridge, MA 02139

Huai-Min Zhang
Woods Hole Oceanographic Institution
Woods Hole, MA 02543